

NASA CR-
141711

(NASA-CR-141711) ANALYSIS OF SRM MODEL
NOZZLE CALIBRATION TEST DATA IN SUPPORT OF
IA12B, IA12C AND IA36 SPACE SHUTTLE LAUNCH
VEHICLE AERODYNAMICS TESTS (Lockheed
Missiles and Space Co.) 82 p HC \$4.75

N75-18294

Unclas
G3/18 12437



Lockheed

HUNTSVILLE RESEARCH & ENGINEERING CENTER

LOCKHEED MISSILES & SPACE COMPANY, INC.
A SUBSIDIARY OF LOCKHEED AIRCRAFT CORPORATION

HUNTSVILLE, ALABAMA

LOCKHEED MISSILES & SPACE COMPANY, INC.
HUNTSVILLE RESEARCH & ENGINEERING CENTER
HUNTSVILLE RESEARCH PARK
4800 BRADFORD DRIVE, HUNTSVILLE, ALABAMA

ANALYSIS OF SRM MODEL NOZZLE
CALIBRATION TEST DATA IN
SUPPORT OF IA12B, IA12C AND
IA36 SPACE SHUTTLE LAUNCH
VEHICLE AERODYNAMICS
TESTS

December 1973

Contract NAS9-13429

by

L. Ray Baker, Jr.
James A. Tevepaugh
Morris M. Penny

APPROVED:



John W. Benefield, Supervisor
Fluid Mechanics Section

FOREWORD

This document is presented in partial fulfillment of the contract requirements of Contract NAS9-13429, "Space Shuttle Plume Impingement Study."

The study was conducted for the Engineering Analysis Division, Johnson Space Center (JSC), Houston, Texas. The NASA-JSC technical monitor for this contract is Mr. Barney B. Roberts, EX32.

Experimental data for this document were provided by the Rocketdyne Division of Rockwell International Corporation.

SUMMARY

Variations of nozzle performance characteristics of the model nozzles used in the Space Shuttle IA12B, IA12C, IA36 power-on launch vehicle test series are shown by comparison between experimental and analytical data. The experimental data are nozzle wall pressure distributions and schlieren photographs of the exhaust plume shapes. The exhaust plume shapes were simulated experimentally with "cold flow" while the analytical data were generated using a method-of-characteristics solution.

Exhaust plume boundaries, boundary shockwave locations and nozzle wall pressure measurements calculated analytically agree favorably with the experimental data from the IA12C and IA36 test series. For the IA12B test series condensation was suspected in the exhaust plumes at the higher pressure ratios required to simulate the prototype plume shapes. Nozzle calibration tests for the series were conducted at pressure ratios where condensation either did not occur or if present did not produce a noticeable effect on the plume shapes. However, at the pressure ratios required in the power-on launch vehicle tests condensation probably occurs and could significantly affect the exhaust plume shapes.

CONTENTS

| Section | | Page |
|----------------|---|------|
| | FOREWORD | ii |
| | SUMMARY | iii |
| | NOMENCLATURE | v |
| 1 | INTRODUCTION | 1 |
| 2 | TECHNICAL DISCUSSION | 3 |
| | 2.1 General Discussion | 3 |
| | 2.2 IA12B | 8 |
| | 2.3 IA12C | 11 |
| | 2.4 IA36 | 13 |
| 3 | GENERAL CONCLUSIONS AND RECOMMENDATIONS | 15 |
| 4 | REFERENCES | 17 |
| Appendixes | | |
| A | Space Shuttle Main Engine Prototype Trajectory Conditions and Predicted Inviscid Plume Boundaries; Model Nozzle Geometry and Operating Conditions Necessary for Simulation of Prototype Plume Boundaries; and Comparison of Predicted Prototype and Simulation (Using Air) Plume Boundary Definitions | A-1 |
| B | Model Nozzle Experimental Pressure Data for Model Nozzle Calibration Test Numbers 41, 45, 48, 49, 55, 57, 59, 65, 67, 68, 72, 73, 81, 83, 88, 90 | B-1 |

NOMENCLATURE

| <u>Symbol</u> | <u>Description</u> |
|-------------------|---|
| A/A^* | area ratio |
| M | Mach number |
| P | pressure, psia |
| R | gas constant (ft-lbf/lbm- $^{\circ}$ R) |
| T | temperature, $^{\circ}$ R |
| t | time, sec |
| u | velocity, ft/sec |
| X, R | axial and radial coordinates of nozzle-plume, in. |
| <u>Greek</u> | |
| γ | ratio of specific heats |
| δ_j | plume initial turning angle, deg |
| θ_N | nozzle lip angle, deg |
| ν | Prandtl-Meyer expansion angle, deg |
| ρ | density, slug/ft ³ |
| <u>Subscripts</u> | |
| l | initial plume boundary |
| c | chamber conditions, curvature |
| e | nozzle exit plane |
| ∞ | freestream conditions |
| F.S. | full-scale |
| M | model nozzle |
| p | plenum |
| t | throat |
| exit | denotes nozzle exit plane |

Section 1 INTRODUCTION

From liftoff to solid rocket motor (SRM) staging, the Space Shuttle vehicle thrust is provided by two solid rocket motors and three Space Shuttle main engines (SSME). Space Shuttle vehicle aerodynamic characteristics are affected by the interaction of the plumes formed by the exhaust gases of the SRMs and SSMEs and the freestream flow field. To accurately predict the aerodynamic characteristics of the Space Shuttle vehicle, the extent of the influence of the exhaust plume-freestream flow field interaction must be determined at various points in the nominal flight trajectory.

Due to the complexity of the gasdynamic problems, a completely analytical treatment of the plume-flow field interaction is not possible. To provide the required data, a series of experimental programs has been undertaken to define the power-on Space Shuttle launch vehicle aerodynamics. Accurate definition of the aerodynamic characteristics requires a technique for scaling or simulating the effects of the full-scale propulsion systems on the vehicle. A "cold gas" technique was utilized during the test series to simulate the full scale SRM and SSME exhaust plumes. For this program "room" temperature air is the "cold gas." Supersonic converging-diverging nozzles designed to flow the air at specified operating pressures are utilized to produce the required plume shapes. This document is concerned with the examination of data from calibration tests conducted with air nozzles designed to meet the simulation requirements of the IA12B, IA12C and IA36 test programs.

In Section 2 of this document (Technical Discussion), Space Shuttle solid rocket motor prototype nozzle geometry, operating and trajectory conditions at freestream Mach numbers of 0.9, 1.25, 2.0, 2.5, 3.0 and 3.5 and the predicted prototype exhaust plumes generated analytically for these trajectory conditions are presented. The methods used in designing model nozzles for simulating the Space Shuttle solid rocket motor exhaust plumes at the above trajectory conditions

are then discussed briefly. The method for predicting analytically the operating conditions of the model nozzles necessary for exhaust plume simulation is presented. Operating conditions obtained analytically for the three model nozzles used to simulate the SRM at the above trajectory conditions are specified and the predicted model exhaust plumes compared with the corresponding prototype exhaust plumes being simulated. Calibration of the model nozzles employed in the IA12B, IA12C and IA36 power-on aerodynamic tests is investigated extensively with emphasis on comparison of nozzle wall static pressure distribution, exhaust plume free boundary shapes and boundary shock shapes obtained experimentally from pressure transducers and schlieren data respectively, with data generated by current analytical techniques.

Although not considered in this study, prototype and plume simulation data for the Space Shuttle main engine have been included in Appendix A as reference material.

Section 2 TECHNICAL DISCUSSION

2.1 GENERAL DISCUSSION

This document reports the results of an examination of experimental data recorded during calibration testing of SRM model nozzles designed for use in the IA12B, IA12C and IA36 Space Shuttle launch configuration power-on aerodynamic test programs. Prior to presenting this information, however, it is appropriate to discuss briefly the methods utilized in the design of the model nozzles. The initial portion of this section addresses the simulation analysis that resulted in the model nozzle contours. The discussion is concluded with a review of the methods utilized in reducing and analyzing the experimental data.

2.1.1 Prototype Plume Definition

The prototype system characteristics are required before a simulation technique can be applied. In this application, the inviscid plume boundary shape at selected trajectory conditions was the prototype characteristic being simulated.

To obtain the required prototype plume boundary shapes, exhaust plume flow fields for the prototype SRM at the trajectory conditions in question were computed. A chemical equilibrium combustion (CEC) computer code (Ref. 1) and a method-of-characteristics (MOC) computer code (Ref. 2) were utilized in the computational process. Initially, thermochemical data for the combustion of the SRM propellant at the chamber pressures corresponding to selected trajectory conditions were computed using the CEC code. To obtain these data, the combustion products were expanded isentropically from the chamber assuming the constituents to be in chemical equilibrium. The thermochemical data along

with the SRM nozzle geometry and the conditions defining the trajectory point were then input to the MOC computer code. Flowfield characteristics were subsequently computed in the supersonic region of the SRM nozzle and in the exhaust plume for a specified distance downstream of the nozzle exit. The exhaust gases from the nozzles were assumed to be expanding into a non-quiet environment. The freestream flow was assumed to be uniform and parallel to the nozzle centerline and to be defined gasdynamically by the specified trajectory conditions. The free boundary of the exhaust plume was defined by balancing the plume static pressure with the component of the Newtonian impact pressure that was normal to local flow direction. Output from the MOC computer code includes the coordinates and gasdynamic properties of the plume free boundary points thereby defining the SRM prototype inviscid exhaust plume boundaries. Exhaust plume boundary shapes for the SRM were defined in the above manner to provide the prototype data upon which the SRM propulsion system simulations were based for each of the subject test programs.

2.1.2 Prototype Plume Simulation

The simulation criteria utilized to determine model design data were based on the work of Herron (Ref. 3). The similarity parameters specified in Ref. 3 were determined for a plume expanding into a quiet environment and therefore were used only as a starting place for obtaining the required data. The similarity parameters of Ref. 3 as interpreted for this application are:

$$\delta_j)_M = \delta_j)_F.S.$$

$$\left. \frac{M_1}{\gamma_1} \right)_M = \left. \frac{M_1}{\gamma_1} \right)_F.S.$$

Knowledge of the full scale plume characteristics (i.e., δ_j , M_1 and γ_1) is required to apply these parameters. In addition to the above parameters, design of the model nozzles is further constrained by consideration of requirements dictated by the aerodynamic model design, the nozzle air supply limitations and the wind tunnel operating characteristics.

In the design procedure, the similarity parameters and other constraints are applied using one-dimensional gasdynamic relationships to arrive at values of nozzle area ratio, lip angle, internal geometry, and a first guess at nozzle operating conditions. This design process is discussed in detail in Ref. 4 in relationship to a similar nozzle design problem for the IA2 and IA7 test series. Nozzles designed in this manner are usually only suitable for plume simulation over a limited range of freestream Mach numbers. Therefore, nozzles unique to each of the subject test series were designed.

Definition of the model nozzle operating pressure which resulted in matching of the model and prototype plume shapes over the region of interest required further computations. The model nozzle geometry, initial plenum pressure estimate, and appropriate trajectory conditions were input to the MOC computer code and the model nozzle and model nozzle exhaust plume flow field calculated. The gas flowing in the nozzle was assumed to behave as a thermally and calorically perfect gas with a constant value of gamma equal to 1.4. Plume boundary shock waves were considered in the exhaust plume flowfield calculations. The computed model nozzle exhaust plume boundary shape was then compared with the SRM prototype plume boundary for the appropriate trajectory condition. If matching of the plume boundary shapes was not achieved, a new estimate of the model nozzle plenum pressure was made and the model nozzle exhaust plume boundary shape recalculated. This "iterative" procedure was continued until satisfactory correlation between the prototype and simulation exhaust plumes was obtained. The nozzle plenum pressure required to achieve correct simulation of the inviscid SRM prototype plume boundary shapes were determined in the above manner for each trajectory condition.

2.1.3 Calibration Testing

Calibration testing of the model nozzles for the IA12B, IA12C and IA36 tests was conducted in the Rocketdyne Rocket Test Facility. Room temperature dry air was utilized as the test medium throughout the calibration tests. The supply pressure to the model nozzle plenum was approximately

constant over most of the calibration test series. Model nozzle exhaust plume shape was varied during the test by adjusting the ambient pressure in the test cell to achieve the desired range of chamber to ambient pressure ratios.

Data recorded during each test included: (1) nozzle chamber pressure and temperature; (2) static pressure along the nozzle walls; (3) ambient pressure in the test cell; and (4) schlieren photographs of the exhaust plumes. The reduced experimental pressure and temperature data utilized in this analysis can be found in Appendix B.

Each calibration test was conducted using the same run procedure. Initially, the nozzle supply pressure was set to the desired level. The test cell ambient pressure then reduced to the level required to achieve the test point pressure ratio. Air flow was then stabilized in the nozzle and the pressure and optical data recorded. The experimental pressure data were subsequently reduced and printed for immediate use. The optical data were processed later and correlated with the pressure data for analysis.

2.1.4 Calibration Data Analysis

An analysis of the experimental data from the calibration testing of IA12B, IA12C and IA36 model nozzles was conducted to determine if the model nozzles performed as expected. The experimental data considered in the analysis included static pressures measured on the nozzle walls and schlieren data showing exhaust plume shapes. The static pressure data were obtained directly from reduced test data sheets (Appendix B). Additional data reduction was required to utilize the schlieren data.

The data of interest to this analysis are the plume boundary and the plume boundary shock shapes. These data were obtained from the schlieren photographs by reading and tabulating the axial and radial coordinates of the locus of plume boundary and shock shapes. Reading and tabulating the locus of plume boundary shock was straightforward since in almost every instance the shock appeared as a narrow well defined line in the photographs.

Locating the inviscid plume boundary on the schlieren photographs is not as straightforward and requires some interpretation of the photograph as well as an explanation of the interaction of the plume flow with the ambient air. The expansion of an exhaust plume into some environment (quiescent or non-quiescent) results in a viscous mixing region occurring along the ambient and plume boundary. The "width" of the mixing zone is a complex function of the gasdynamic characteristics of the plume and ambient flow and the "axial" distance over which the mixing occurs. Over the region of interest for the plume simulation, the mixing zone lies outside the plume boundary shock so that comparison of analytical and experimental shock locations can easily be made. The problem then becomes one of locating an "inviscid" plume boundary on the schlieren optical data which permits meaningful comparisons to be made with analytically computed inviscid plume boundaries. This in essence is locating a streamline on the schlieren photo which contains a mass equal to 100% of the mass emitted from the nozzle.

To locate the "inviscid" plume boundary in the mixing zone, one of two approximate approaches must be adopted. Either a detailed mixing analysis must be conducted for each case to define the mixing zone and then the plume boundary determined from these data or a consistent estimate of the boundary location made from optical data without the aid of analysis. Both of these approaches involve assumptions and interpretations and, therefore, do not yield exact information. Since conducting a detailed mixing analysis for each case was considered too time consuming for this investigation, the latter approach was adopted.

Approximate mixing calculations assume the mixing to occur about an inviscid plume boundary which is the basic assumption used in this study. The inviscid plume boundary was assumed to lie on a locus of points that equally divides the region of density gradient that appears on each schlieren photograph at the intersection of the plume and ambient gases. Although, not exact, the inviscid plume boundary data obtained from this approach are consistent with the mixing phenomena. To augment and support this assumption, additional work

has been undertaken to better define the location of the inviscid plume boundary. This information will be reported in a subsequent document.

To assess the performance of the model nozzles, a method-of-characteristics flowfield analysis was conducted for each of the calibration test cases being examined. Baseline model nozzle geometry and corresponding operating conditions along with the ambient pressure for each case were input to the MOC program. The air flowing through the model nozzles was assumed to behave as an ideal gas. Calculated nozzle wall static pressure distributions were nondimensionalized with respect to chamber pressure and plotted as function of axial distance from the nozzle geometric throat. The calculated coordinates of the plume boundary and shock points were nondimensionalized with respect to the nozzle exit radius and also plotted.

Experimental and computed nozzle and plume characteristics were compared when the data reduction and computational processes were completed. The remainder of this document discusses the results of these comparisons. Analysis of the calibration data associated with each launch vehicle test series is discussed as a separate item and conclusions pertinent to that test are stated.

2.2 IA12B

SRM prototype nozzle geometry and motor characteristics utilized as the baseline for the IA12B Space Shuttle launch vehicle aerodynamic tests are given in Table 1a. The trajectory conditions being investigated in this test are summarized in Table 2. The information given in Tables 1 and 2 was utilized to generate the plume boundary shown in Fig. 1 for freestream Mach numbers of 1.55 and 2.0. Application of the simulation technique discussed in Section 2.1 resulted in a model nozzle with the geometric characteristics given in Fig. 2a. The operating pressure ratio (model chamber pressure to ambient static pressure) required to achieve matching of the prototype plume boundary is given in Table 3. The computed prototype and simulant gas plume boundary shapes are compared in Figs. 3 and 4 for freestream Mach numbers of 1.55 and 2.0, respectively. Good agreement

was obtained between the prototype and simulation plume boundary. Also presented in Figs. 3 and 4 are predicted plume boundaries for pressure ratios run during the IA12B aerodynamic tests which were greater than the pressure ratios required for prototype plume simulation.

Calibration testing of the IA12B model nozzles was conducted in the Rocketdyne Rocket Nozzle Test Facility prior to the IA12B aerodynamic test series. From the series of calibration test points obtained with the IA12B SRM nozzles (test 41 through 50 of Table 4), four test points were selected for in-depth analysis. The highest pressure ratio (chamber-to-ambient pressure), the lowest pressure ratio and two intermediate pressure ratios were selected for analysis. The pressure ratios for these points are summarized in Table 5.

Experimental plume boundary and boundary shock definitions were obtained from schlieren photographs of the exhaust plume at each test point. Coordinates of points along the plume boundary and boundary shock were measured with respect to their distance from the nozzle exit plane and the nozzle centerline. The coordinates of the points were nondimensionalized with respect to the nozzle exit radius and compared with the predicted values in Figs. 6, 8, 10 and 12. Figure 6a compares the predicted plume boundary and shock shape with schlieren photograph data for test 41. This comparison indicates the method of locating the plume boundary (Section 2.1.4) and shock shape from the schlieren photograph and is typical of the data comparisons presented throughout the remainder of the report. Nozzle wall static pressure distributions nondimensionalized with respect to chamber pressure were obtained directly from the calibration data summary sheets (Appendix B) provided by the Rocketdyne Rocket Nozzle Test Facility. These data are compared with the computed wall pressure distributions in Figs. 5, 7, 9 and 11.

Comparison of the experimental and nozzle wall static pressure distributions for the four test points showed fair agreement. The experimental data consistently fell below the predicted distribution, indicating that the measured

static pressure at the wall of the model nozzle was greater than the predicted static pressure. The differences noted between the experimental and predicted wall pressure data could result from: (1) instrumentation error; (2) boundary layer growth in the nozzle; (3) condensation or liquefaction in the flow; or (4) deviation of the actual nozzle geometry from design baselines. Review of the test procedures has eliminated instrumentation error as a probable source. Boundary layer growth in the nozzle was investigated using the computer code of Ref. 5. A displacement thickness distribution was calculated and the nozzle flow field recalculated. A slight shift in the predicted static wall pressure distribution was noted but it was not of the magnitude required to explain the noted differences.

The nozzle flow was then examined to determine if conditions existed in the nozzle which would be conducive to the onset of condensation or liquefaction. To produce the measured nozzle wall pressure trends liquefaction of the air (or condensation) would have had to occur at an axial location corresponding to a rather low area ratio (see Figs. 6, 8, 10 and 12). Examination of the vapor pressure curves for oxygen and equilibrium air indicated that liquefaction in this region of the flow is highly unlikely. In addition, data taken with nozzles having much higher area ratios (Ref. 4) in which condensation was observed showed a much more severe effect on the wall static pressure than was observed in this test. The conclusion was that differences in the nozzle wall static distribution did not result from condensation or liquefaction.

It was thus concluded that the differences noted in the nozzle wall static pressure distributions were caused by deviation of the model nozzle geometry from the design baseline (probably a difference in nozzle wall angle). Model nozzle inspection data were not available to confirm this conclusion.

Comparison of the experimentally determined and analytically predicted plume boundary and boundary shock shapes yielded only fair agreement. The experimental plume boundary shapes corresponding to the higher pressure ratios (Figs. 8 and 12) fell considerably above the predicted plume boundaries.

This result was caused by the exaggeration at the high pressure ratios of the difference between the experimentally measured and the predicted static pressure at the nozzle lip. The higher static pressures measured at the model nozzle exit would result in a greater expansion of the nozzle exhaust gases for a fixed ambient condition producing a larger plume. This trend is substantiated by the plume boundaries for the lower pressure ratios presented in Figs. 6 and 10. At the lower pressure ratios the difference in the experimental and predicted plume boundaries is very small but nonetheless present with the experimental data falling slightly above the predicted plume boundaries.

Comparison of the boundary shock location data (Figs. 6, 8, 10 and 12) indicated a trend similar to that observed with the plume boundaries. For the case of the higher pressure ratios the experimentally determined boundary shock data plotted considerably above the predicted shock curves. At the lower pressure ratios, the experimental and predicted boundary shock data generally coincided.

From the analysis conducted on the IA12B nozzle calibration data it was concluded that matching of the inviscid prototype plume boundary could be accomplished with the model nozzles operated at the pressure ratios shown in Table 3. The differences noted in the nozzle wall static pressure distribution did not produce a significant influence on the plume boundary shape at the pressure ratio level required for plume simulation.

2.3 IA12C

The characteristics of Space Shuttle solid rocket motor used as the baseline for IA12C launch vehicle aerodynamic test series are given in Table 1b. Trajectory conditions being investigated by this test series correspond to the freestream Mach numbers of 2.5, 3.0 and 3.5 given in Table 6. Prototype plume shapes were generated for these trajectory conditions using the methods outlined in Section 2.1.

An area ratio of 7.0 conical nozzle was utilized to simulate SRM exhaust plumes for this test series. The geometric characteristics of this nozzle are summarized in Fig. 2a. The ratio of nozzle chamber to ambient pressure required to achieve prototype plume boundary shape at each trajectory test condition are given in Table 3. Comparison of the predicted prototype and simulation plume shapes are presented in Figs. 13, 14 and 15 for trajectory conditions corresponding to the freestream Mach numbers of 2.5, 3.0 and 3.5, respectively. Good agreement was achieved in each case. Also presented in Figs. 13, 14 and 15 are predicted plume boundaries for pressure ratios run during the IA12C aerodynamic tests which were greater or less than the pressure ratios required for prototype plume simulation.

Calibration testing of the model nozzles for the IA12C experimental program was conducted in the Rocketdyne Rocket Nozzle Test Facility after completion of the launch vehicle experimental program. Four calibration data points representative of the high, intermediate and low values of the chamber to ambient pressure ratios were selected for analysis. The test conditions for these data points are summarized in Table 5. A complete list of IA12C calibration data points is contained in Table 4 (test 73 through 90). The calibration test procedure and type of data obtained during the test were previously discussed in Sections 2.1.3 and 2.1.4, respectively.

The calibration test conditions (chamber pressures and ambient cell pressures) were input along with the IA12C model nozzle geometry into a method-of-characteristics computer code (Ref. 2). Nozzle and exhaust plume flow fields were subsequently defined for each of the four calibration test conditions selected for analysis. Experimental and predicted nozzle wall static pressure distributions are compared in Figs. 16, 18, 20 and 22 for calibration tests 81, 83, 88 and 90, respectively. Good agreement was obtained between experimental and predicted data.

Experimental and predicted plume boundary and boundary shock data are compared in Figs. 17, 19, 21 and 23 for the four calibration tests being analyzed. Good agreement was obtained between the experimental and predicted data at

each test point. It was therefore concluded that the IA12C model nozzles performed as expected. However, plume simulation conditions (i.e., pressure ratios) required for matching the prototype exhaust plume shapes the IA12C trajectory conditions were not obtained during the calibration test. To achieve the required pressure ratios during the IA12C test the model nozzles were operated at chamber pressures of about 1500 psia. The use of the high chamber pressures aggravates the problem of liquefaction of the constituents of the air in the nozzle flows. Thus, even if liquefaction effects were not noted during the calibration testing, such effects may have influenced the plume boundary shapes during the aerodynamic test series. Data from the calibration series are not adequate to assess this problem.

2.4 IA36

The SRM prototype baseline characteristics for the IA36 test series are given in Table 1b. This information together with the trajectory data for free-stream Mach numbers of 0.9 and 1.25 were utilized to compute the prototype plume shapes presented in Fig. 1. Model nozzle geometry for use in matching the prototype plume shapes was defined using the simulation process discussed in Section 2.1. A 0.019-scale model of the prototype nozzle was used as the simulant nozzle for this test series. Pertinent dimensions of this nozzle are given in Fig. 2b. The exhaust plume boundary shapes predicted for the prototype and simulant systems at the specified trajectory conditions are presented in Figs. 24 and 25. The operating pressure ratios (chamber pressure to ambient pressure) required to obtain the matching of the prototype plume boundaries are given in Table 3. As shown in Figs. 24 and 25, good agreement between the predicted simulant and prototype plume boundaries was obtained. Also presented in Figs. 24 and 25 are predicted plume boundaries for pressure ratios run during the IA36 aerodynamic tests which were greater than the pressure ratios required for prototype plume simulation.

Calibration testing of these nozzles was also conducted in the Rocketdyne Rocket Nozzle Test Facility. The testing procedure and the data acquired during the tests were previously discussed in Sections 2.1.3 and 2.1.4. Four calibration

test points were selected from the list of calibration test conditions (tests 51 through 72, Table 4) for analysis. These points, summarized in Table 5, were selected to sample the complete range of pressure ratios tested during the nozzle calibration.

Experimental values of nondimensionalized nozzle wall static pressures are compared with the predicted wall static pressure distribution in Figs. 26, 28, 30 and 32 for calibration tests 55, 57, 72 and 73, respectively. As can be seen from these curves, good agreement was obtained between experimental and analytical results for each of the calibration test points.

Exhaust plume boundary and boundary shock shapes from experimental and predicted data are compared in Figs. 27, 29, 31 and 33. The agreement indicated by these data was generally good. Some difference in the experimental and predicted shock locations was noted; however, these differences were considered to be acceptable.

Based on the results of the calibration data analysis, it was concluded that the nozzles designed for exhaust plume simulation during the IA36 test series performed as was expected.

Section 3

GENERAL CONCLUSIONS AND RECOMMENDATIONS

The following general conclusions were reached during the course of this study.

- The nozzle used in the IA12B calibration test did not perform as expected. It is suspected that the performance difference resulted from a deviation of the nozzle geometry from design baseline. Model inspection data was not available to substantiate this, however. The effect on the plume simulation at the required pressure ratios was considered to be slight.
- The nozzles used in the IA12C calibration tests performed as expected.
- The nozzles used in the IA36 calibration tests performed as expected.
- Use of schlieren photographs in the evaluation of the calibration data taken for a plume expanding to ambient conditions provides a good assessment of plume boundary shock location. However, due to the relatively large width of the viscous mixing zone, a certain amount of interpretation is required to ascertain an equivalent location of the inviscid plume boundary. Since the method used to interpret the optical data directly influences various aspects of the study results, additional effort has been undertaken to better define the mixing region at the plume boundary. The results of this additional effort will be reported on in a future document.
- The use of dry unheated air as the simulant gas in the nozzle calibration and launch vehicle tests can result in the liquefaction of the constituents of the air (nitrogen and oxygen) in the exhaust plumes. Techniques for predicting the onset of the liquefaction and its effect on the plume boundary shape are not available for use in readily assessing these effects for the test program. However, examination of vapor pressure data and Mollier curves for equilibrium air and oxygen indicate that conditions suitable for liquefaction to occur do exist in the exhaust plumes. It is also evident that the chamber pressure used in the launch vehicle test (higher by a factor of three over the calibration test chamber pressures) will aggravate the liquefaction problem.

- To prevent the introduction of "unknowns" into the plume simulation problem, it is therefore recommended that future nozzle calibration tests be conducted with nozzle supply pressures equal to that which will be used during the testing. It is also recommended that provisions for heating the air be provided so that the liquefaction problem can be eliminated.
- The experimental calibration data utilized in this study were obtained with one nozzle of each pair provided for the IA12B, IA12C and IA36 launch vehicle tests. A cursory dimensional inspection was made for both nozzles in each pair to determine if the nozzles were geometrically matched. A decision to test only one nozzle in each pair was made based on the inspection results. Although this approach is probably adequate it is recommended that both nozzles to be used in simulating the SRM plumes be calibrated prior to future launch vehicle aerodynamic tests.

Section 4
REFERENCES

1. Gordon, S., and Bonnie J. McBride, "Computer Program for Calculation of Complex Chemical Equilibrium Compositions, Rocket Performance, Incident and Reflected Shocks, and Chapman-Jouquet Detonations," NASA-SP-273, NASA-Lewis Research Center, Cleveland, Ohio, 1971.
2. Prozan, R.J., "Development of a Method of Characteristics Solution for the Supersonic Flow of an Ideal, Frozen or Equilibrium Reacting Gas/Mixture," LMSC-HREC D16220-III, Lockheed Missiles & Space Company, Huntsville, Ala., May 1970.
3. Pindzola, M., "Jet Simulation in Ground Test Facilities," AGARDograph 79, North Atlantic Treaty Organization Advisory Group for Aeronautical Research and Development, November 1963.
4. Baker, L.R., M.M. Penny and R.W. McCanna, "Design and Calibration of Model Nozzles for Use in Gasdynamic Simulation of the Space Shuttle Propulsion System Exhaust Plumes," LMSC-HREC TR D306555, Lockheed Missiles & Space Company, Huntsville, Ala., April 1973.
5. Hoenig, R.J., "Boundary Layer Computer Program Users Manual," LMSC-HREC A782404, Lockheed Missiles & Space Company, Huntsville, Ala., August 1966.

Table 1
SPACE SHUTTLE SOLID ROCKET BOOSTER CHARACTERISTICS

A. Prototype SRM Characteristics for IA12B

Nozzle Characteristics

$$A/A^* = 11$$

$$D_e = 88.05 \text{ in}$$

Contoured Bell

$$\theta_{\text{lip}} = 11 \text{ deg}$$

Propellant - PBAN/(16 - 18% Al)

Chamber conditions: P_c variable along trajectory

B. Prototype SRM Characteristics for IA12C and IA36

Nozzle Characteristics

$$A/A^* = 7$$

$$D_e = 141.7 \text{ in.}$$

Contoured Bell

$$\theta_{\text{lip}} = 11 \text{ deg}$$

Propellant - PBAN/(16 - 18% Al)

Chamber conditions: P_c variable along trajectory

Table 2
 SPACE SHUTTLE TRAJECTORY CONDITIONS UNDER
 INVESTIGATION FOR THE IA12B AERODYNAMICS TESTS

| Mach Number | Altitude (ft) | Ambient Pressure (psfa) |
|-------------|------------------|----------------------------|
| 1.55 | 42,075 | 387.7 |
| 2.00 | 56,304 | 201.1 |

Table 3
 SRM MODEL NOZZLE OPERATING CONDITIONS NECESSARY
 FOR SIMULATION OF PROTOTYPE PLUME DEFINITIONS

| Test Series | Trajectory Mach No. Being Simulated | Model Nozzle Pressure Ratio Required for Simulation (P_c/P_a) |
|-------------|--|--|
| IA36 | 0.90 | 115.0 |
| | 1.25 | 200.0 |
| IA12B | 1.55 | 284.7 |
| | 2.00 | 670.61 |
| IA12C | 2.50 | 1490.0 |
| | 3.00 | 2686.0 |
| | 3.50 | 6000.0 |

Table 4
 MODEL NOZZLE CALIBRATION TEST CONDITIONS FOR IA12B, IA12C, IA36

| | Test Number | Model Nozzle Chamber Pressure (psia) | Test Cell Ambient Pressure (psia) |
|-------|-------------|--------------------------------------|-----------------------------------|
| IA12B | 41 | 548.563 | 1.947 |
| | 42 | 549.070 | 0.871 |
| | 43 | 549.196 | 0.816 |
| | 44 | 549.906 | 0.530 |
| | 45 | 550.110 | 0.503 |
| | 46 | 547.234 | 0.350 |
| | 48 | 547.297 | 0.723 |
| | 49 | 546.196 | 0.339 |
| | 50 | 546.196 | 0.640 |
| | IA36 | 51 | 548.737 |
| 52 | | 548.830 | 2.165 |
| 53 | | 548.356 | 1.466 |
| 54 | | 549.842 | 1.110 |
| 55 | | 549.345 | 0.797 |
| 57 | | 548.921 | 0.319 |
| 58 | | 549.261 | 0.775 |
| 59 | | 550.123 | 1.133 |
| 60 | | 551.489 | 1.466 |
| 61 | | 550.424 | 2.181 |
| 62 | | 551.150 | 0.681 |
| 63 | | 551.407 | 0.776 |
| 64 | | 551.616 | 2.791 |
| 65 | | 551.658 | 0.680 |
| IA12C | 66 | 548.815 | 2.049 |
| | 67 | 549.445 | 4.235 |
| | 68 | 549.936 | 0.307 |
| | 71 | 547.516 | 0.703 |
| | 72 | 548.701 | 2.074 |
| | 73 | 548.629 | 4.265 |
| | 74 | 548.492 | 0.360 |
| | 76 | | |
| | 77 | 250.143 | 0.790 |
| | 81 | 254.504 | 0.198 |
| | 82 | 252.083 | 0.325 |
| | 83 | 514.856 | 0.722 |
| | 84 | 516.182 | 0.769 |
| | 85 | 516.724 | 0.322 |
| 86 | 516.928 | 0.342 | |
| 87 | 515.736 | 0.343 | |
| 88 | 515.474 | 0.290 | |
| 89 | 513.104 | 0.362 | |
| 90 | 508.204 | 0.825 | |

ORIGINAL PAGE IS
 OF POOR QUALITY

Table 5
 MODEL NOZZLE CALIBRATION TEST CONDITIONS
 SELECTED FOR ANALYSIS

| Test Series | Test Number | Pressure Ratio (Chamber Pressure/Ambient Pressure) |
|-------------|-------------|--|
| IA12B | 41 | 281.72 |
| | 45 | 1092.59 |
| | 48 | 756.92 |
| | 49 | 1610.70 |
| IA12C | 81 | 1288.21 |
| | 83 | 713.22 |
| | 88 | 1777.92 |
| | 90 | 615.86 |
| IA36 | 55 | 689.19 |
| | 57 | 1718.67 |
| | 72 | 264.59 |
| | 73 | 128.64 |

Table 6
 SPACE SHUTTLE TRAJECTORY CONDITIONS UNDER INVESTIGATION
 FOR THE IA12C AND IA36 AERODYNAMIC TESTS

| Mach Number | Altitude (ft) | Ambient Pressure (psfa) |
|-------------|---------------|-------------------------|
| 0.90 | 18,428 | 1084.7 |
| 1.25 | 32,160 | 607.9 |
| 2.50 | 69,590 | 96.85 |
| 3.00 | 83,464 | 50.13 |
| 3.50 | 97,152 | 26.86 |

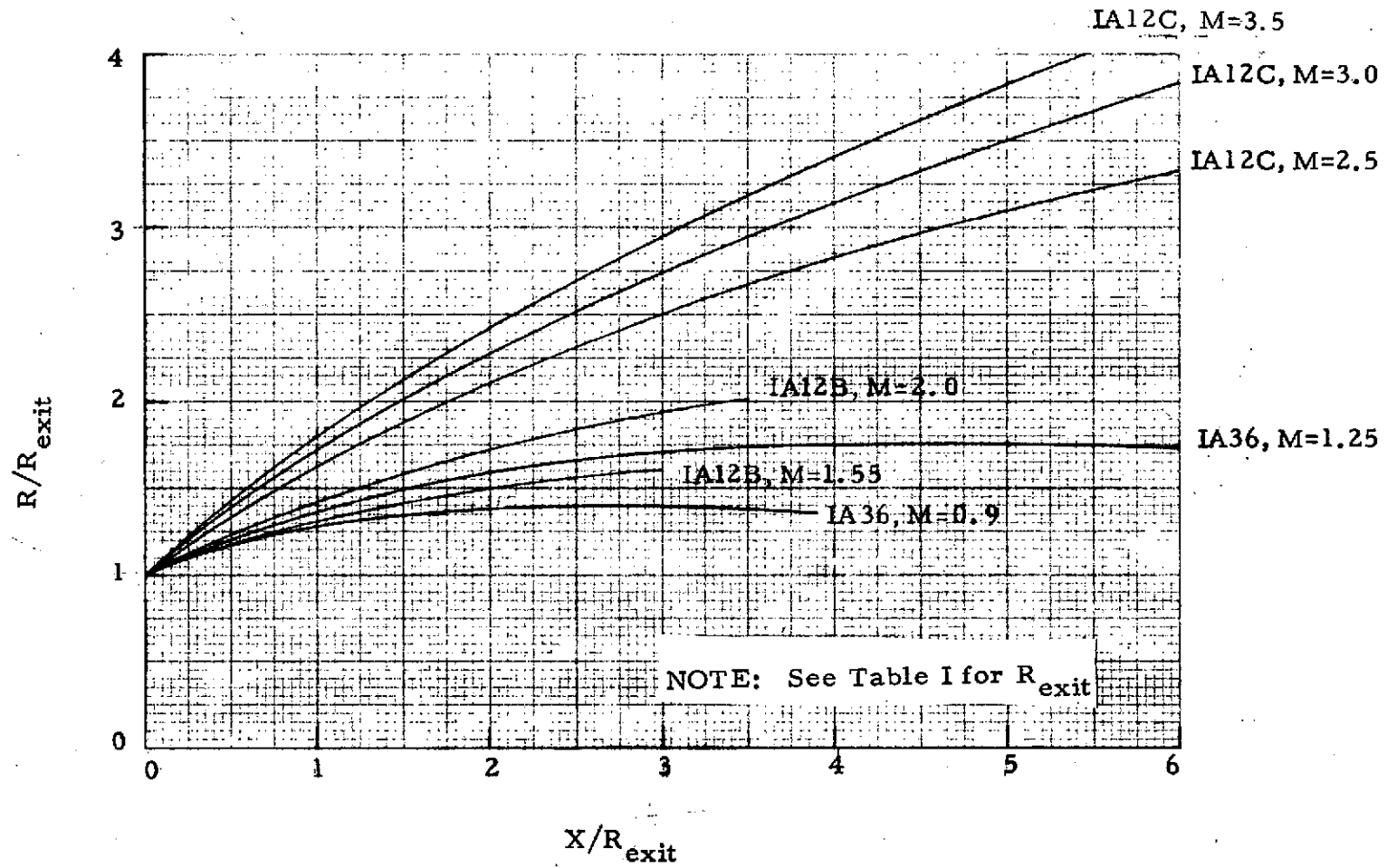
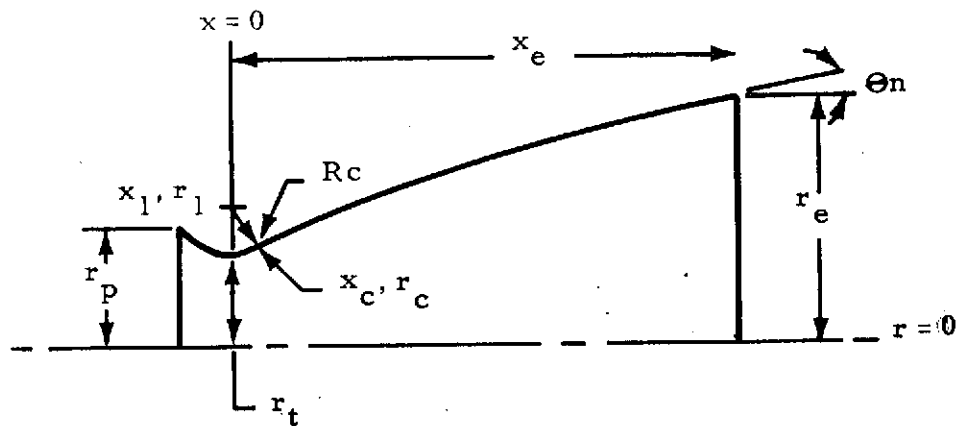


Fig. 1 - Space Shuttle Solid Rocket Motor Prototype Plume Boundaries



| Parameter | SRM Contoured Model Nozzle |
|------------------|----------------------------|
| r_t | 0.509 |
| r_e | 1.3467 |
| θ_n (deg) | 11 |
| R_c | 0.3027 |
| x_c | 0.1134 |
| r_c | 0.5265 |
| x_1 | 0.0 |
| r_1 | 0.8097 |
| R_{cz} | — |
| x_z | — |
| r_z | — |
| r_p | 1.317 |
| x_e | 2.759 |

*Dimensions in inches

Fig. 2b - Space Shuttle Solid Rocket Motor Model Nozzle Geometry for the IA36 Launch Vehicle Test Series.

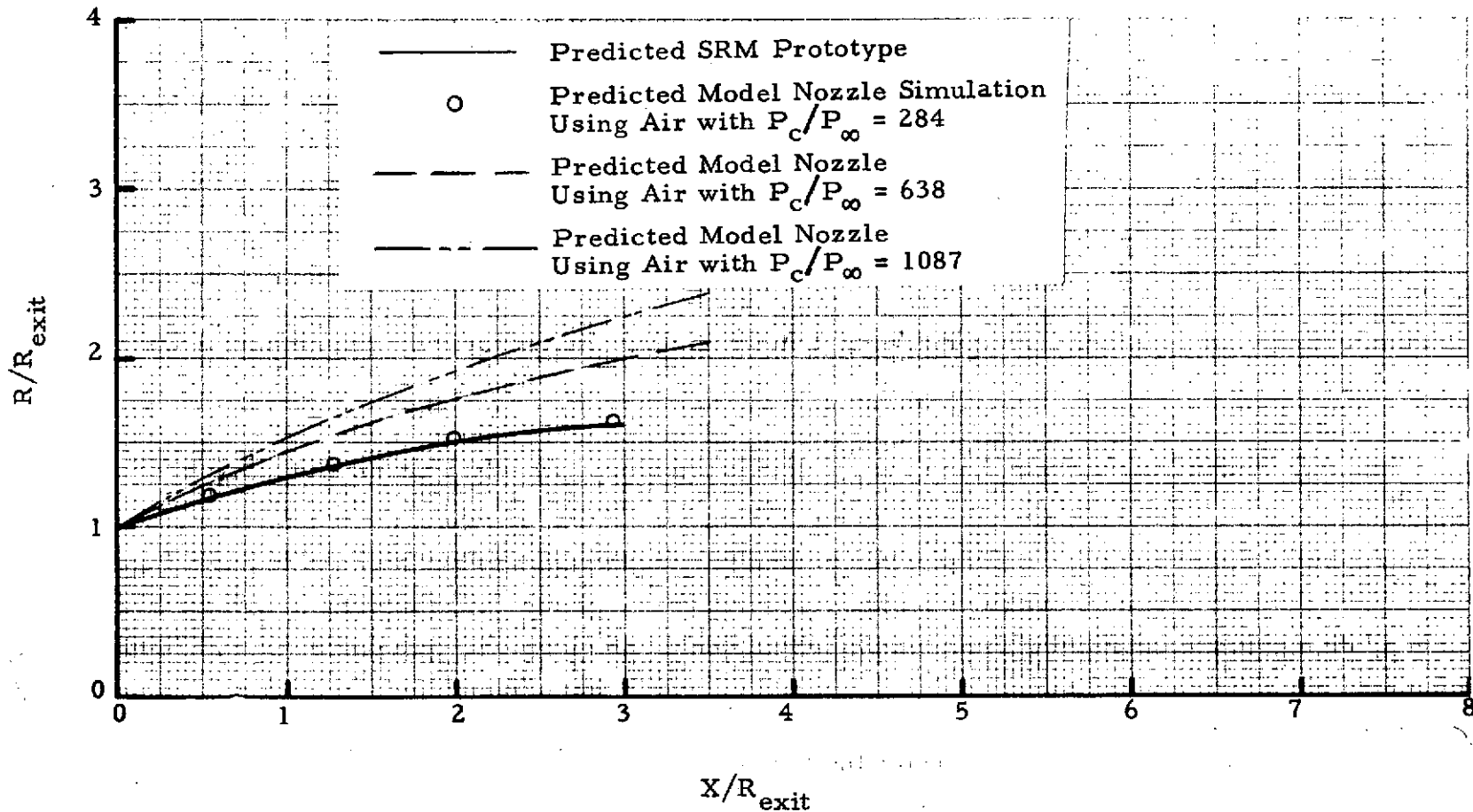


Fig. 3 - Comparison of the Space Shuttle SRM Prototype and Model Nozzle Plume Boundary Definition at Conditions Corresponding to a Trajectory Mach Number of 1.55

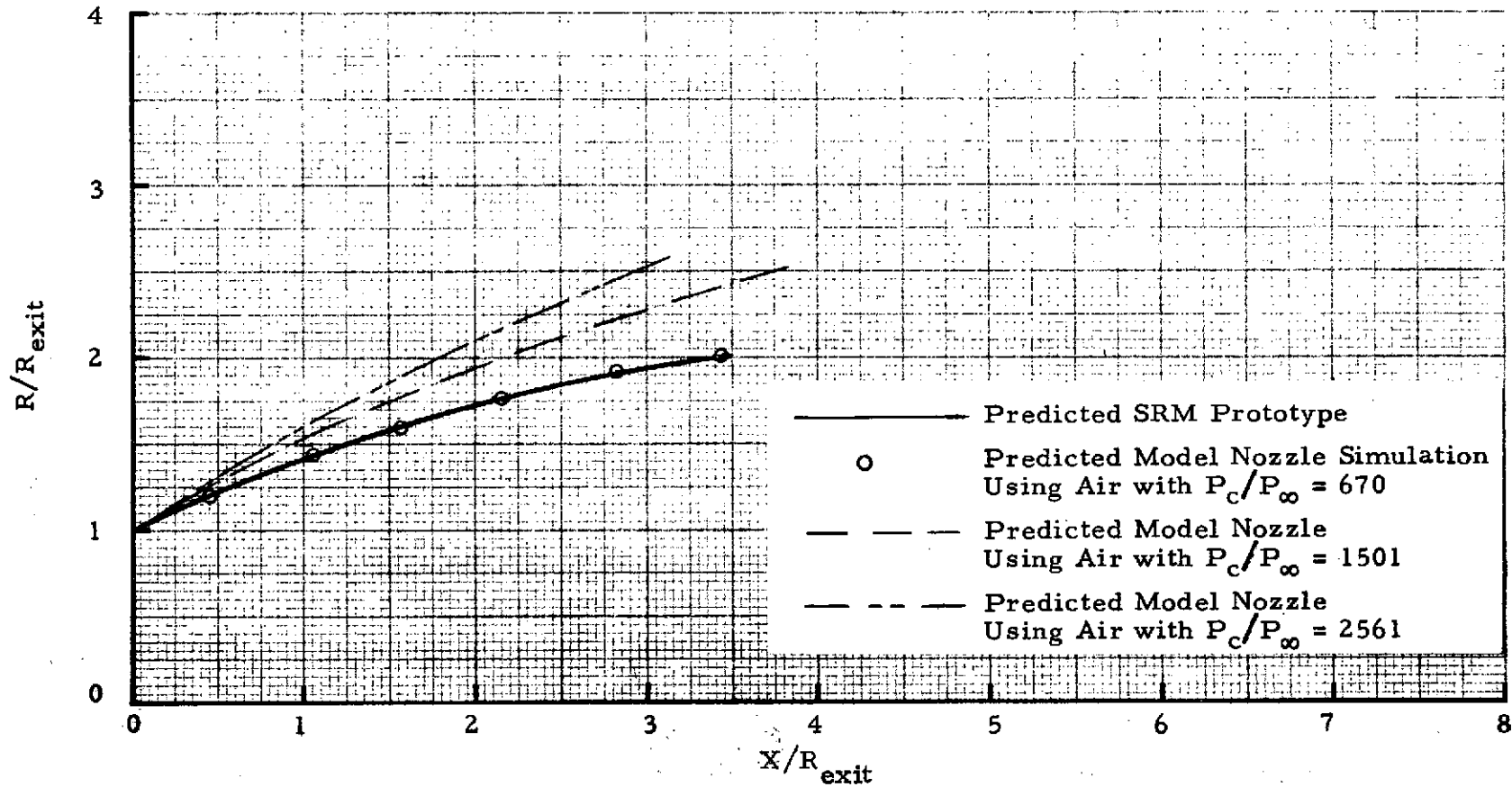


Fig. 4 - Comparison of the Space Shuttle SRM Prototype and Model Nozzle Plume Boundary Definition at Conditions Corresponding to a Trajectory Mach Number of 2.0

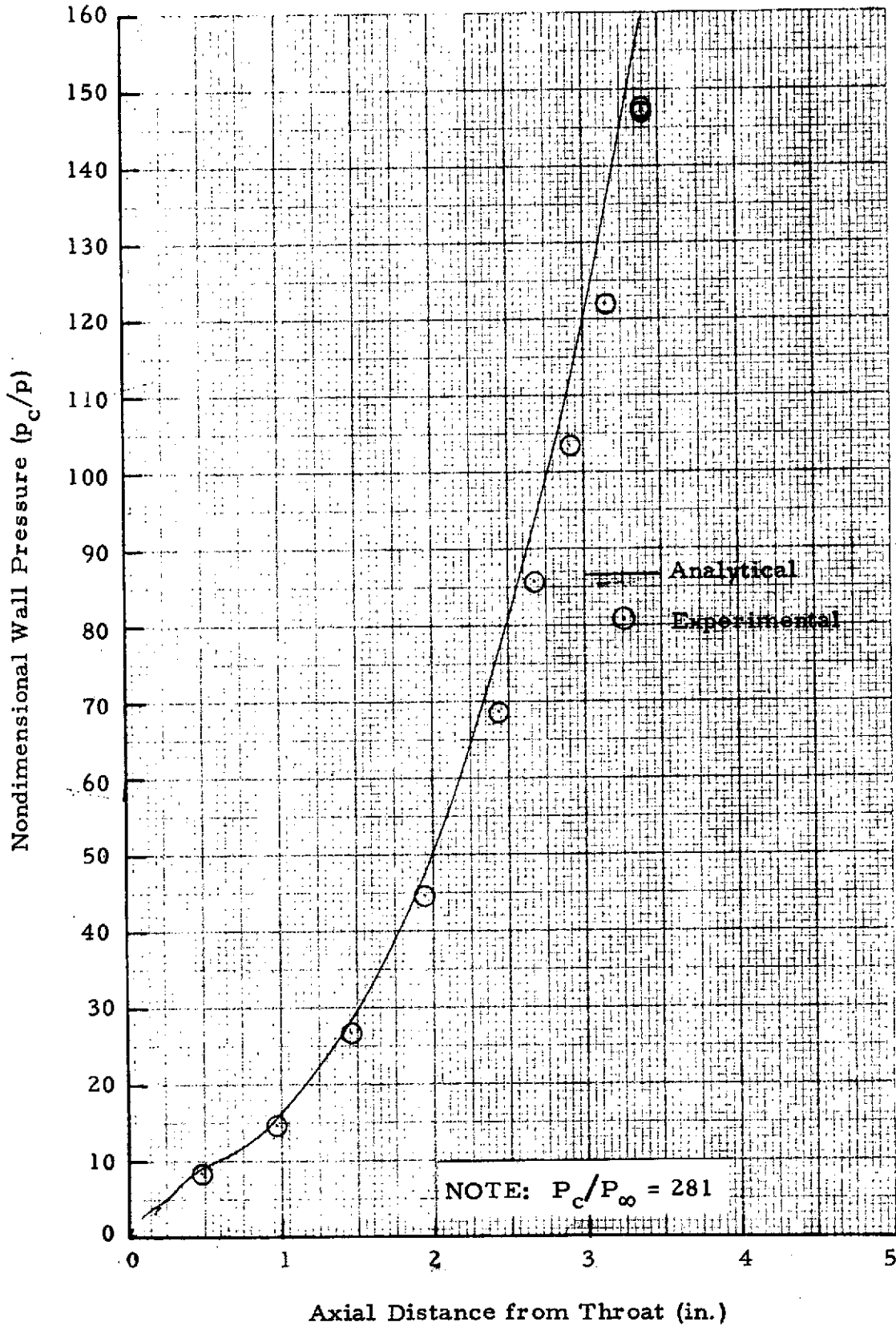


Fig. 5 - Comparison of Experimental and Predicted SRM Model Nozzle Nondimensional Wall Pressure at Conditions Corresponding to Model Nozzle Calibration Test 41

ORIGINAL PAGE IS
OF POOR QUALITY

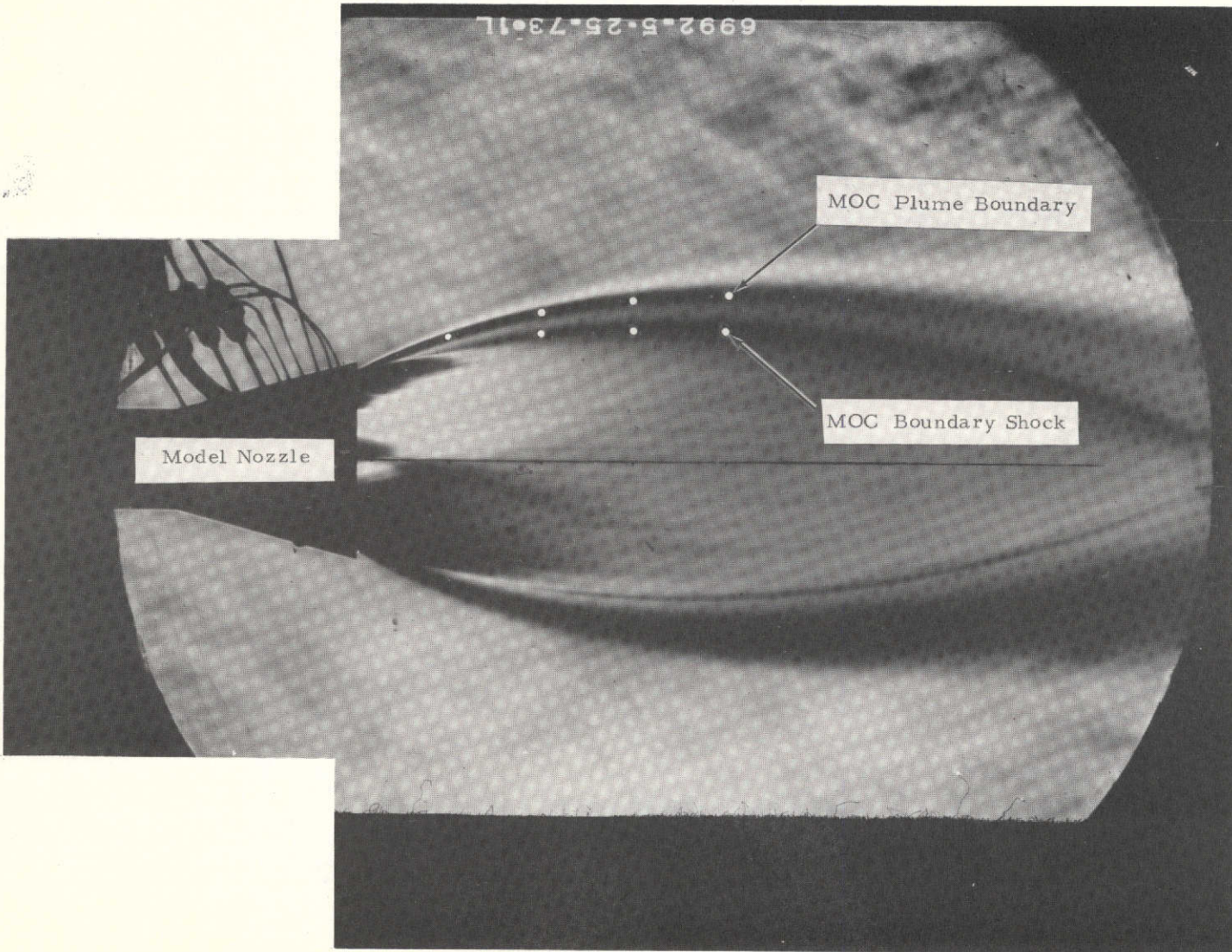


Fig. 6a - Comparison of Predicted SRM Model Nozzle Plume Boundary and Boundary Shock with Schlieren Data for the Model Nozzle Calibration Test Point 41

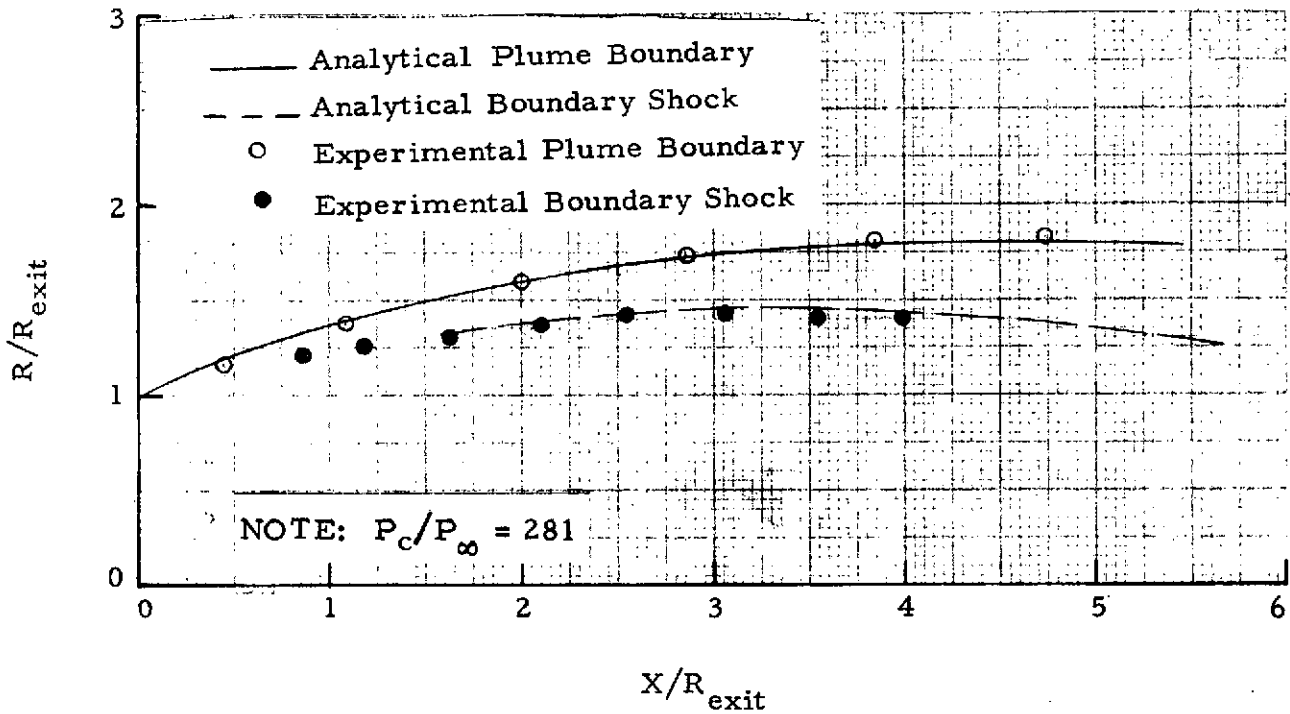


Fig. 6b - Comparison of Experimental and Predicted SRM Model Nozzle Plume Boundary and Boundary Shock Definitions at Conditions Corresponding to Model Nozzle Calibration Test 41

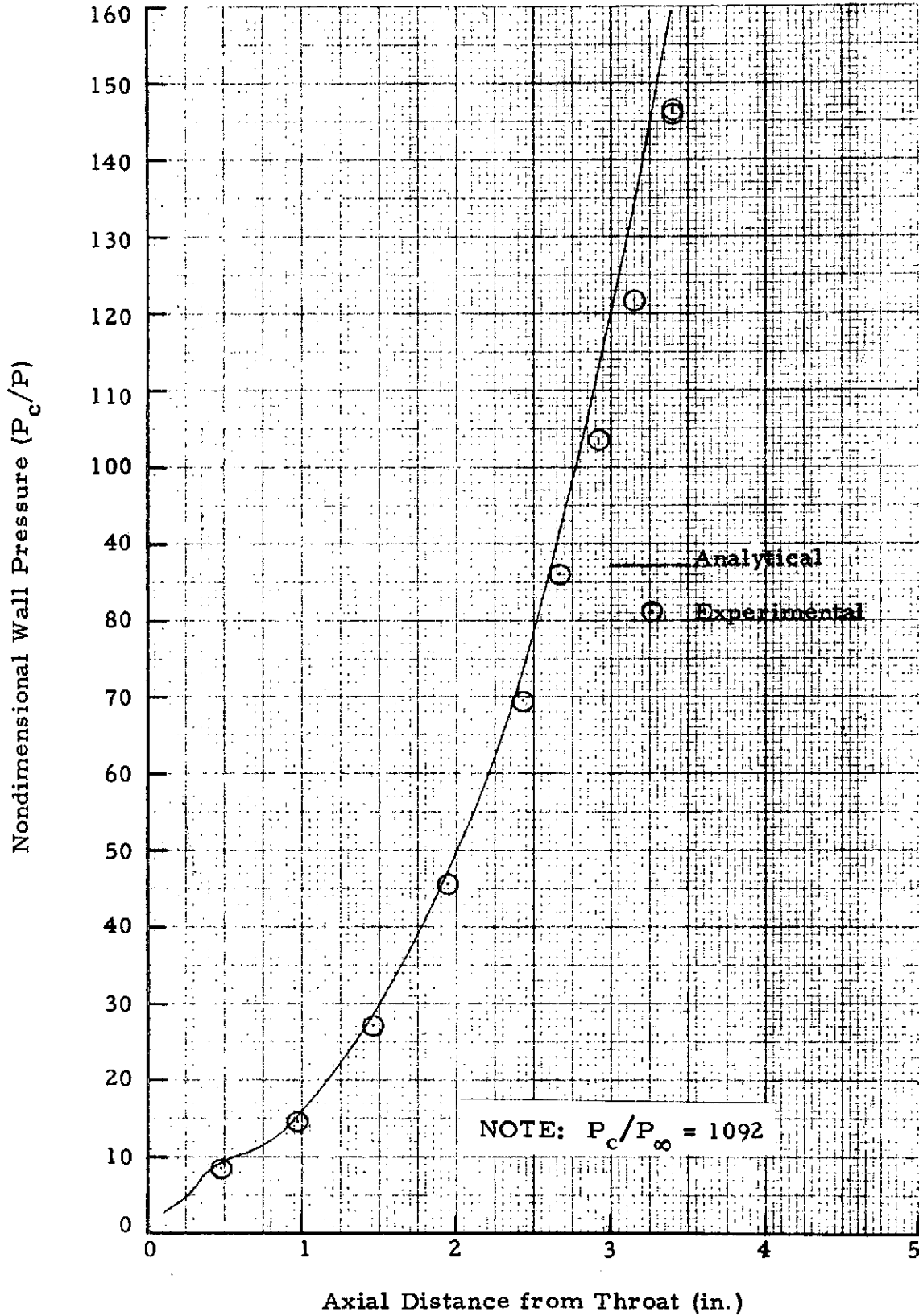


Fig. 7 - Comparison of Experimental and Predicted SRM Model Nozzle Nondimensional Wall Pressure at Conditions Corresponding to Model Nozzle Calibration Test 45

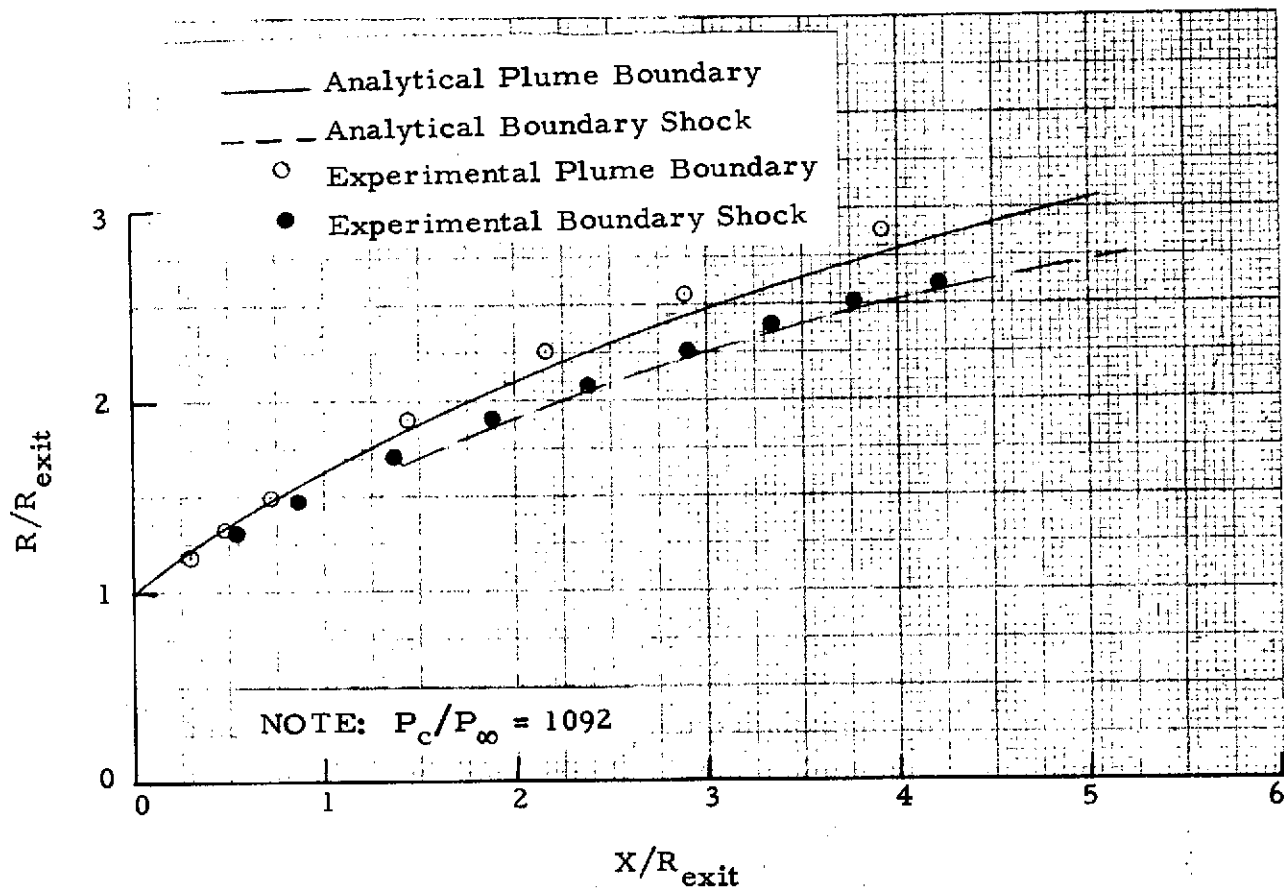


Fig. 8 - Comparison of Experimental and Predicted SRM Model Nozzle Plume Boundary and Boundary Shock Definitions at Conditions Corresponding to Model Nozzle Calibration Test 45

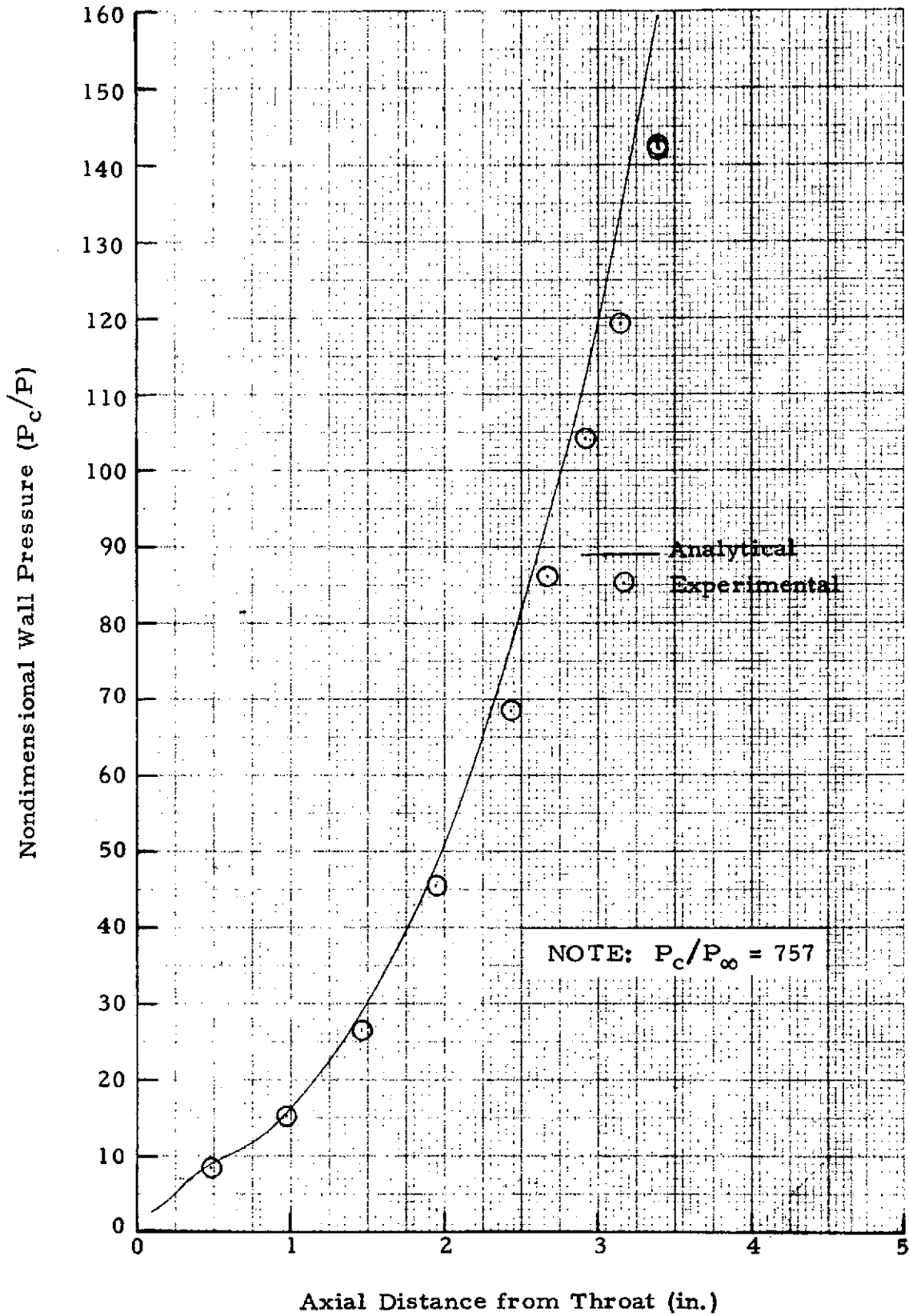


Fig. 9 - Comparison of Experimental and Predicted SRM Model Nozzle Nondimensional Wall Pressure at Conditions Corresponding to Model Nozzle Calibration Test 48

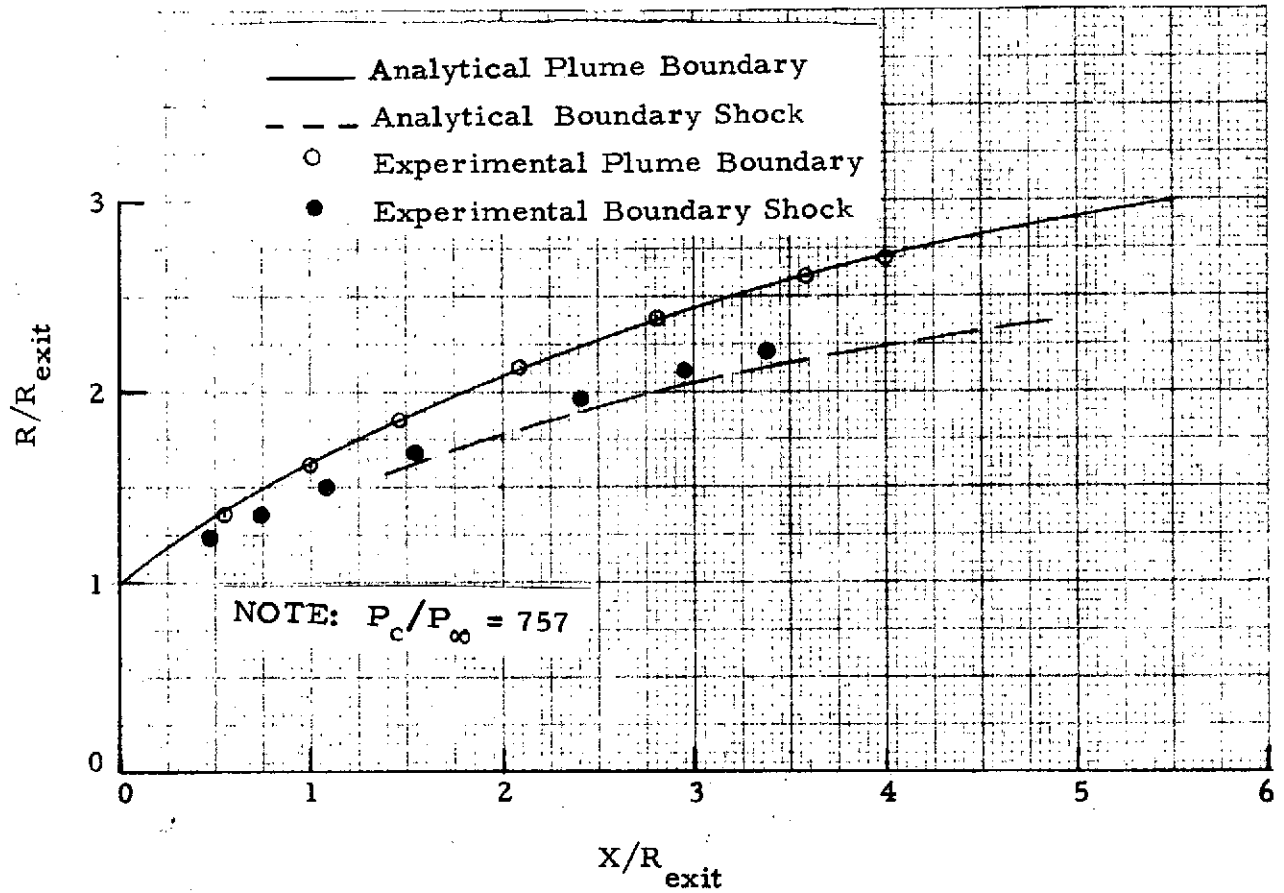


Fig. 10 - Comparison of Experimental and Predicted SRM Model Nozzle Plume Boundary and Boundary Shock Definitions at Conditions Corresponding to Model Nozzle Calibration Test 48

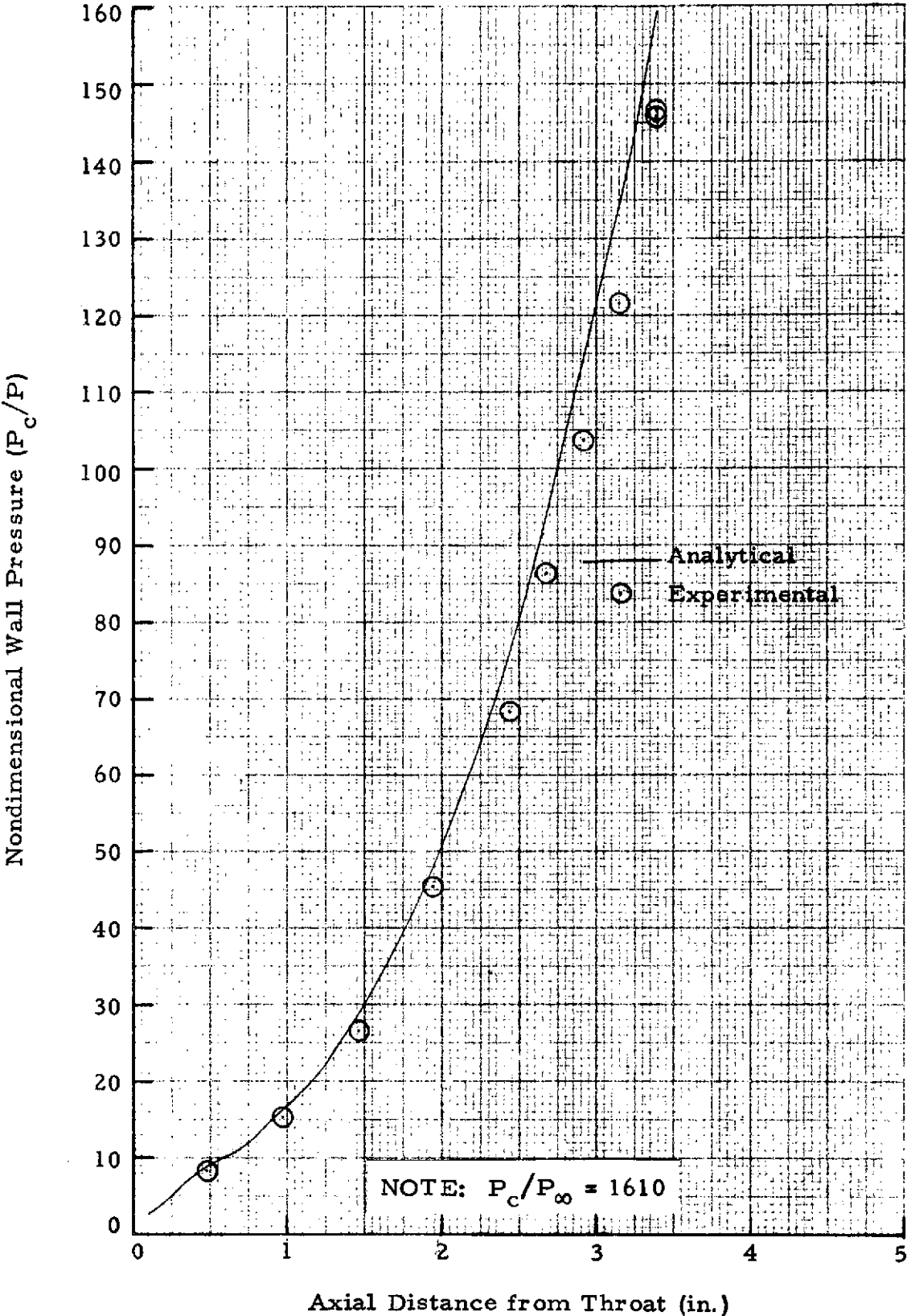


Fig. 11 - Comparison of Experimental and Predicted SRM Model Nozzle Nondimensional Wall Pressure at Conditions Corresponding to Model Nozzle Calibration Test 49

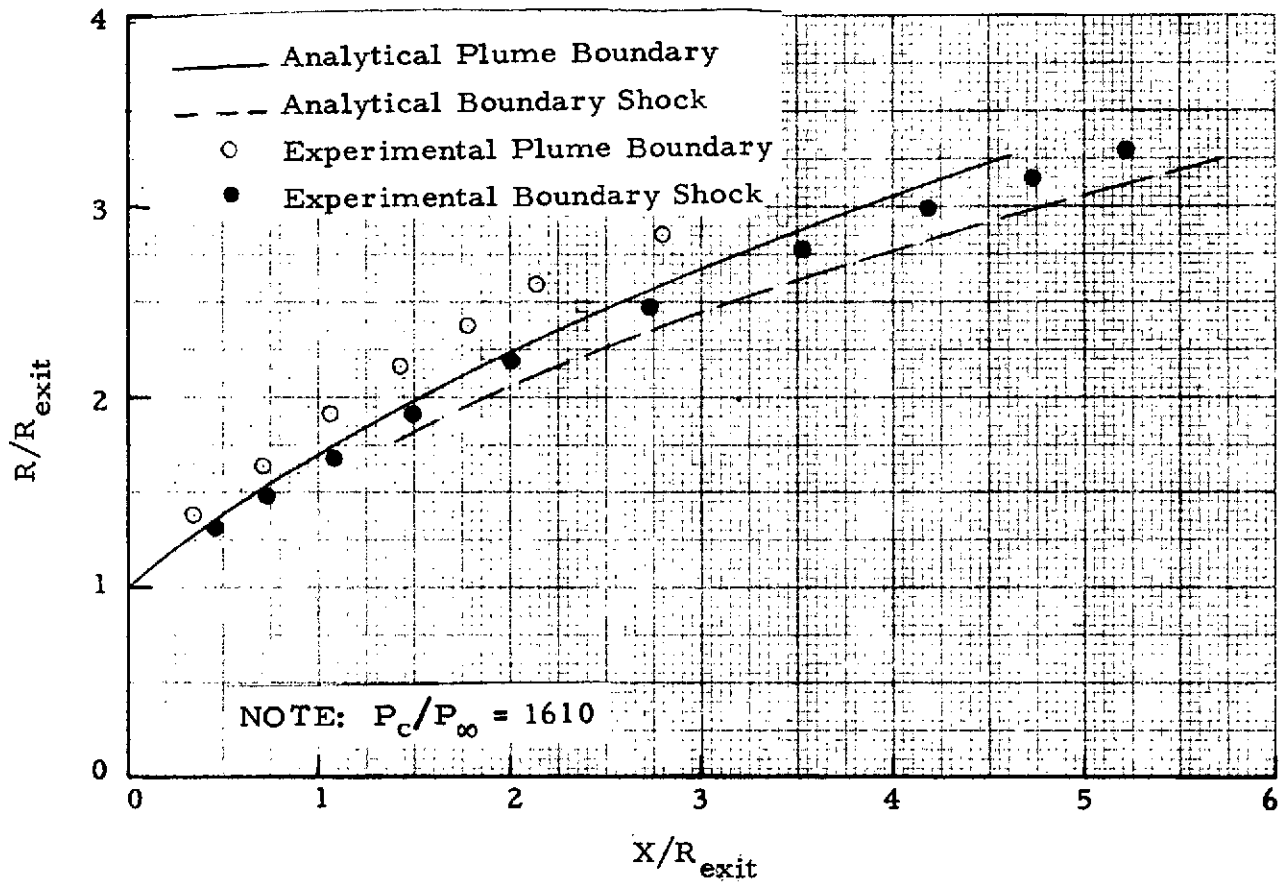


Fig. 12 - Comparison of Experimental and Predicted SRM Model Nozzle Plume Boundary and Boundary Shock Definitions at Conditions Corresponding to Model Nozzle Calibration Test 49

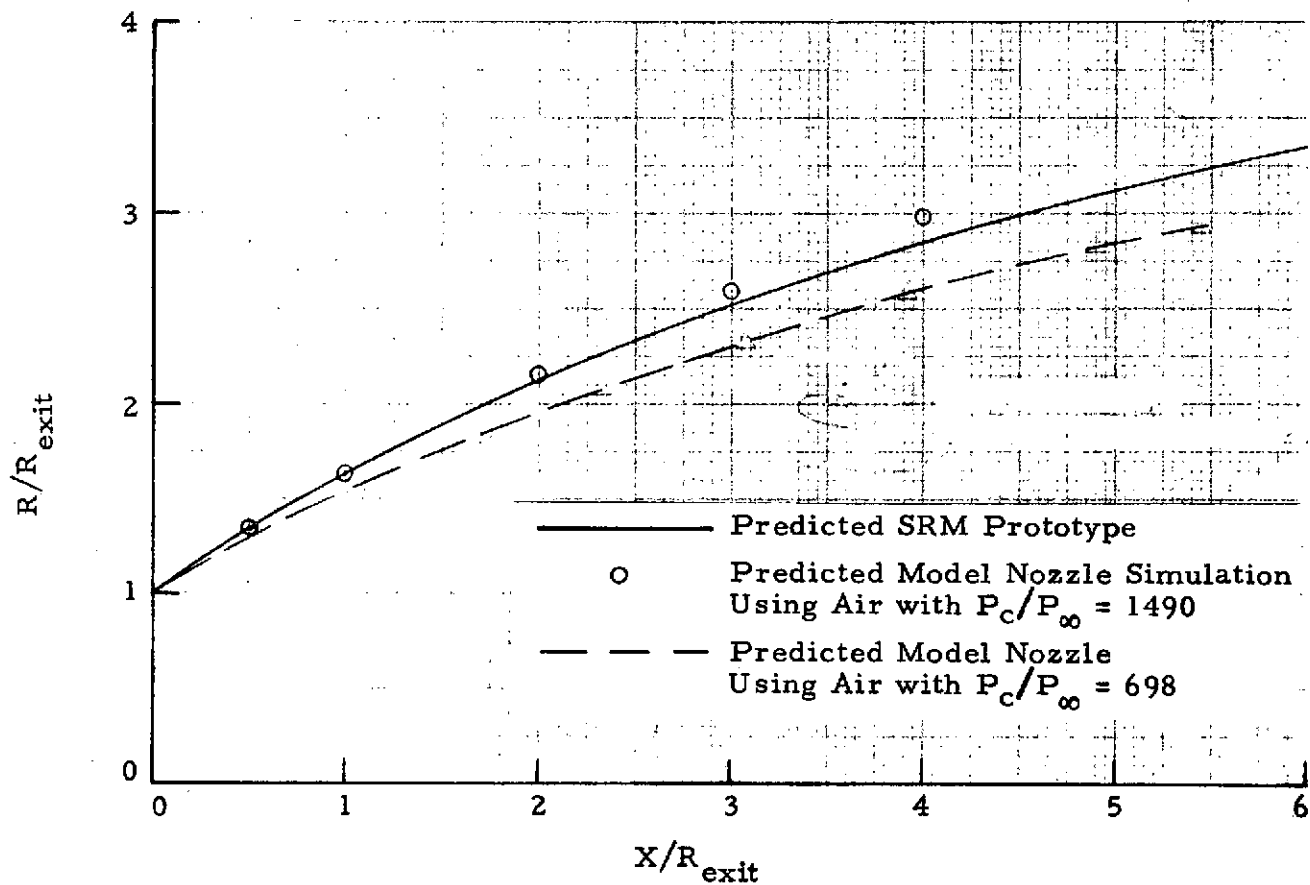


Fig. 13 - Comparison of the Space Shuttle SRM Prototype and Model Nozzle Plume Boundary Definition at Conditions Corresponding to a Trajectory Mach Number of 2.5

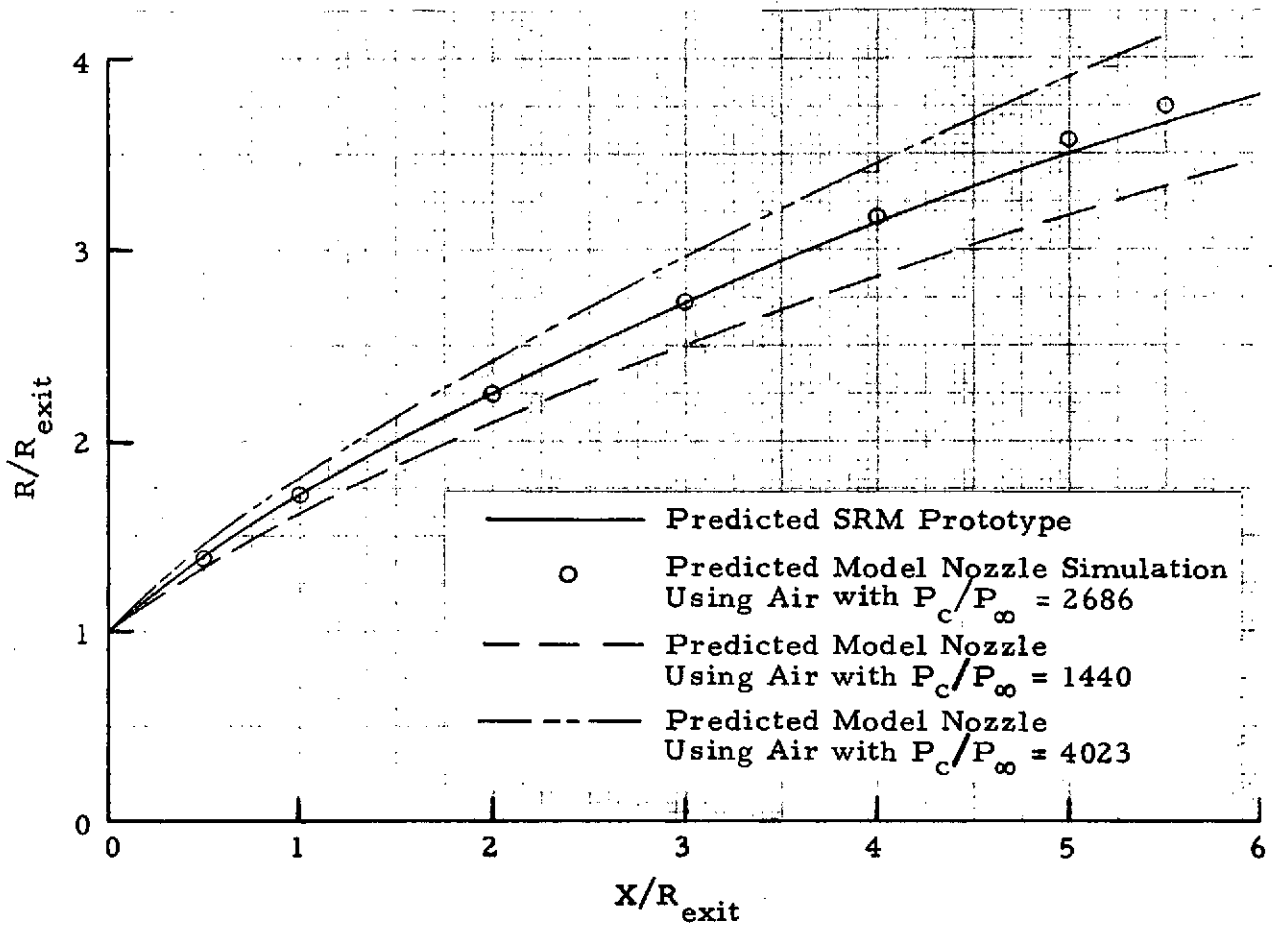


Fig. 14 - Comparison of the Space Shuttle SRM Prototype and Model Nozzle Plume Boundary Definition at Conditions Corresponding to a Trajectory Mach Number of 3.0

ORIGINAL PAGE IS
OF POOR QUALITY

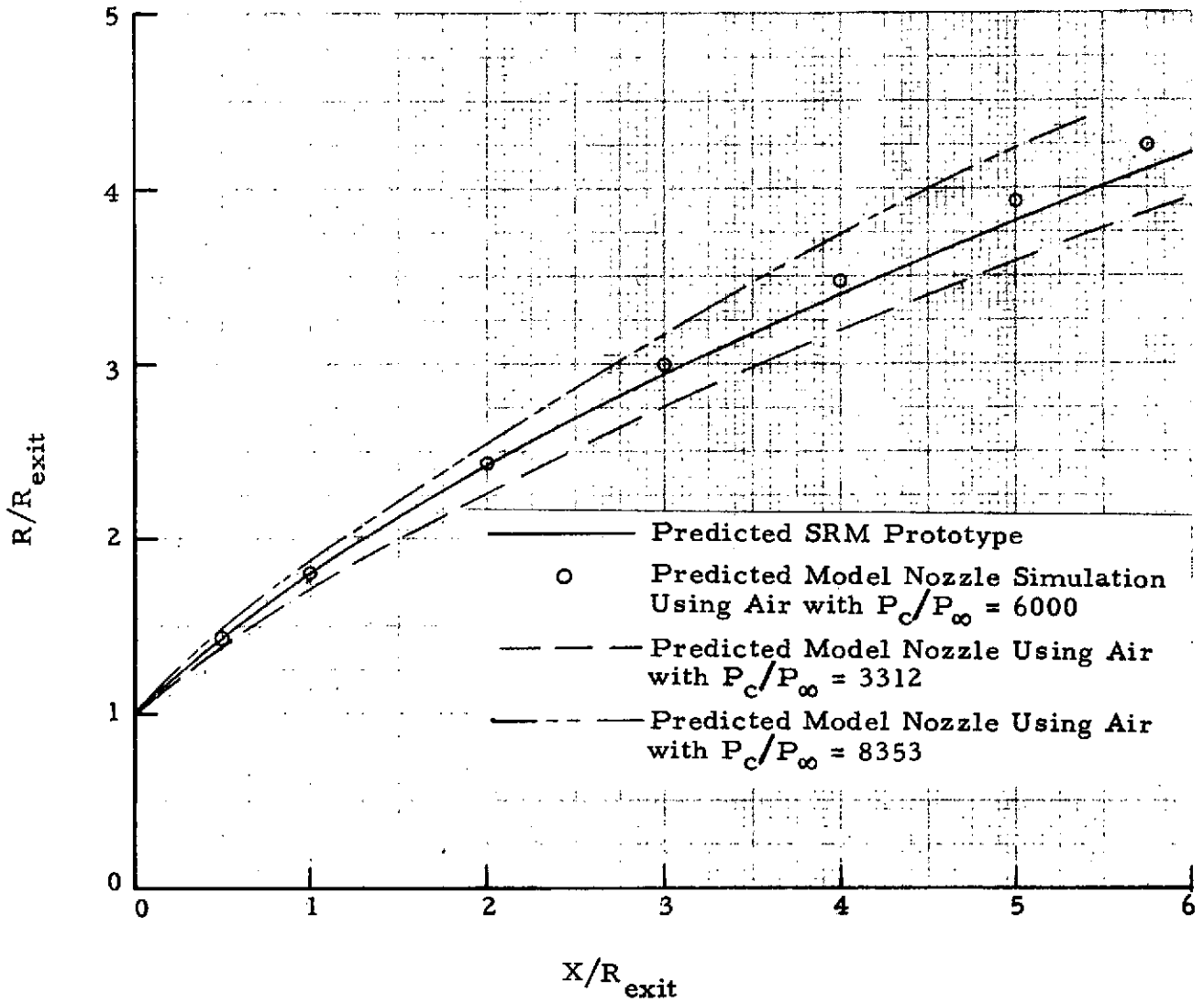


Fig. 15 - Comparison of the Space Shuttle SRM Prototype and Model Nozzle Plume Boundary Definition at Conditions Corresponding to a Trajectory Mach Number of 3.5

ORIGINAL PAGE IS
OF POOR QUALITY

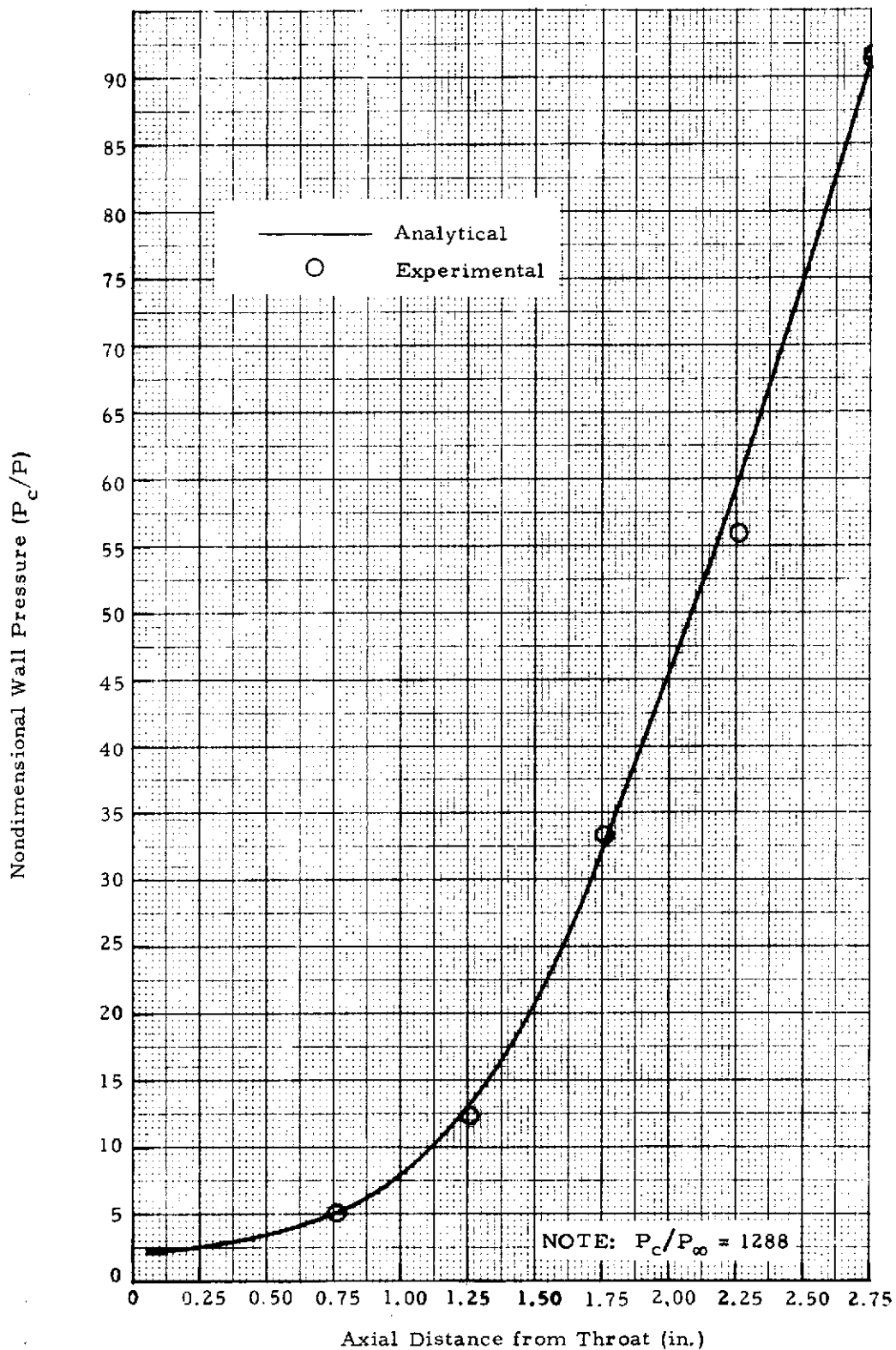


Fig. 16 - Comparison of Experimental and Predicted SRM Model Nozzle Nondimensional Wall Pressure at Conditions Corresponding to Model Nozzle Calibration Test 81

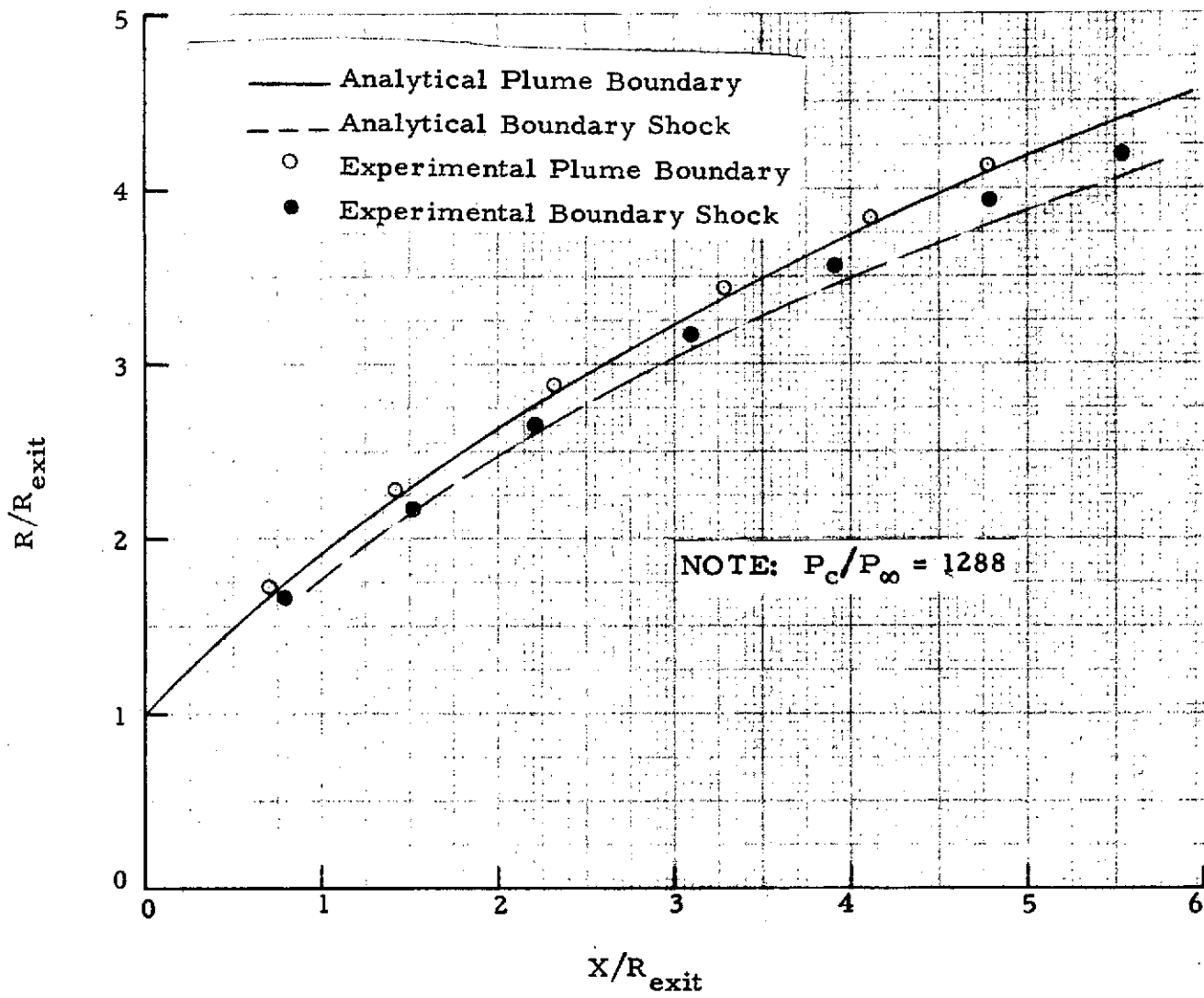


Fig. 17 - Comparison of Experimental and Predicted SRM Model Nozzle Plume Boundary and Boundary Shock Definitions at Conditions Corresponding to Model Nozzle Calibration Test 81

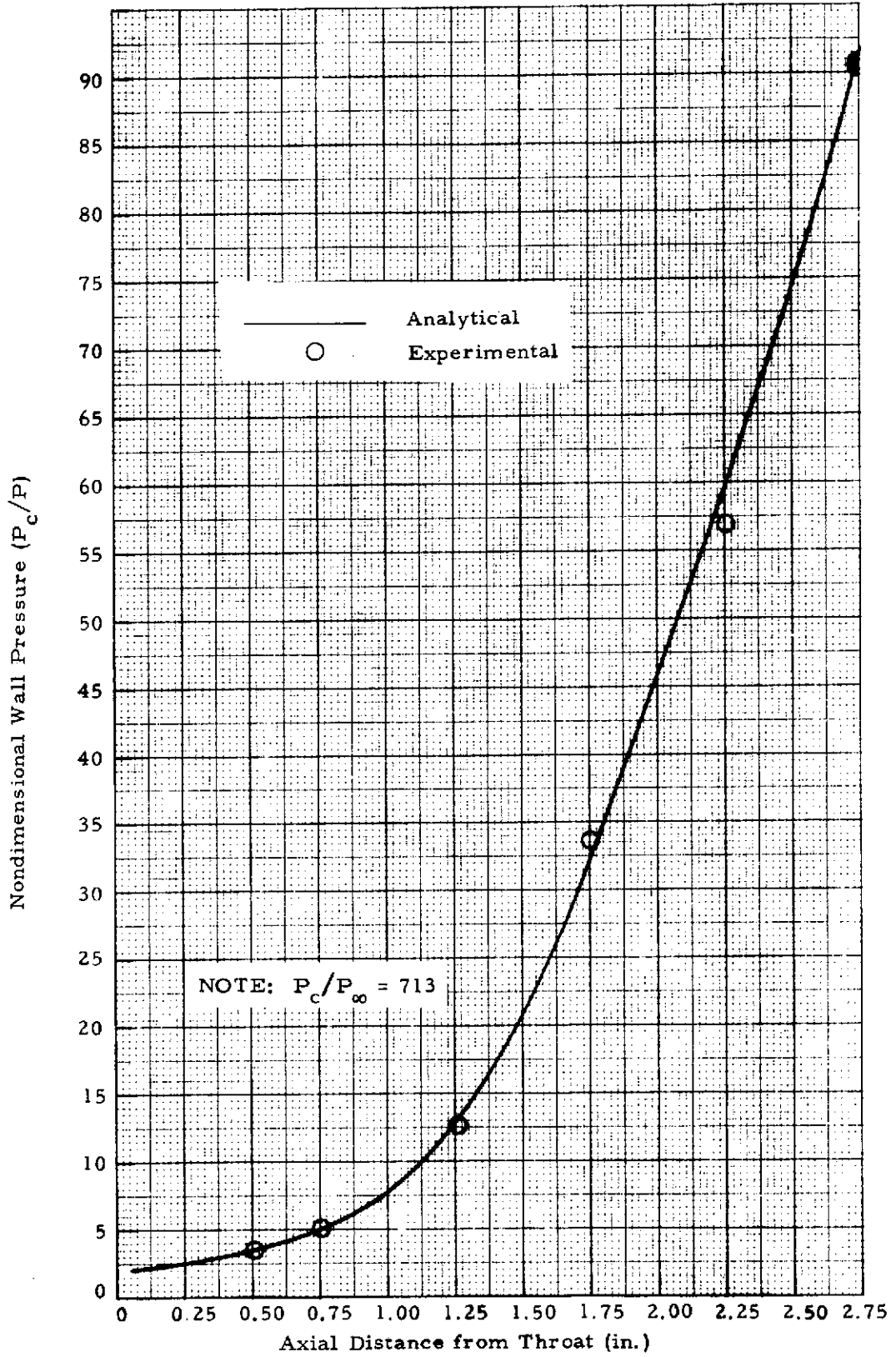


Fig. 18 - Comparison of Experimental and Predicted SRM Model Nozzle Nondimensional Wall Pressure at Conditions Corresponding to Model Nozzle Calibration Test 83

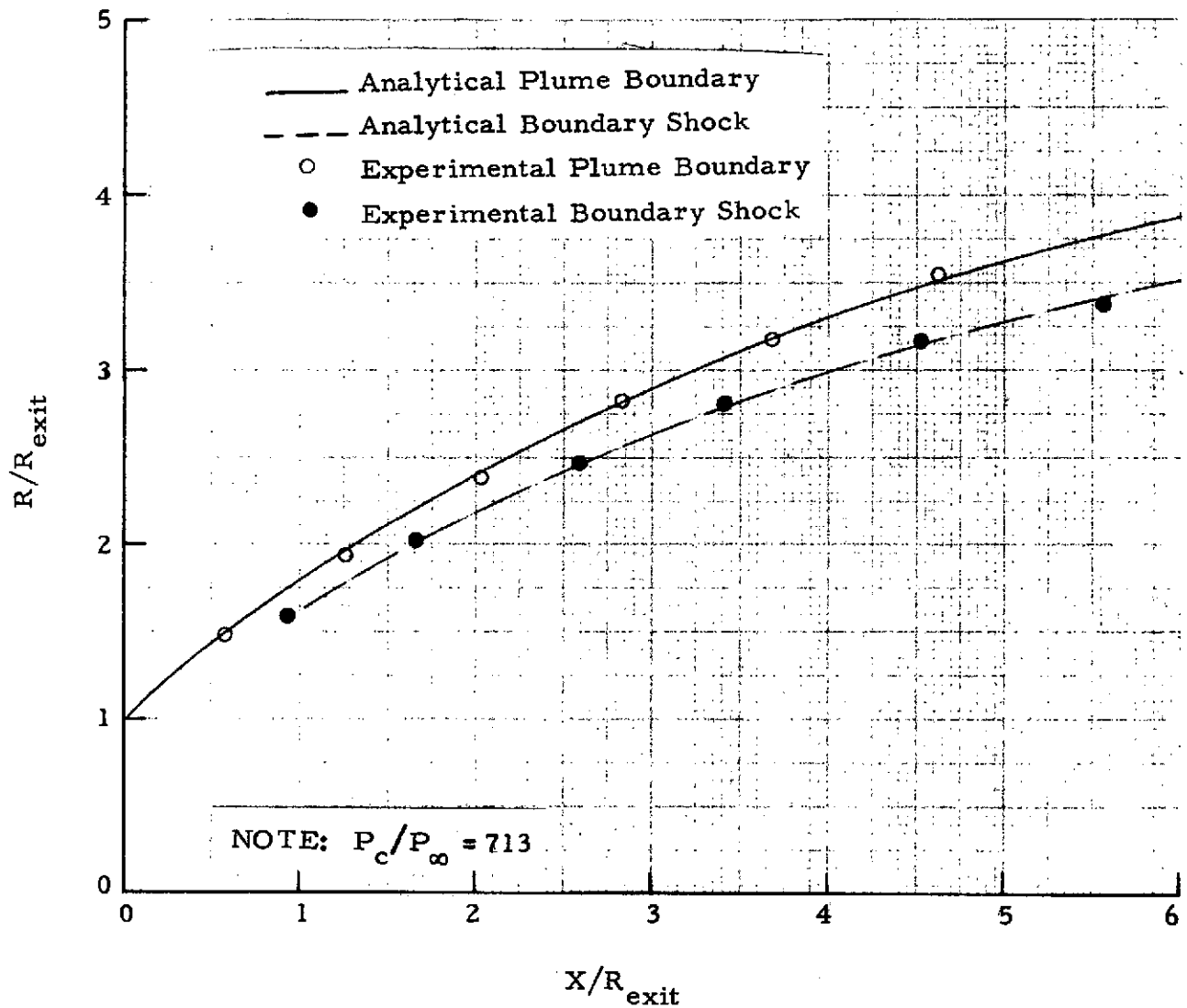


Fig. 19 - Comparison of Experimental and Predicted SRM Model Nozzle Plume Boundary and Boundary Shock Definitions at Conditions Corresponding to Model Nozzle Calibration Test 83

ORIGINAL PAGE IS
OF POOR QUALITY

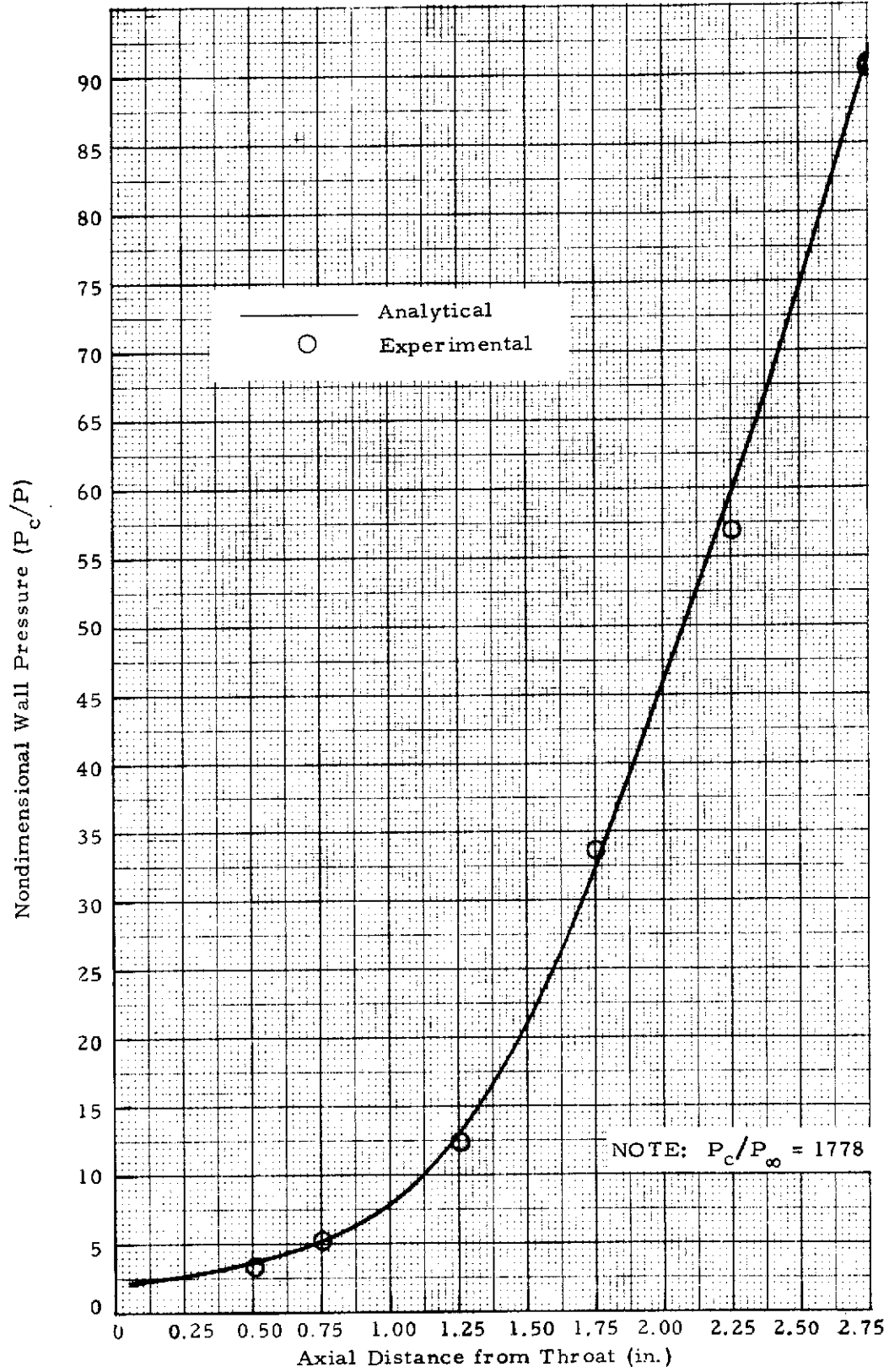


Fig. 20 - Comparison of Experimental and Predicted SRM Model Nozzle Nondimensional Wall Pressure at Conditions Corresponding to Model Nozzle Calibration Test 88

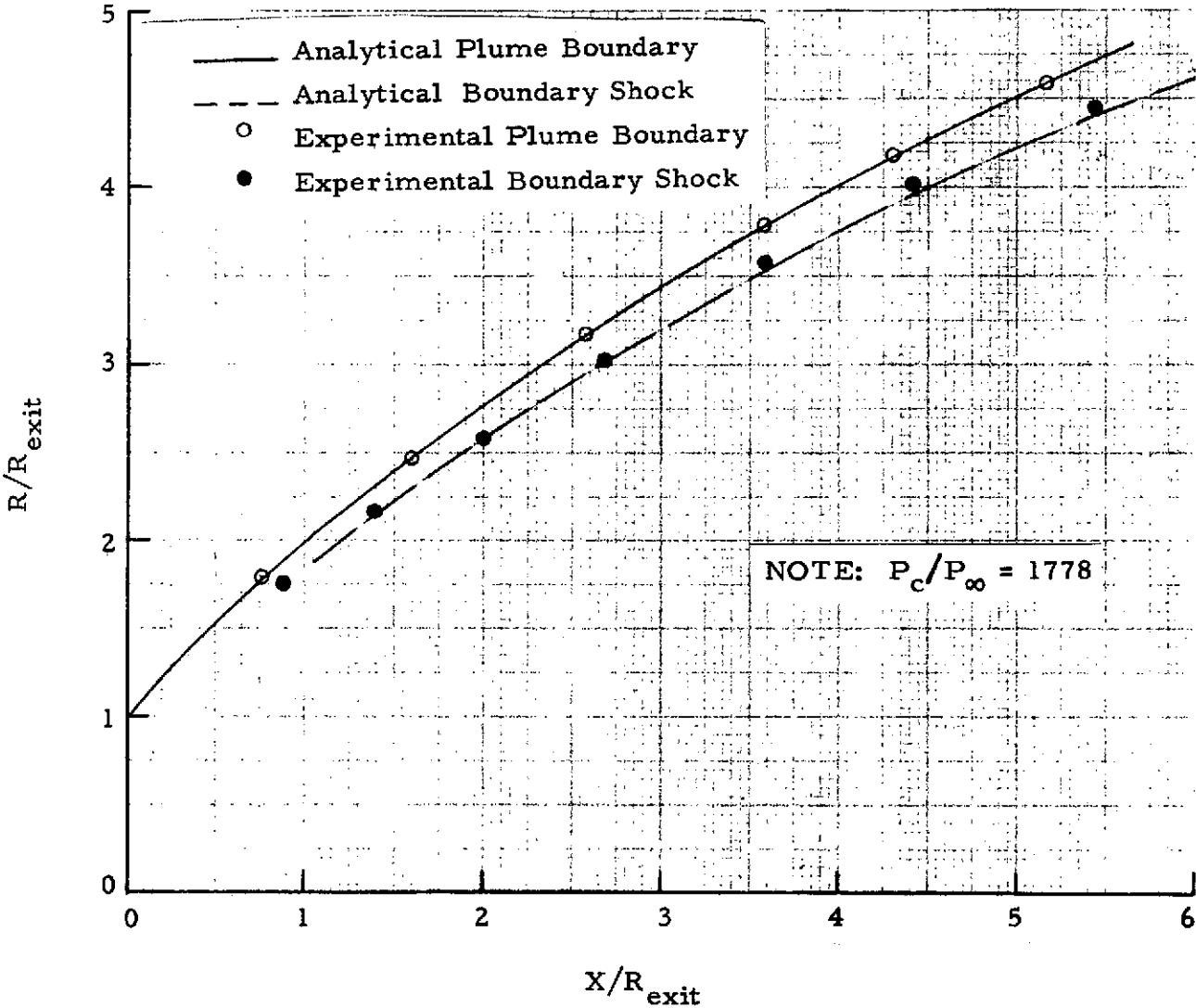


Fig. 21 - Comparison of Experimental and Predicted SRM Model Nozzle Plume Boundary and Boundary Shock Definitions at Conditions Corresponding to Model Nozzle Calibration Test 88

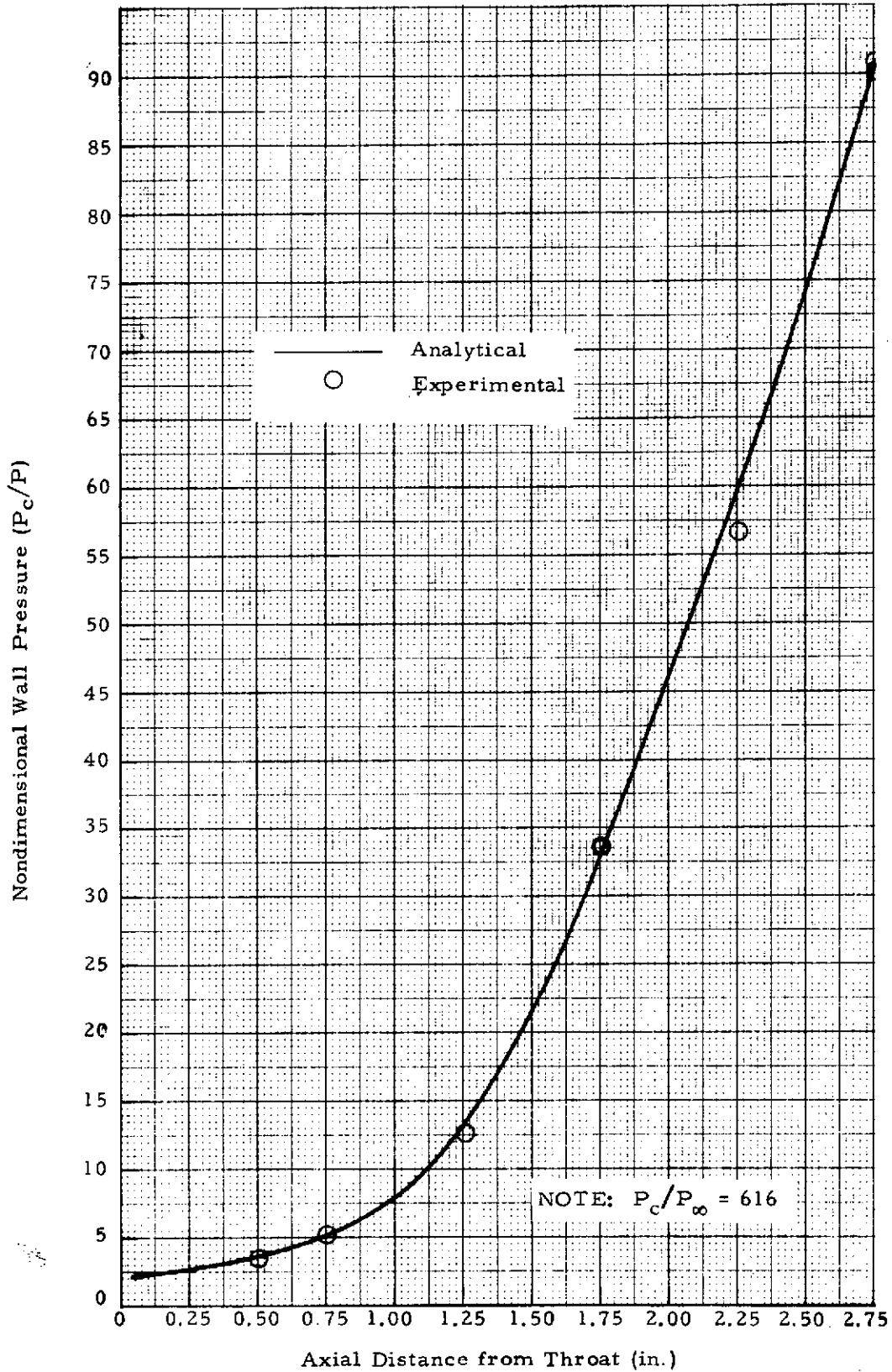


Fig. 22 - Comparison of Experimental and Predicted SRM Model Nozzle Nondimensional Wall Pressure at Conditions Corresponding to Model Nozzle Calibration Test 90

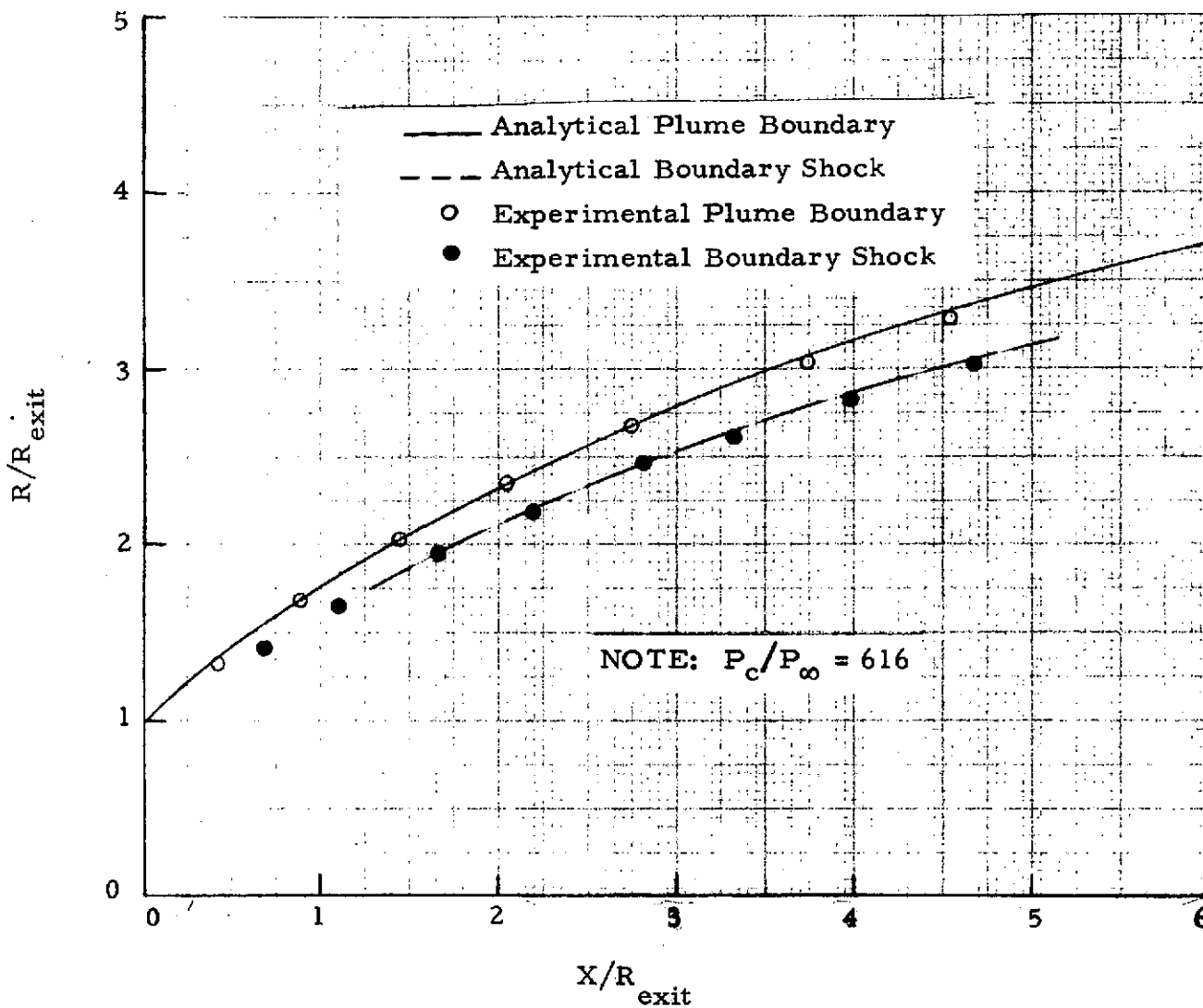


Fig. 23 - Comparison of Experimental and Predicted SRM Model Nozzle Plume Boundary and Boundary Shock Definitions at Conditions Corresponding to Model Nozzle Calibration Test 90

ORIGINAL PAGE IS
OF POOR QUALITY

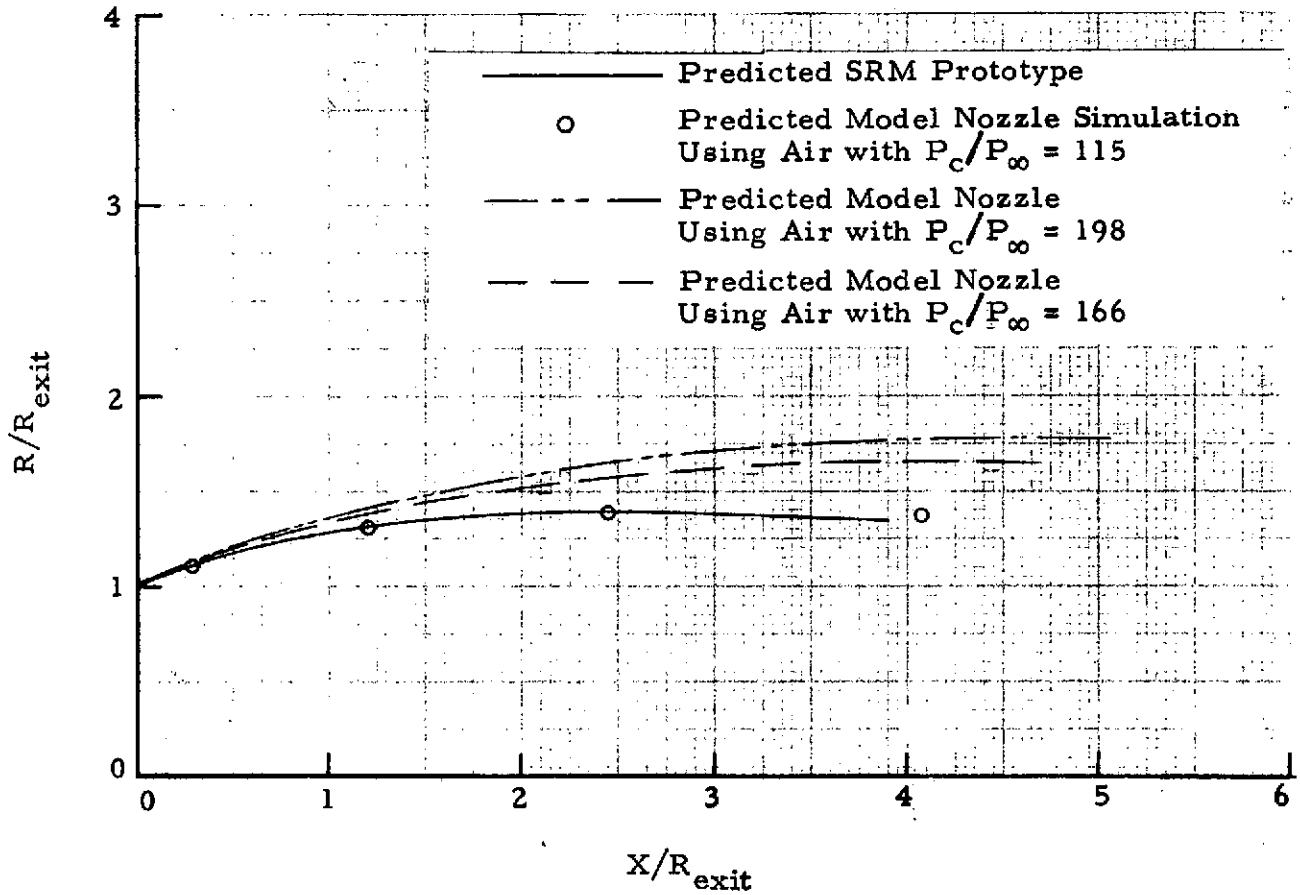


Fig. 24 - Comparison of the Space Shuttle SRM Prototype and Model Nozzle Plume Boundary Definition at Conditions Corresponding to a Trajectory Mach Number of 0.9

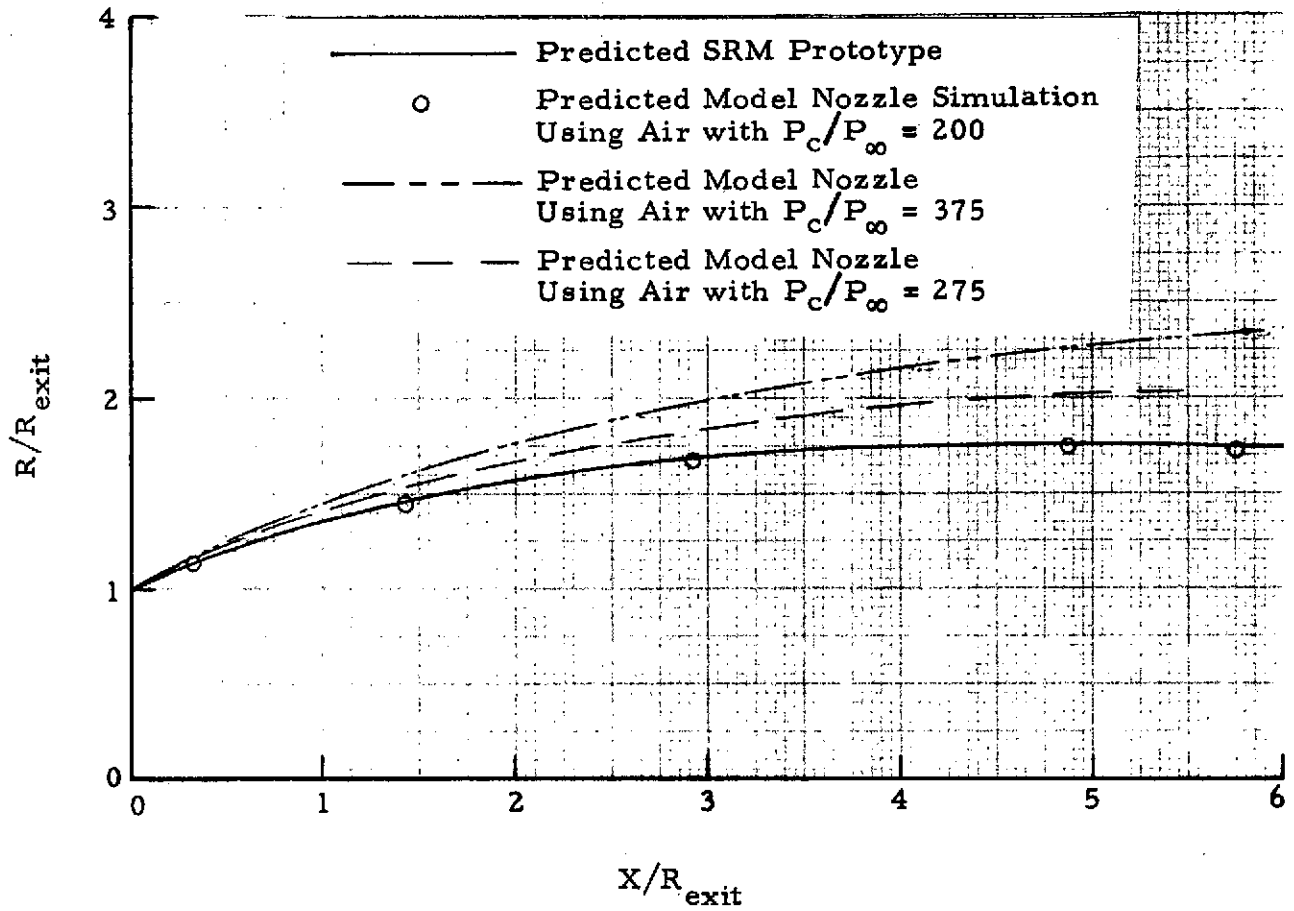


Fig. 25 - Comparison of the Space Shuttle SRM Prototype and Model Nozzle Plume Boundary Definition at Conditions Corresponding to a Trajectory Mach Number of 1.25

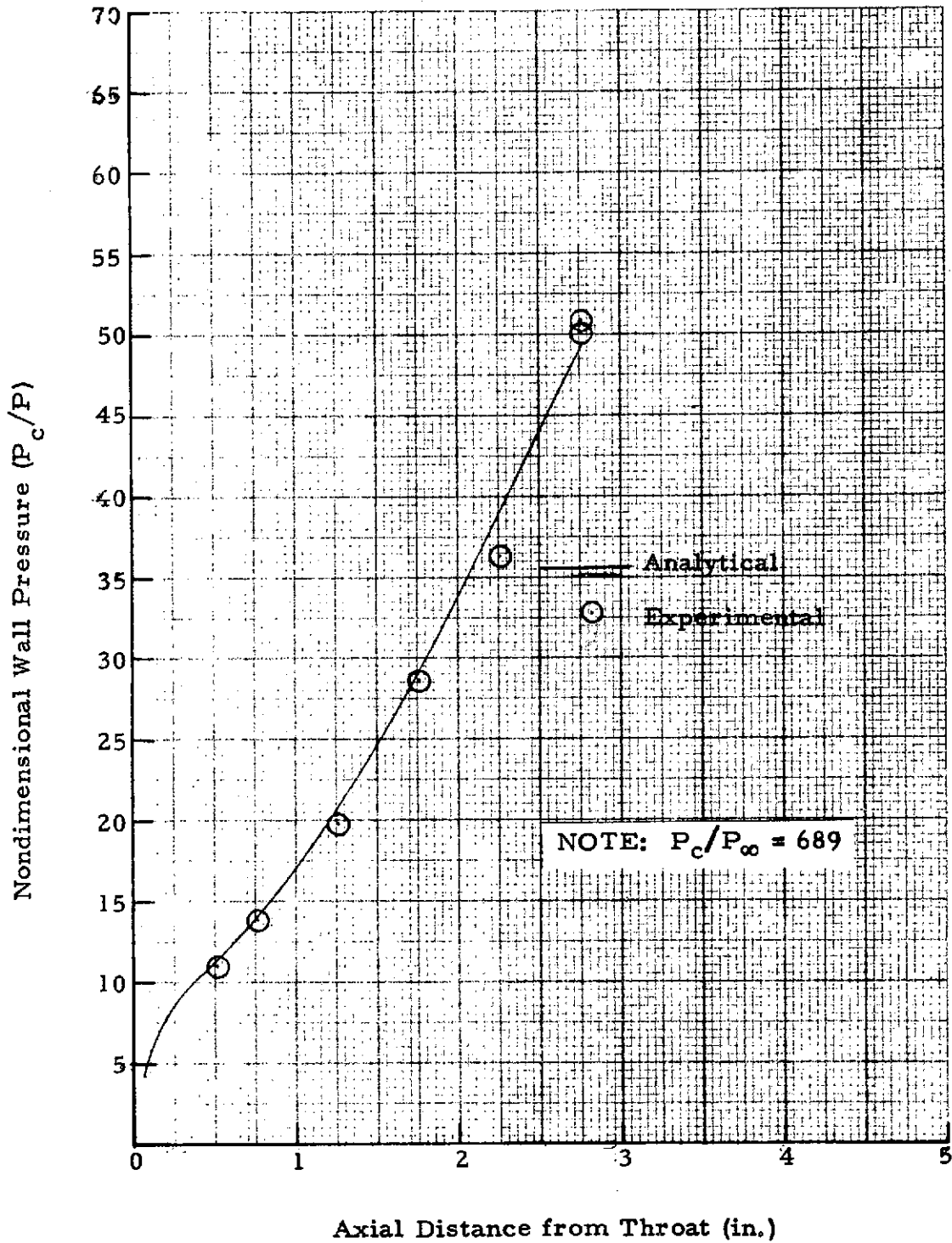


Fig. 26 - Comparison of Experimental and Predicted SRM Model Nozzle Nondimensional Wall Pressure at Conditions Corresponding to Model Nozzle Calibration Test 55

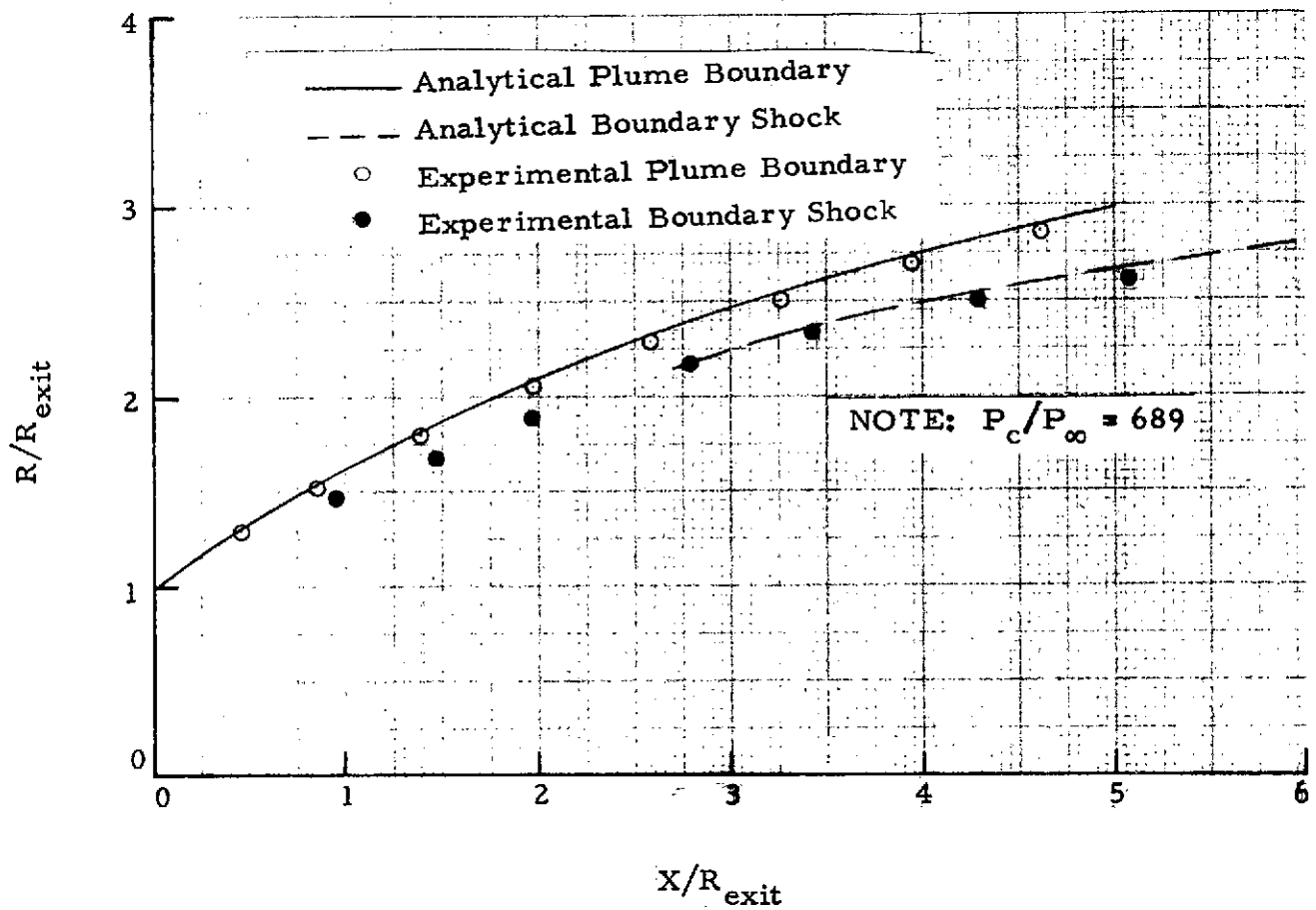


Fig. 27 - Comparison of Experimental and Predicted SRM Model Nozzle Plume Boundary and Boundary Shock Definitions at Conditions Corresponding to Model Nozzle Calibration Test 55

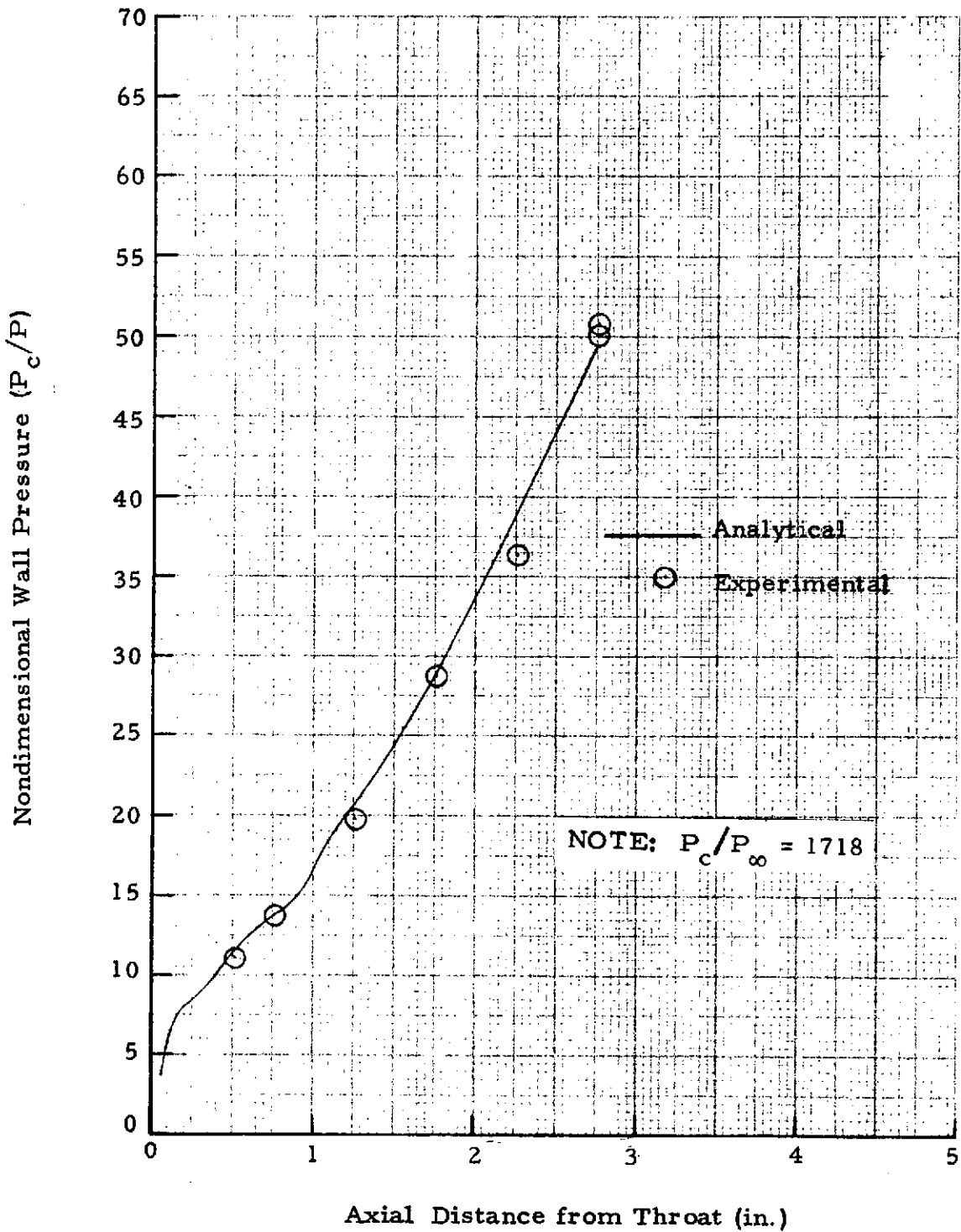


Fig. 28 - Comparison of Experimental and Predicted SRM Model Nozzle Nondimensional Wall Pressure at Conditions Corresponding to Model Nozzle Calibration Test 57

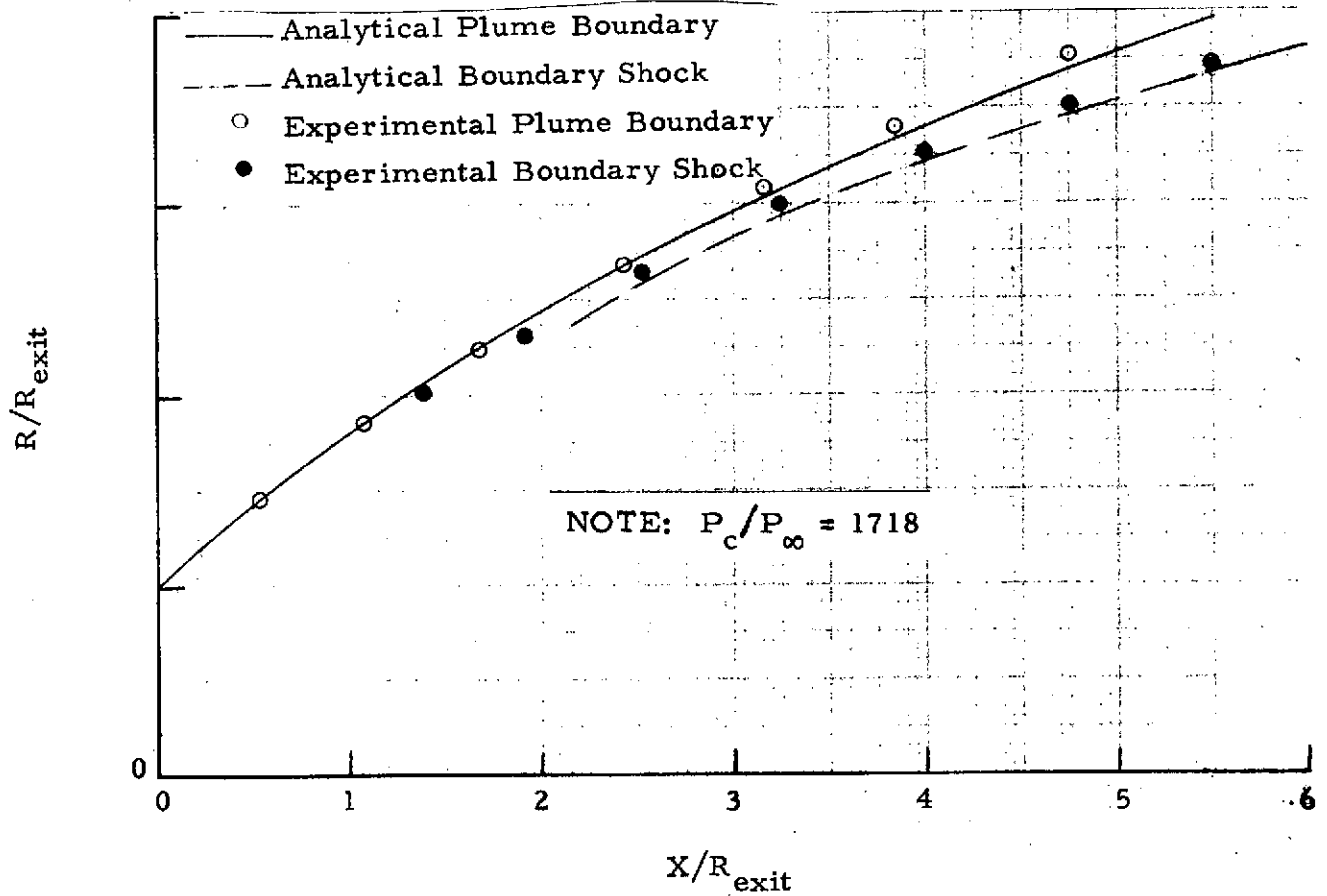


Fig. 29 - Comparison of Experimental and Predicted SRM Model Nozzle Plume Boundary and Boundary Shock Definitions at Conditions Corresponding to Model Nozzle Calibration Test 57

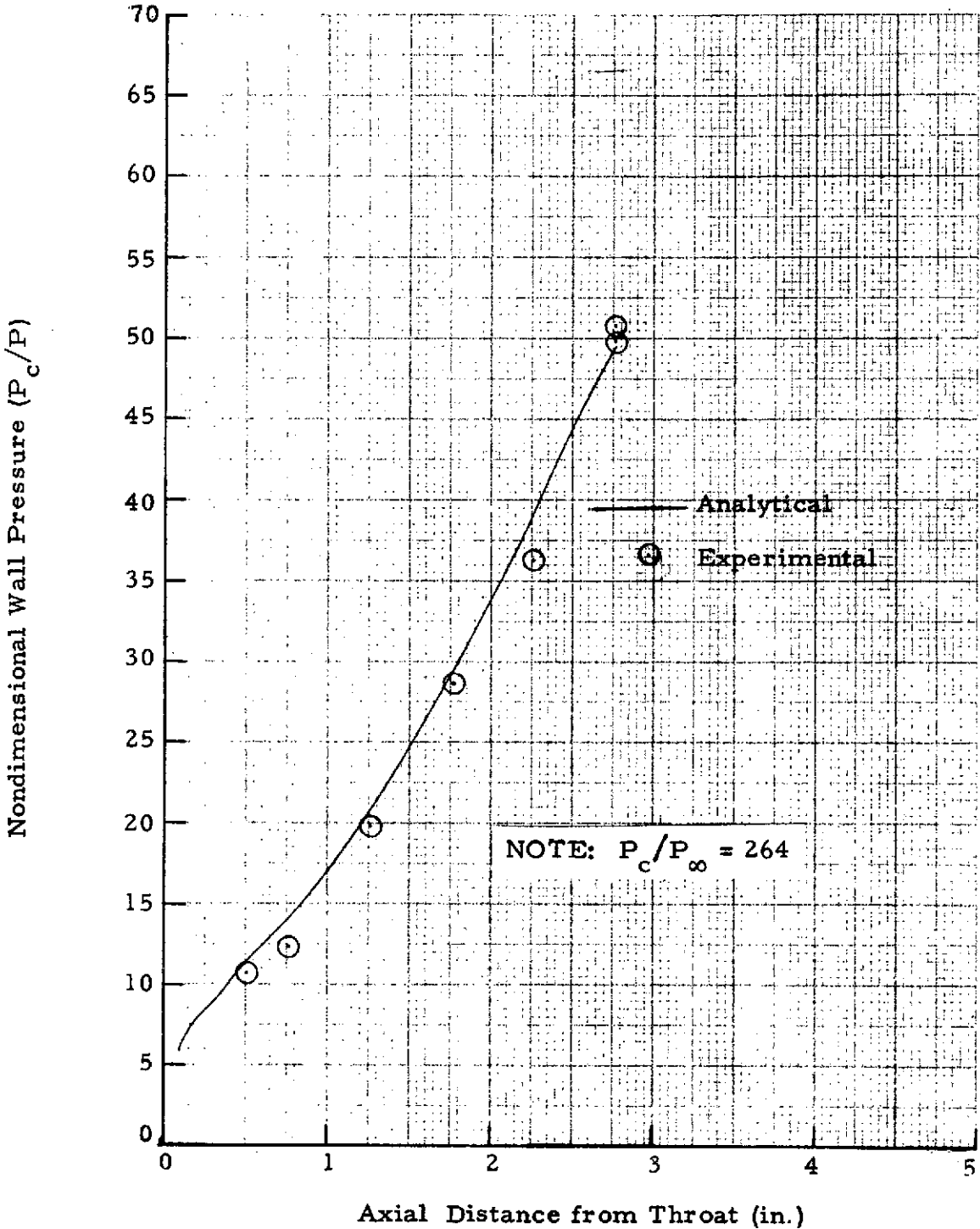


Fig. 30 - Comparison of Experimental and Predicted SRM Model Nozzle Nondimensional Wall Pressure at Conditions Corresponding to Model Nozzle Calibration Test 72

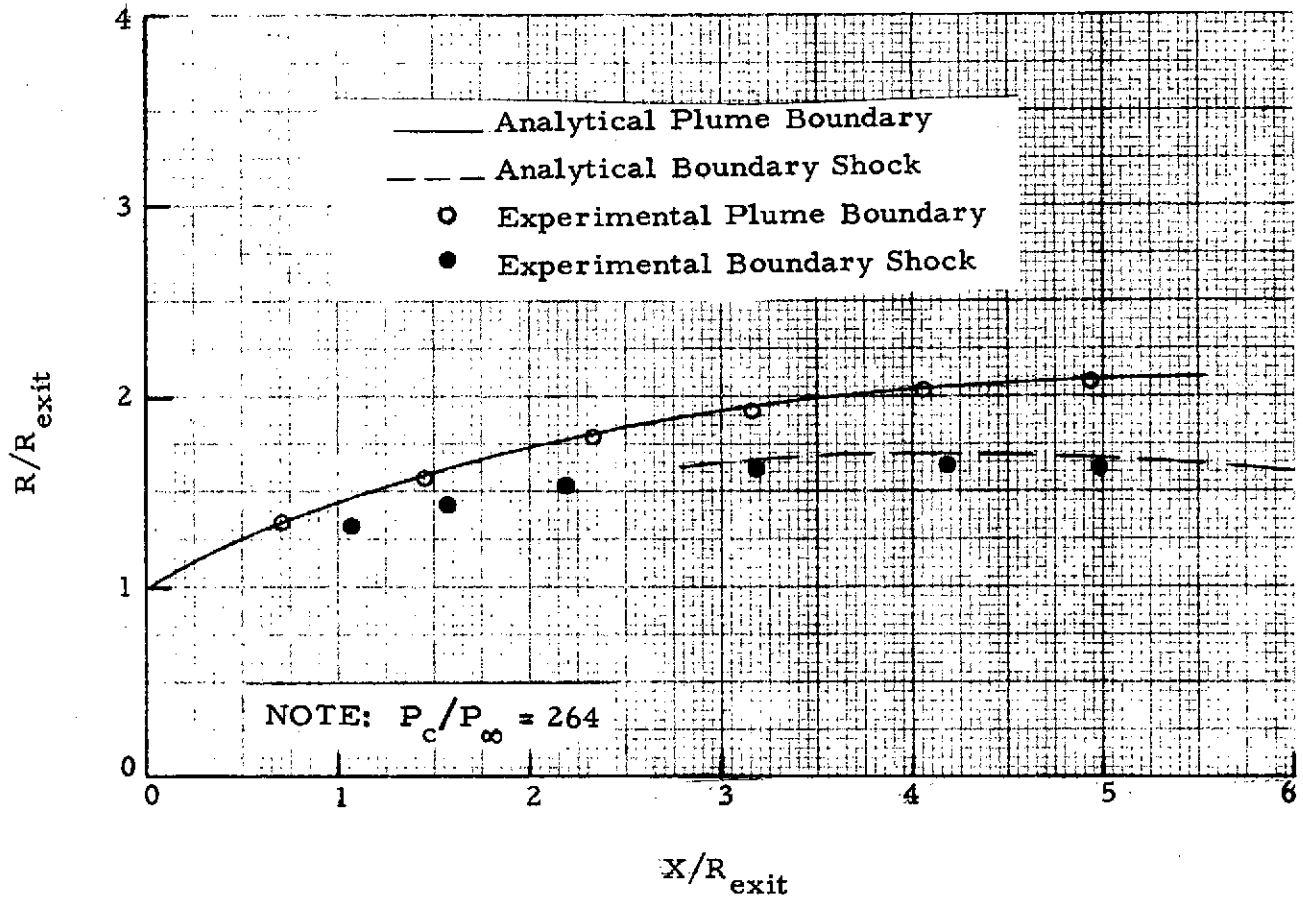


Fig. 31 - Comparison of Experimental and Predicted SRM Model Nozzle Plume Boundary and Boundary Shock Definitions at Conditions Corresponding to Model Nozzle Calibration Test 72

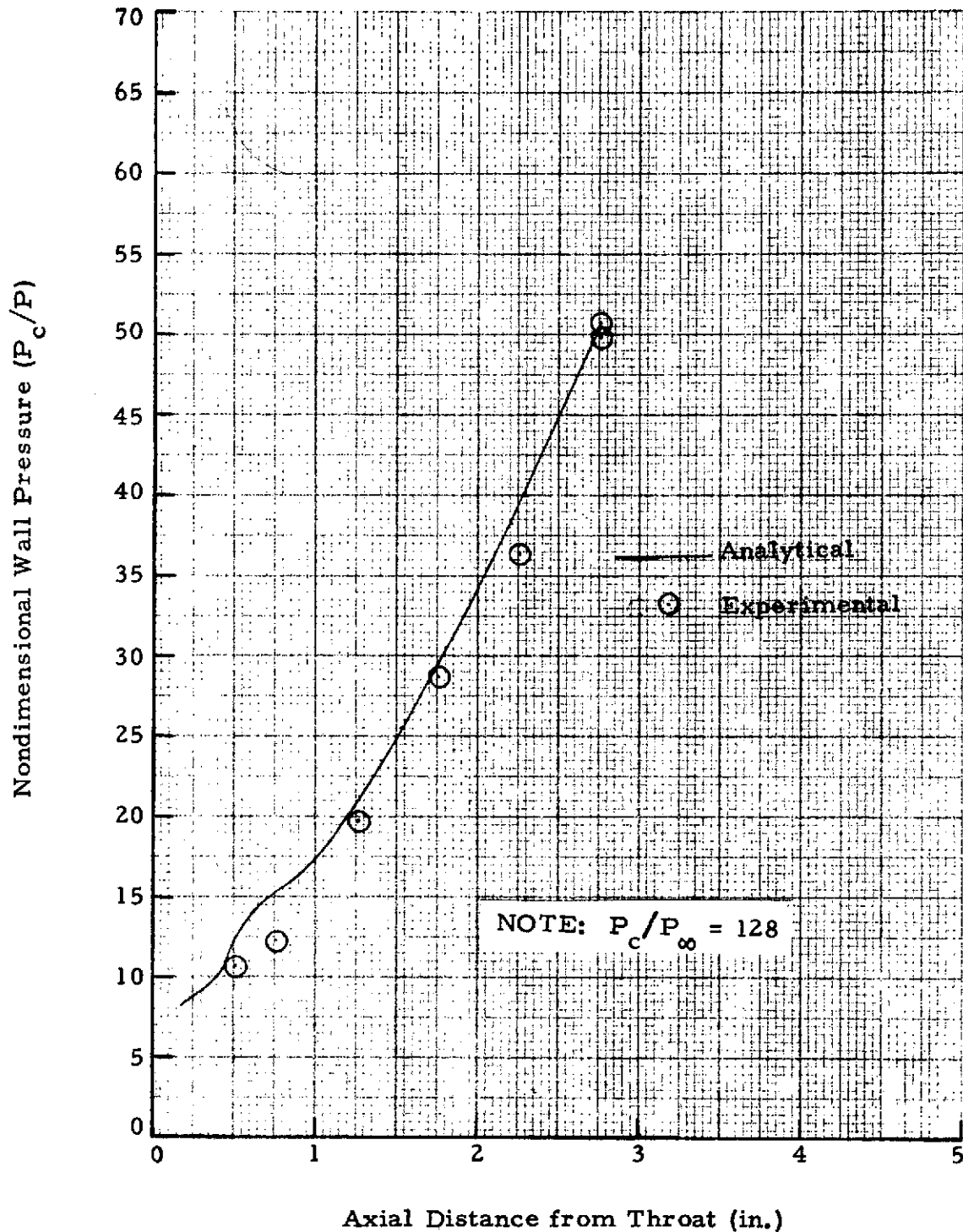


Fig. 32 - Comparison of Experimental and Predicted SRM Model Nozzle Nondimensional Wall Pressure at Conditions Corresponding to Model Nozzle Calibration Test 73

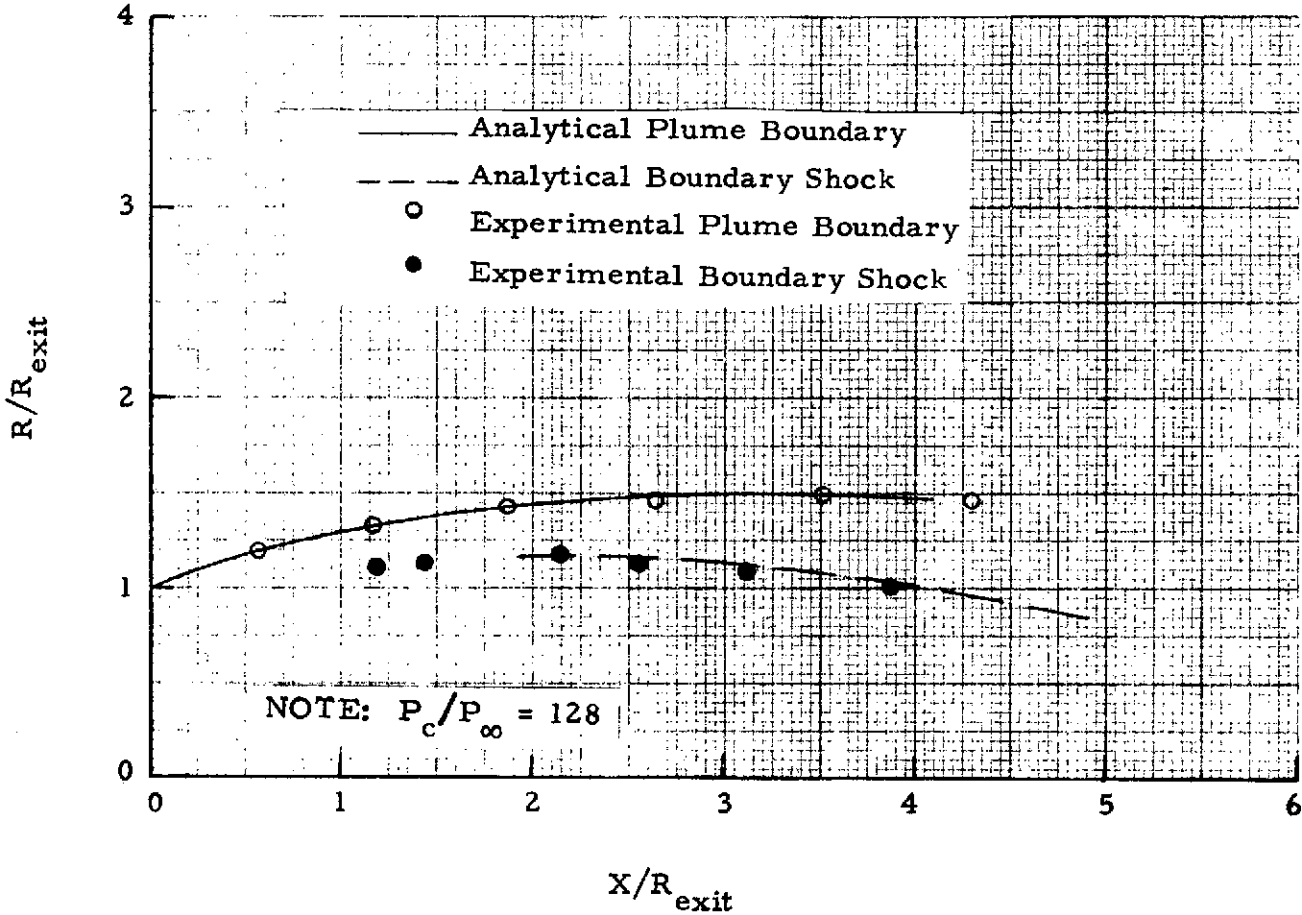


Fig. 33 - Comparison of Experimental and Predicted SRM Model Nozzle Plume Boundary and Boundary Shock Definitions at Conditions Corresponding to Model Nozzle Calibration Test 73

Appendix A

SPACE SHUTTLE MAIN ENGINE PROTOTYPE TRAJECTORY
CONDITIONS AND PREDICTED INVISCID PLUME BOUNDARIES;
MODEL NOZZLE GEOMETRY AND OPERATING CONDITIONS
NECESSARY FOR SIMULATION OF PROTOTYPE PLUME
BOUNDARIES; AND COMPARISON OF PREDICTED
PROTOTYPE AND SIMULATION (USING AIR)
PLUME BOUNDARY DEFINITIONS

PRECEDING PAGE BLANK NOT FILMED

Table A-1
 SPACE SHUTTLE MAIN ENGINE PROTOTYPE
 TRAJECTORY CONDITIONS

| Test Series | Trajectory Mach. No. | Trajectory Ambient Pressure (psfa) |
|-------------|----------------------|------------------------------------|
| IA36 | 0.90 | 1084.7 |
| | 1.25 | 607.9 |
| IA12B | 1.55 | 387.7 |
| | 2.00 | 201.1 |
| IA12C | 2.50 | 96.85 |
| | 3.00 | 50.13 |
| | 3.50 | 26.86 |

Table A-2
 SSME 0.019 SCALE MODEL NOZZLE OPERATING CONDITIONS
 NECESSARY FOR SIMULATION OF PROTOTYPE PLUME DEFINITIONS

| Test Series | Trajectory Mach No. Being Simulated | Model Nozzle Pressure Ratio Required for Simulation ($P_{\text{chamber}}/P_{\text{ambient}}$) |
|-------------|-------------------------------------|---|
| IA36 | 0.90 | 60.0 |
| | 1.25 | 94.0 |
| IA12B | 1.55 | 145.0 |
| | 2.00 | 265.0 |
| IA12C | 2.50 | 534.1 |
| | 3.00 | 987.4 |
| | 3.50 | 1820.0 |

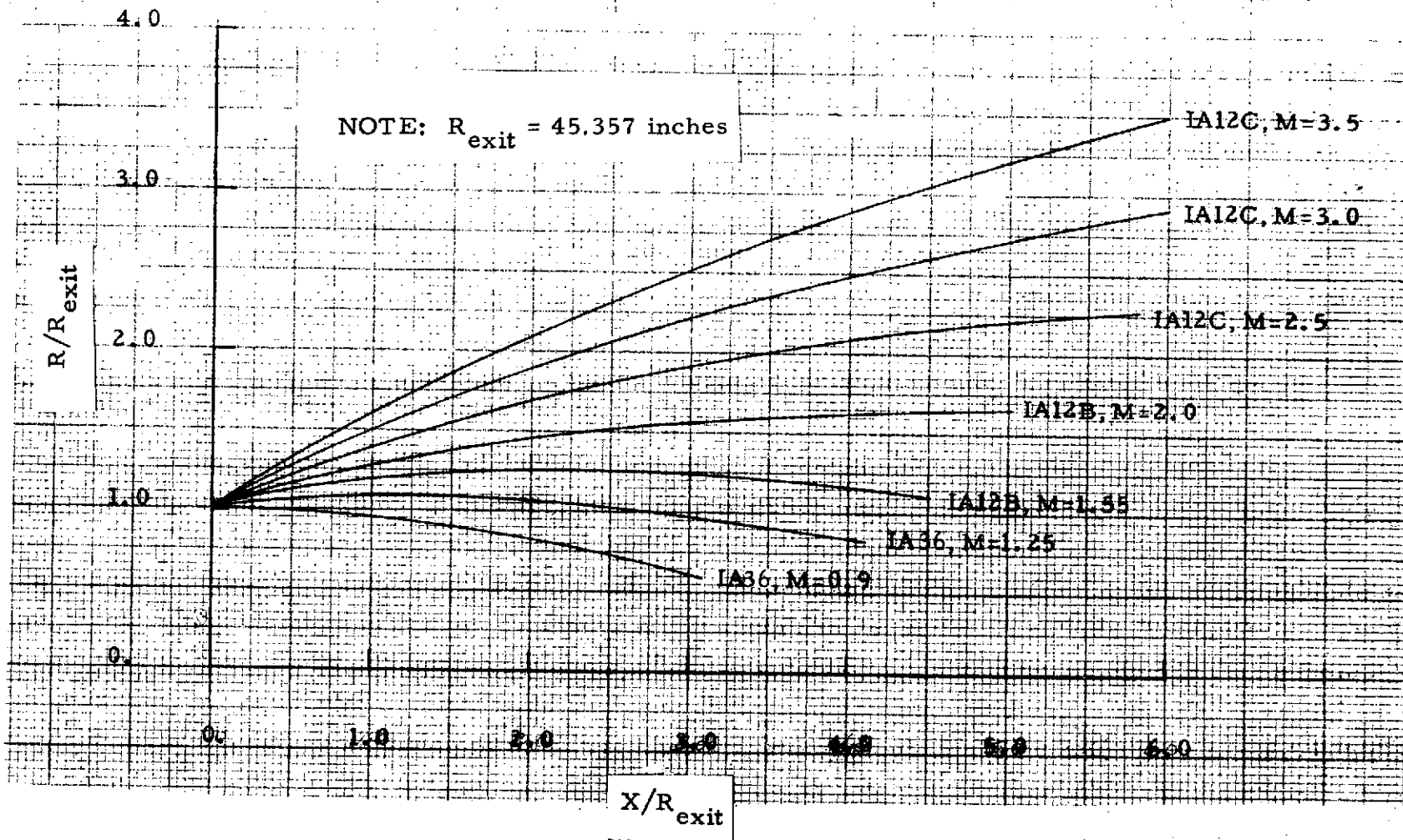
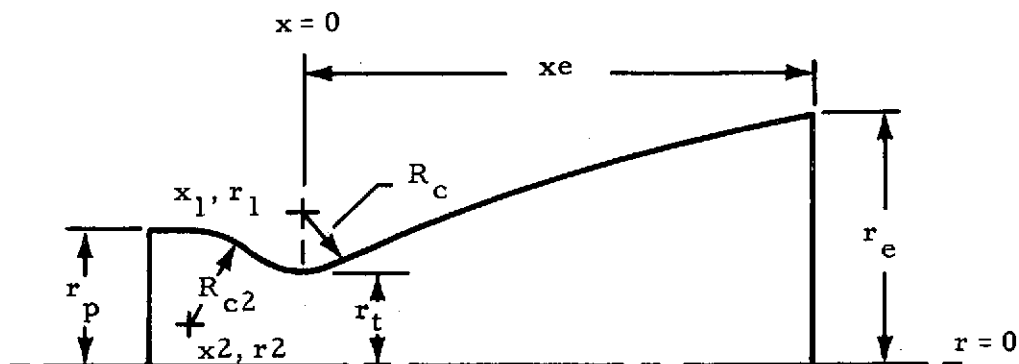


Fig. A-1 - Space Shuttle Main Engine Prototype Plume Boundaries



| Parameter | SSME Contoured Model Nozzle |
|-----------|-----------------------------|
| r_t | 0.2672 |
| r_e | 0.8618 |
| R_c | 0.2003 |
| x_c | 0.0986 |
| r_c | 0.2931 |
| x_1 | 0.0 |
| r_1 | 0.4675 |
| R_{cz} | 0.3759 |
| x_2 | -0.3053 |
| r_2 | -0.0212 |
| r_p | 0.3547 |
| x_e | 2.1178 |

* Dimensions in Inches

Fig. A.2 - Space Shuttle Main Engine 0.019 Scale Model Nozzle Geometry

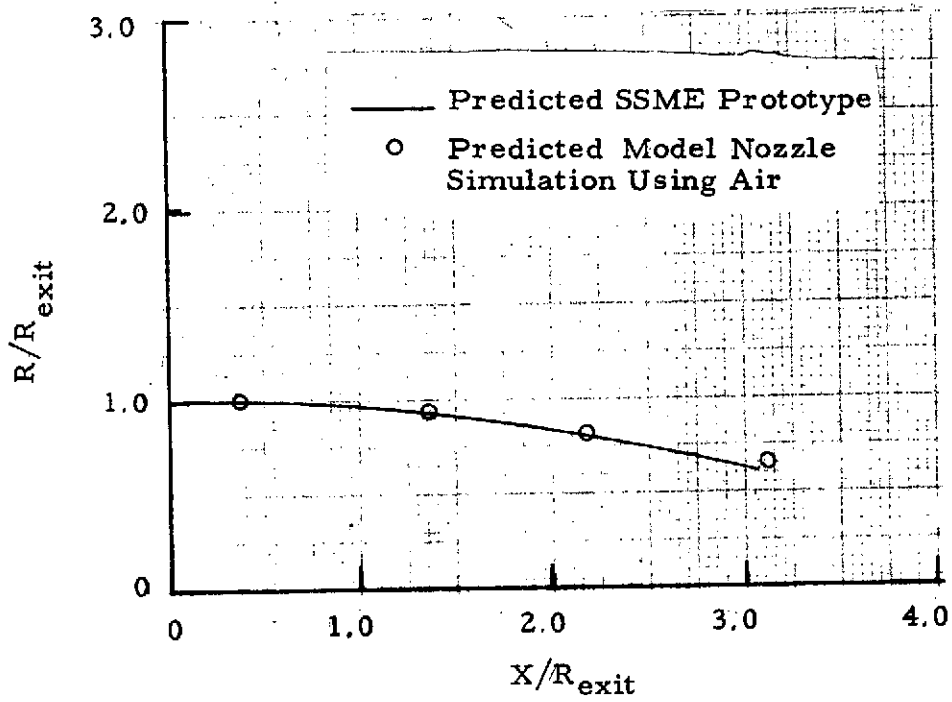


Fig. A-3 - Comparison of the Space Shuttle SSME Prototype and Model Nozzle Plume Boundary Definition at Conditions Corresponding to a Trajectory Mach Number of 0.9

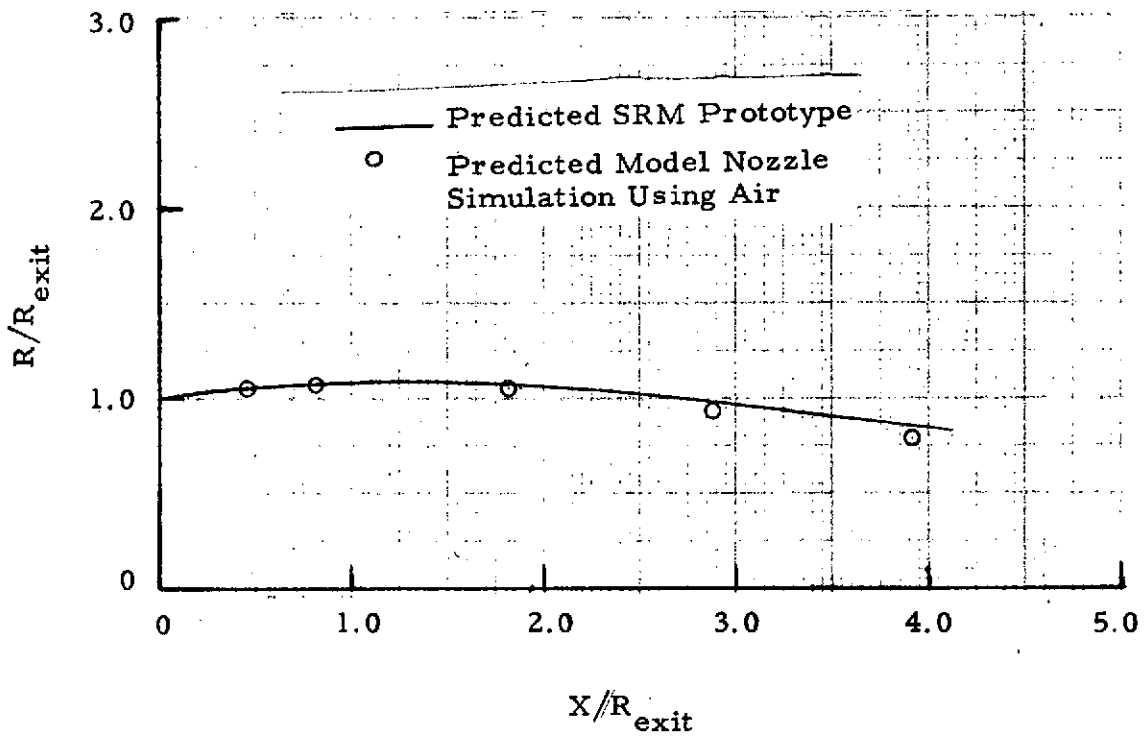


Fig. A-4 - Comparison of the Space Shuttle SSME Prototype and Model Nozzle Plume Boundary Definition at Conditions Corresponding to a Trajectory Mach Number of 1.25

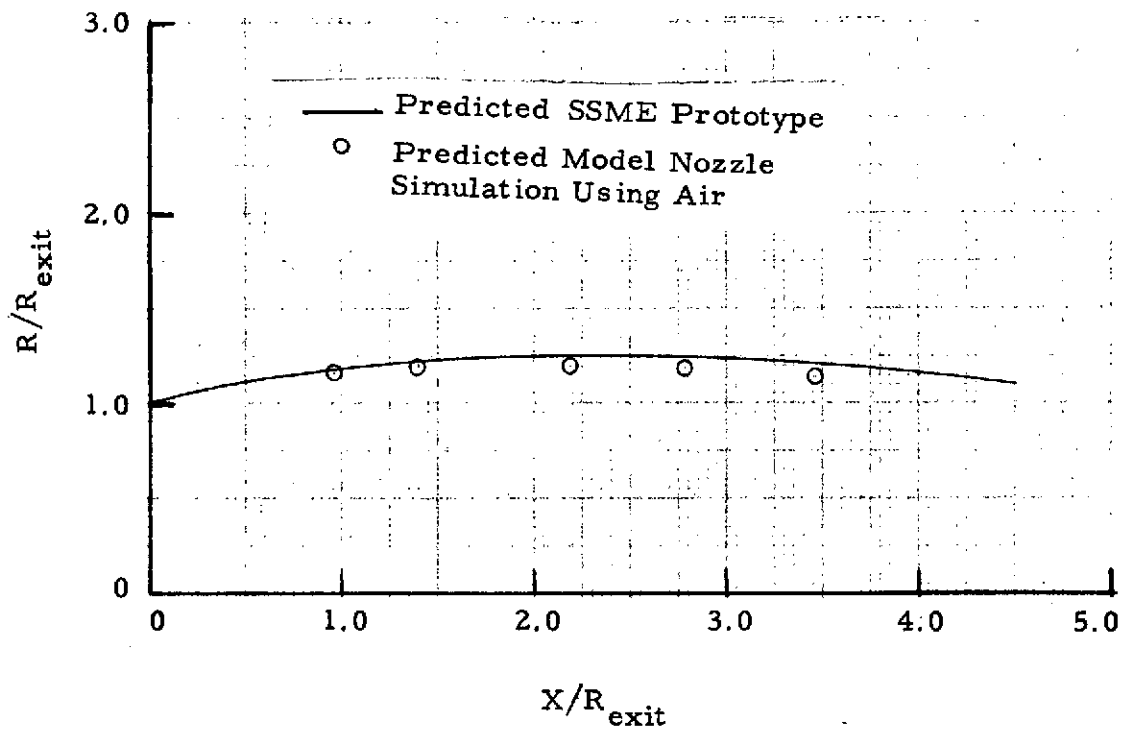


Fig. A-5 - Comparison of the Space Shuttle SSME Prototype and Model Nozzle Plume Boundary Definition at Conditions Corresponding to a Trajectory Mach Number of 1.55

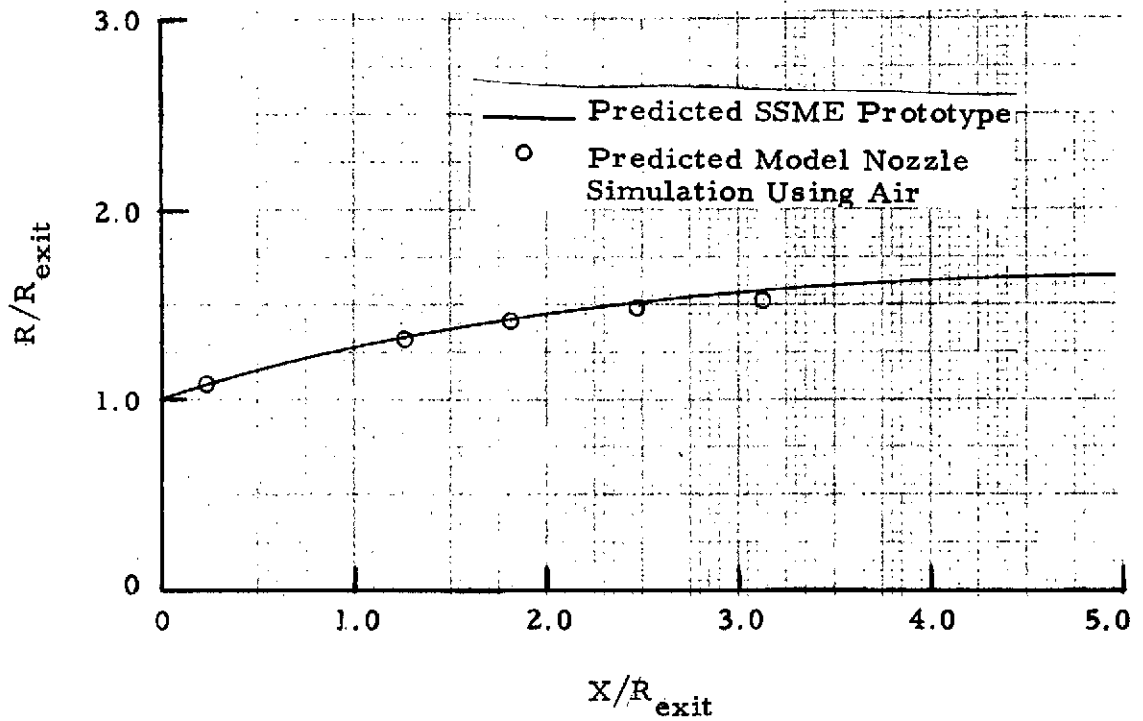


Fig. A-6 - Comparison of the Space Shuttle SSME Prototype and Model Nozzle Plume Boundary Definition at Conditions Corresponding to a Trajectory Mach Number of 2.0

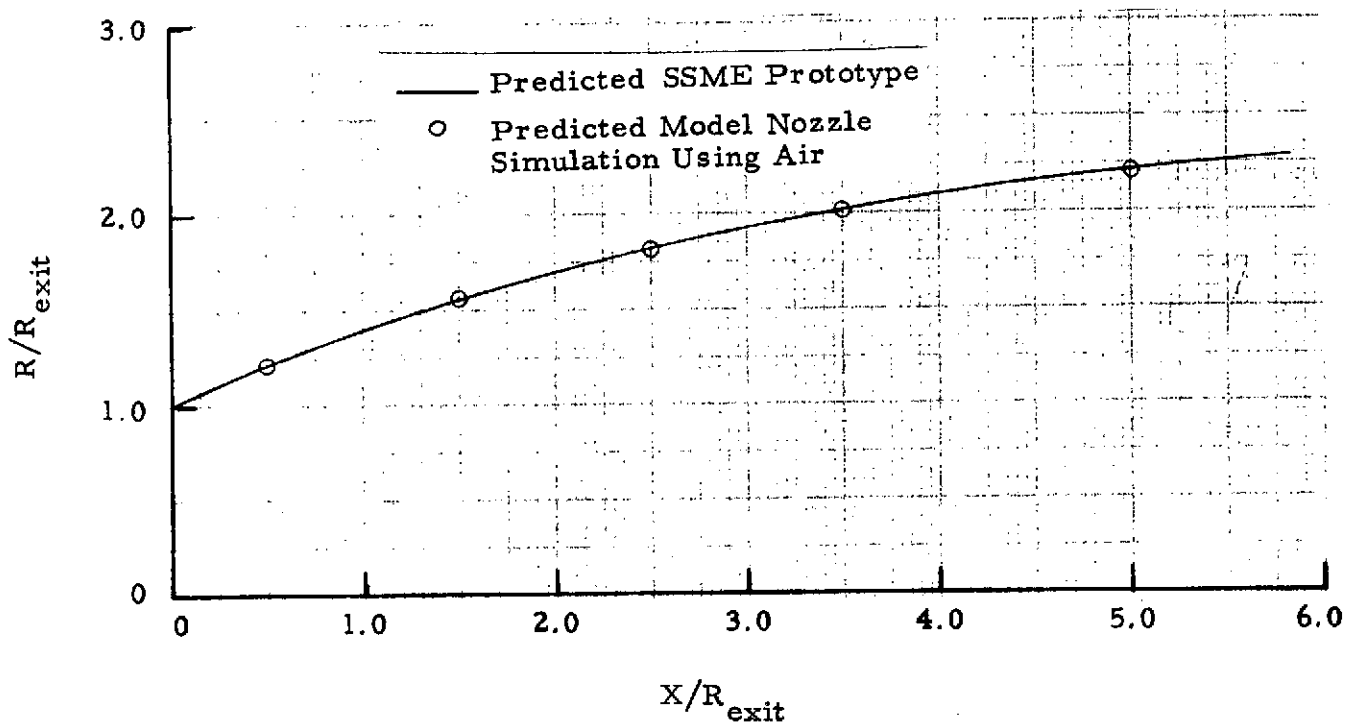


Fig. A-7 - Comparison of the Space Shuttle SSME Prototype and Model Nozzle Plume Boundary Definition at Conditions Corresponding to a Trajectory Mach Number of 2.5

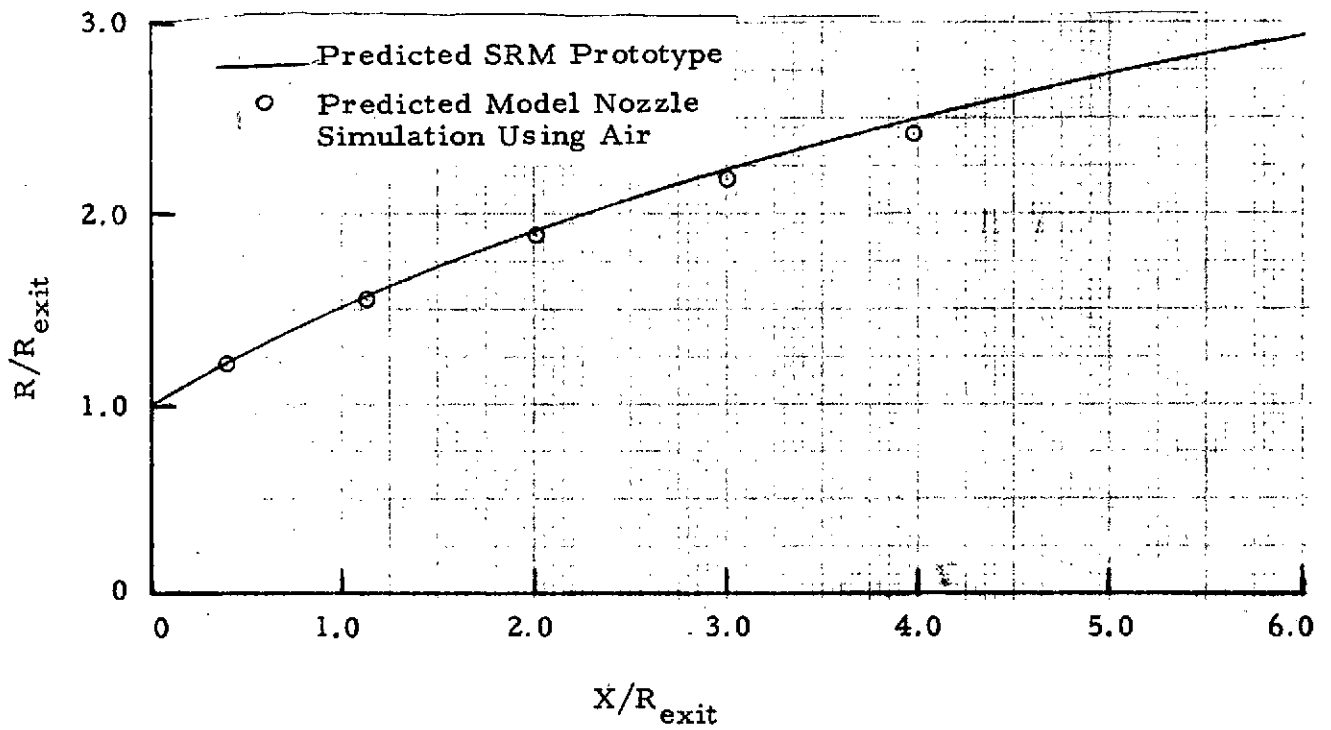


Fig. A-8 - Comparison of the Space Shuttle SSME Prototype and Model Nozzle Plume Boundary Definition at Conditions Corresponding to a Trajectory Mach Number of 3.0

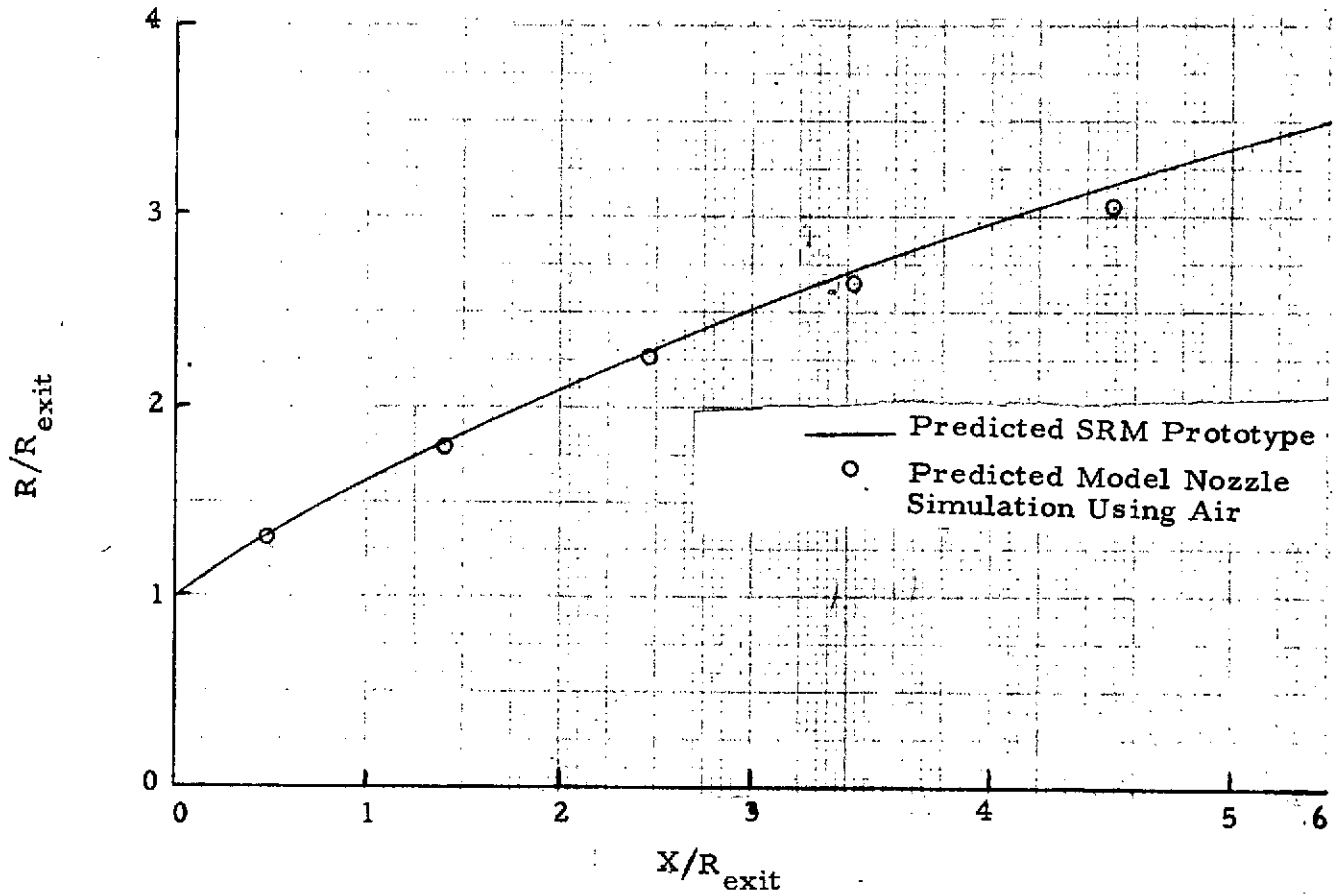


Fig. A-9 - Comparison of the Space Shuttle SSME Prototype and Model Nozzle Plume Boundary Definitions at Conditions Corresponding to a Trajectory Mach Number of 3.5

Appendix B

MODEL NOZZLE EXPERIMENTAL PRESSURE DATA
FOR MODEL NOZZLE CALIBRATION TEST NUMBERS
41, 45, 48, 49, 55, 57, 59, 65, 67, 68, 72, 73, 81, 83, 88, 90

ORIGINAL PAGE IS
OF POOR QUALITY

B-1

ROCKETDYNE ROCKET NOZZLE TEST FACILITY BRISTOL RECORDED (DATEX) TEST DATA

22 MAY 1973

TEST PROGRAM NO. 7307...JET PLUME AND WALL PRESSURE CALIBRATION OF THE 0.019 SCALE S.S.V.NOZZLES

CONFIGURATION NO. 120 TEST MEDIUM = AIR

TEST NO. 41 CASE NO. 1 SINGLE COMPONENT FORCE BALANCE

AVERAGE VALUES FOR EACH TAP ARE DIVIDED INTO THE AVERAGE MODEL TOTAL PRESSURE(PT)

AVERAGE MODEL TOTAL PRESSURE(PT)= 548.563, AVERAGE TEST CELL AMBIENT PRESSURE(PA)= 1.947, PT/PA=281.723

| | | | | | | | |
|----------|----------|----------|----------|---------|---------|---------|-----------|
| 147.0347 | 147.4995 | 122.0064 | 103.4937 | 85.9211 | 68.9102 | TAP NO. | 1 - 6 |
| 44.8305 | 26.9104 | 14.8259 | 8.3542 | 0.0 | 0.0 | TAP NO. | 7 - 12 |
| 1.0000 | 0.9997 | 1.0003 | 0.0 | 0.0 | 0.0 | TAP NO. | 25 - 30 |
| 0.0 | 0.0 | 0.0 | 281.7234 | 0.0 | 0.0 | TAP NO. | 97 - 102 |
| 0.0 | 0.0 | 0.0 | 0.0 | 1.1008 | 1.1024 | TAP NO. | 121 - 126 |

ROCKETDYNE ROCKET NOZZLE TEST FACILITY BRISTOL RECORDED (DATEX) TEST DATA

22 MAY 1973

TEST PROGRAM NO. 7307...JET PLUME AND WALL PRESSURE CALIBRATION OF THE 0.019 SCALE S.S.V.NOZZLES

CONFIGURATION NO. 120 TEST MEDIUM = AIR

TEST NO. 45 CASE NO. 1 SINGLE COMPONENT FORCE BALANCE

AVERAGE VALUES FOR EACH TAP ARE DIVIDED INTO THE AVERAGE MODEL TOTAL PRESSURE(PT)

AVERAGE MODEL TOTAL PRESSURE(PT)= 550.110, AVERAGE TEST CELL AMBIENT PRESSURE(PA)= 0.503, PT/PA=1092.591

| | | | | | | | |
|----------|----------|----------|-----------|---------|---------|---------|-----------|
| 146.3067 | 146.6917 | 121.8402 | 103.7092 | 86.0504 | 69.4224 | TAP NO. | 1 - 6 |
| 45.8718 | 27.0811 | 14.9741 | 8.2960 | 0.0 | 0.0 | TAP NO. | 7 - 12 |
| 1.0000 | 1.0002 | 1.0008 | 0.0 | 0.0 | 0.0 | TAP NO. | 25 - 30 |
| 0.0 | 0.0 | 0.0 | 1092.5906 | 0.0 | 0.0 | TAP NO. | 97 - 102 |
| 0.0 | 0.0 | 0.0 | 0.0 | 1.1065 | 1.1086 | TAP NO. | 121 - 126 |

LMSC-HREC TM D306990

ORIGINAL PAGE IS
OF POOR QUALITY

B-2

ROCKETDYNE ROCKET NOZZLE TEST FACILITY BRISTOL RECORDED (DATEX) TEST DATA

22 MAY 1973

TEST PROGRAM NO. 7307...JET PLUME AND WALL PRESSURE CALIBRATION OF THE 0.019 SCALE S.S.V.NOZZLES

CONFIGURATION NO. 120 TEST MEDIUM = AIR

TEST NO. 48 CASE NO. 1 SINGLE COMPONENT FORCE BALANCE

AVERAGE VALUES FOR EACH TAP ARE DIVIDED INTO THE AVERAGE MODEL TOTAL PRESSURE(PT)

AVERAGE MODEL TOTAL PRESSURE(PT)= 547.297, AVERAGE TEST CELL AMBIENT PRESSURE(PA)= 0.723, PT/PA=756.926

| | | | | | | | |
|----------|----------|----------|----------|---------|---------|---------|-----------|
| 142.3800 | 142.7903 | 119.3738 | 103.8868 | 86.0785 | 68.5210 | TAP NO. | 1 - 6 |
| 45.3954 | 26.8403 | 15.1556 | 8.2988 | 0.0 | 0.0 | TAP NO. | 7 - 12 |
| 1.0000 | 1.0002 | 1.0010 | 0.0 | 0.0 | 0.0 | TAP NO. | 25 - 30 |
| 0.0 | 0.0 | 0.0 | 756.9258 | 0.0 | 0.0 | TAP NO. | 97 - 102 |
| 0.0 | 0.0 | 0.0 | 0.0 | 1.1231 | 1.1244 | TAP NO. | 121 - 126 |

ROCKETDYNE ROCKET NOZZLE TEST FACILITY BRISTOL RECORDED (DATEX) TEST DATA

22 MAY 1973

TEST PROGRAM NO. 7307...JET PLUME AND WALL PRESSURE CALIBRATION OF THE 0.019 SCALE S.S.V.NOZZLES

CONFIGURATION NO. 120 TEST MEDIUM = AIR

TEST NO. 49 CASE NO. 1 SINGLE COMPONENT FORCE BALANCE

AVERAGE VALUES FOR EACH TAP ARE DIVIDED INTO THE AVERAGE MODEL TOTAL PRESSURE(PT)

AVERAGE MODEL TOTAL PRESSURE(PT)= 546.196, AVERAGE TEST CELL AMBIENT PRESSURE(PA)= 0.339, PT/PA=1617.702

| | | | | | | | |
|----------|----------|----------|-----------|---------|---------|---------|-----------|
| 145.9092 | 146.7444 | 121.8055 | 103.9537 | 86.2176 | 68.3153 | TAP NO. | 1 - 6 |
| 45.4262 | 26.7442 | 15.1914 | 8.3425 | 0.0 | 0.0 | TAP NO. | 7 - 12 |
| 1.0000 | 1.0001 | 1.0009 | 0.0 | 0.0 | 0.0 | TAP NO. | 25 - 30 |
| 0.0 | 0.0 | 0.0 | 1610.7021 | 0.0 | 0.0 | TAP NO. | 97 - 102 |
| 0.0 | 0.0 | 0.0 | 0.0 | 1.1016 | 1.1019 | TAP NO. | 121 - 126 |

LMSC-HREC IM D306990

ORIGINAL PAGE IS
OF POOR QUALITY

ROCKETDYNE ROCKET NOZZLE TEST FACILITY BRISTOL RECORDED (DATEX) TEST DATA

22 MAY 1973

TEST PROGRAM NO. 7307...JET PLUME AND WALL PRESSURE CALIBRATION OF THE 0.019 SCALE S.S.V.NOZZLES

CONFIGURATION NO. 700 TEST MEDIUM = AIR

TEST NO. 55 CASE NO. 1 SINGLE COMPONENT FORCE BALANCE

AVERAGE VALUES FOR EACH TAP ARE DIVIDED INTO THE AVERAGE MODEL TOTAL PRESSURE(PT)

AVERAGE MODEL TOTAL PRESSURE(PT)= 549.345, AVERAGE TEST CELL AMBIENT PRESSURE(PA)= 0.797, PT/PA= 689.195

| | | | | | | |
|---------|---------|---------|----------|---------|---------|-------------------|
| 50.8697 | 50.0041 | 36.4258 | 28.6358 | 19.7999 | 13.8343 | TAP NO. 1 - 6 |
| 11.0566 | 0.0 | 0.0 | 0.0 | 0.0 | 0.0 | TAP NO. 7 - 12 |
| 1.0000 | 0.9997 | 1.0003 | 0.0 | 0.0 | 0.0 | TAP NO. 25 - 30 |
| 0.0 | 0.0 | 0.0 | 689.1951 | 0.0 | 0.0 | TAP NO. 97 - 102 |
| 0.0 | 0.0 | 0.0 | 0.0 | 1.1013 | 1.1020 | TAP NO. 121 - 126 |

ROCKETDYNE ROCKET NOZZLE TEST FACILITY BRISTOL RECORDED (DATEX) TEST DATA

22 MAY 1973

TEST PROGRAM NO. 7307...JET PLUME AND WALL PRESSURE CALIBRATION OF THE 0.019 SCALE S.S.V.NOZZLES

CONFIGURATION NO. 700 TEST MEDIUM = AIR

TEST NO. 57 CASE NO. 1 SINGLE COMPONENT FORCE BALANCE

AVERAGE VALUES FOR EACH TAP ARE DIVIDED INTO THE AVERAGE MODEL TOTAL PRESSURE(PT)

AVERAGE MODEL TOTAL PRESSURE(PT)= 548.921, AVERAGE TEST CELL AMBIENT PRESSURE(PA)= 0.319, PT/PA= 1718.677

| | | | | | | |
|---------|---------|---------|-----------|---------|---------|-------------------|
| 50.8957 | 50.0411 | 36.4179 | 28.6768 | 19.8336 | 13.9114 | TAP NO. 1 - 6 |
| 11.0649 | 0.0 | 0.0 | 0.0 | 0.0 | 0.0 | TAP NO. 7 - 12 |
| 1.0000 | 1.0001 | 1.0007 | 0.0 | 0.0 | 0.0 | TAP NO. 25 - 30 |
| 0.0 | 0.0 | 0.0 | 1718.6775 | 0.0 | 0.0 | TAP NO. 97 - 102 |
| 0.0 | 0.0 | 0.0 | 0.0 | 1.0904 | 1.0907 | TAP NO. 121 - 126 |

B-3

LMSC-HREC TM D306990

ROCKETDYNE ROCKET NOZZLE TEST FACILITY BRISTOL RECORDED (DATEX) TEST DATA

22 MAY 1973

TEST PROGRAM NO. 7307...JET PLUME AND WALL PRESSURE CALIBRATION OF THE 0.019 SCALE S.S.V.NOZZLES

CONFIGURATION NO. 707 TEST MEDIUM = AIR

TEST NO. 59 CASE NO. 1 SINGLE COMPONENT FORCE BALANCE

AVERAGE VALUES FOR EACH TAP ARE DIVIDED INTO THE AVERAGE MODEL TOTAL PRESSURE(PT)

AVERAGE MODEL TOTAL PRESSURE(PT)= 550.123, AVERAGE TEST CELL AMBIENT PRESSURE(PA)= 1.133, PT/PA= 485.415

| | | | | | | | |
|---------|---------|---------|----------|---------|---------|---------|-----------|
| 50.8684 | 50.0579 | 26.4100 | 28.6543 | 19.7864 | 13.9209 | TAP NO. | 1 - 6 |
| 11.0315 | 0.0 | 0.0 | 0.0 | 0.0 | 0.0 | TAP NO. | 7 - 12 |
| 1.0000 | 1.0001 | 1.0010 | 0.0 | 0.0 | 0.0 | TAP NO. | 25 - 30 |
| 0.0 | 0.0 | 0.0 | 485.4148 | 0.0 | 0.0 | TAP NO. | 97 - 102 |
| 0.0 | 0.0 | 0.0 | 0.0 | 1.1243 | 1.1265 | TAP NO. | 121 - 126 |

ROCKETDYNE ROCKET NOZZLE TEST FACILITY BRISTOL RECORDED (DATEX) TEST DATA

22 MAY 1973

TEST PROGRAM NO. 7307...JET PLUME AND WALL PRESSURE CALIBRATION OF THE 0.019 SCALE S.S.V.NOZZLES

CONFIGURATION NO. 707 TEST MEDIUM = AIR

TEST NO. 65 CASE NO. 1 SINGLE COMPONENT FORCE BALANCE

AVERAGE VALUES FOR EACH TAP ARE DIVIDED INTO THE AVERAGE MODEL TOTAL PRESSURE(PT)

AVERAGE MODEL TOTAL PRESSURE(PT)= 551.658, AVERAGE TEST CELL AMBIENT PRESSURE(PA)= 0.680, PT/PA= 811.513

| | | | | | | | |
|---------|---------|---------|----------|---------|---------|---------|-----------|
| 50.9197 | 50.0735 | 36.4736 | 28.6543 | 19.6295 | 13.8070 | TAP NO. | 1 - 6 |
| 11.0363 | 0.0 | 0.0 | 0.0 | 0.0 | 0.0 | TAP NO. | 7 - 12 |
| 1.0000 | 1.0001 | 1.0008 | 0.0 | 0.0 | 0.0 | TAP NO. | 25 - 30 |
| 0.0 | 0.0 | 0.0 | 811.5132 | 0.0 | 0.0 | TAP NO. | 97 - 102 |
| 0.0 | 0.0 | 0.0 | 0.0 | 1.0894 | 1.0901 | TAP NO. | 121 - 126 |

ORIGINAL PAGE 13
B-4 FOR POOR QUALITY

B-4

LMSC-HREC TM D306990

ORIGINAL PAGE IS
OF POOR QUALITY

ROCKETDYNE ROCKET NOZZLE TEST FACILITY BRISTOL RECORDED (DATEX) TEST DATA

22 MAY 1973

TEST PROGRAM NO. 7307...JET PLUME AND WALL PRESSURE CALIBRATION OF THE 0.019 SCALE S.S.V.NOZZLES

CONFIGURATION NO. 707 TEST MEDIUM = AIR

TEST NO. 67 CASE NO. 1 SINGLE COMPONENT FORCE BALANCE

AVERAGE VALUES FOR EACH TAP ARE DIVIDED INTO THE AVERAGE MODEL TOTAL PRESSURE(PT)

AVERAGE MODEL TOTAL PRESSURE(PT)= 549.445, AVERAGE TEST CELL AMBIENT PRESSURE(PA)= 4.235, PT/PA=127.749

| | | | | | | |
|---------|---------|---------|----------|---------|---------|-------------------|
| 50.9029 | 50.0546 | 36.4629 | 28.6225 | 19.8016 | 13.8092 | TAP NO. 1 - 6 |
| 11.0327 | 0.0 | 0.0 | 0.0 | 0.0 | 0.0 | TAP NO. 7 - 12 |
| 1.0000 | 1.0003 | 1.0012 | 0.0 | 0.0 | 0.0 | TAP NO. 25 - 30 |
| 0.0 | 0.0 | 0.0 | 129.7494 | 0.0 | 0.0 | TAP NO. 97 - 102 |
| 0.0 | 0.0 | 0.0 | 0.0 | 1.0806 | 1.0807 | TAP NO. 121 - 126 |

ROCKETDYNE ROCKET NOZZLE TEST FACILITY BRISTOL RECORDED (DATEX) TEST DATA

25 MAY 1973

TEST PROGRAM NO. 7307...JET PLUME AND WALL PRESSURE CALIBRATION OF THE 0.019 SCALE S.S.V.NOZZLES

CONFIGURATION NO. 707 TEST MEDIUM = AIR

TEST NO. 68 CASE NO. 1 SINGLE COMPONENT FORCE BALANCE

AVERAGE VALUES FOR EACH TAP ARE DIVIDED INTO THE AVERAGE MODEL TOTAL PRESSURE(PT)

AVERAGE MODEL TOTAL PRESSURE(PT)= 549.936, AVERAGE TEST CELL AMBIENT PRESSURE(PA)= 0.307, PT/PA=1791.43

| | | | | | | |
|---------|---------|---------|-----------|---------|---------|-------------------|
| 50.8988 | 50.0094 | 36.3384 | 28.6388 | 19.7838 | 13.2334 | TAP NO. 1 - 6 |
| 11.0848 | 0.0 | 0.0 | 0.0 | 0.0 | 0.0 | TAP NO. 7 - 12 |
| 1.0000 | 1.0002 | 1.0014 | 0.0 | 0.0 | 0.0 | TAP NO. 25 - 30 |
| 0.0 | 0.0 | 0.0 | 1791.4033 | 0.0 | 0.0 | TAP NO. 97 - 102 |
| 0.0 | 0.0 | 0.0 | 0.0 | 1.1016 | 1.1019 | TAP NO. 121 - 126 |

B-5

LMSC-HREC TM D306990

ORIGINAL PAGE IS
OF POOR QUALITY

ROCKETDYNE ROCKET NOZZLE TEST FACILITY BRISTOL RECORDED (DATEX) TEST DATA

25 MAY 1973

TEST PROGRAM NO. 7307...JET PLUME AND WALL PRESSURE CALIBRATION OF THE 0.019 SCALE S.S.V.NOZZLES

CONFIGURATION NO. 700 TEST MEDIUM = AIR

TEST NO. 72 CASE NO. 1 SINGLE COMPONENT FORCE BALANCE

AVERAGE VALUES FOR EACH TAP ARE DIVIDED INTO THE AVERAGE MODEL TOTAL PRESSURE(PT)

AVERAGE MODEL TOTAL PRESSURE(PT)= 548.701, AVERAGE TEST CELL AMBIENT PRESSURE(IPA)= 2.074, PT/PA=264.590

| | | | | | | |
|---------|---------|---------|----------|---------|---------|-------------------|
| 50.9658 | 49.9816 | 36.4701 | 28.6706 | 19.7858 | 12.4543 | TAP NO. 1 - 6 |
| 10.6942 | 0.0 | 0.0 | 0.0 | 0.0 | 0.0 | TAP NO. 7 - 12 |
| 1.0000 | 1.0001 | 1.0012 | 0.0 | 0.0 | 0.0 | TAP NO. 25 - 30 |
| 0.0 | 0.0 | 0.0 | 264.5901 | 0.0 | 0.0 | TAP NO. 97 - 102 |
| 0.0 | 0.0 | 0.0 | 0.0 | 1.0904 | 1.0912 | TAP NO. 121 - 126 |

ROCKETDYNE ROCKET NOZZLE TEST FACILITY BRISTOL RECORDED (DATEX) TEST DATA

25 MAY 1973

TEST PROGRAM NO. 7307...JET PLUME AND WALL PRESSURE CALIBRATION OF THE 0.019 SCALE S.S.V.NOZZLES

CONFIGURATION NO. 700 TEST MEDIUM = AIR

TEST NO. 73 CASE NO. 2 SINGLE COMPONENT FORCE BALANCE

AVERAGE VALUES FOR EACH TAP ARE DIVIDED INTO THE AVERAGE MODEL TOTAL PRESSURE(PT)

AVERAGE MODEL TOTAL PRESSURE(PT)= 548.629, AVERAGE TEST CELL AMBIENT PRESSURE(IPA)= 4.265, PT/PA=128.639

| | | | | | | |
|---------|---------|---------|----------|---------|---------|-------------------|
| 50.8442 | 49.8972 | 36.4159 | 28.6393 | 19.7707 | 12.4127 | TAP NO. 1 - 6 |
| 10.6631 | 0.0 | 0.0 | 0.0 | 0.0 | 0.0 | TAP NO. 7 - 12 |
| 1.0000 | 0.9998 | 1.0009 | 0.0 | 0.0 | 0.0 | TAP NO. 25 - 30 |
| 0.0 | 0.0 | 0.0 | 128.6390 | 0.0 | 0.0 | TAP NO. 97 - 102 |
| 0.0 | 0.0 | 0.0 | 0.0 | 1.0990 | 1.0989 | TAP NO. 121 - 126 |

B-6

LMSC-HREC TM D306990

ROCKETDYNE ROCKET NOZZLE TEST FACILITY BRISTOL RECORDED (DATEX) TEST DATA

12 SEP 1973

TEST PROGRAM NO. 7307...JET PLUME AND WALL PRESSURE CALIBRATION OF THE 0.019 SCALE S.S.V.NOZZLES

CONFIGURATION NO. 900 TEST MEDIUM = AIR

TEST NO. 81 CASE NO. 1 SINGLE COMPONENT FORCE BALANCE

AVERAGE VALUES FOR EACH TAP ARE DIVIDED INTO THE AVERAGE MODEL TOTAL PRESSURE (PT)

AVERAGE MODEL TOTAL PRESSURE (PT) = 254.504, AVERAGE TEST CELL AMBIENT PRESSURE (PA) = 0.198, PT/PA = 1288.210

| | | | | | | |
|---------|---------|---------|-----------|---------|--------|-------------------|
| 91.6482 | 51.9703 | 56.0196 | 33.3439 | 12.4127 | 5.1211 | TAP NO. 1 - 6 |
| 1.0000 | 1.0019 | 1.0011 | 0.0 | 0.0 | 0.0 | TAP NO. 25 - 30 |
| 0.0 | 0.0 | 0.0 | 1288.2097 | 0.0 | 0.0 | TAP NO. 97 - 102 |
| 0.0 | 0.0 | 0.0 | 0.0 | 0.5137 | 0.0 | TAP NO. 121 - 126 |

ROCKETDYNE ROCKET NOZZLE TEST FACILITY BRISTOL RECORDED (DATEX) TEST DATA

12 SEP 1973

TEST PROGRAM NO. 7307...JET PLUME AND WALL PRESSURE CALIBRATION OF THE 0.019 SCALE S.S.V.NOZZLES

CONFIGURATION NO. 900 TEST MEDIUM = AIR

TEST NO. 83 CASE NO. 1 SINGLE COMPONENT FORCE BALANCE

AVERAGE VALUES FOR EACH TAP ARE DIVIDED INTO THE AVERAGE MODEL TOTAL PRESSURE (PT)

AVERAGE MODEL TOTAL PRESSURE (PT) = 514.856, AVERAGE TEST CELL AMBIENT PRESSURE (PA) = 0.722, PT/PA = 713.221

| | | | | | | |
|---------|---------|---------|----------|---------|--------|-------------------|
| 90.0234 | 90.8684 | 56.8323 | 33.5409 | 12.5460 | 5.1310 | TAP NO. 1 - 6 |
| 3.4403 | 0.0 | 0.0 | 0.0 | 0.0 | 0.0 | TAP NO. 7 - 12 |
| 1.0000 | 0.0 | 0.9597 | 0.0 | 0.0 | 0.0 | TAP NO. 25 - 30 |
| 0.0 | 0.0 | 0.0 | 713.2214 | 0.0 | 0.0 | TAP NO. 97 - 102 |
| 0.0 | 0.0 | 0.0 | 0.0 | 1.0404 | 0.0 | TAP NO. 121 - 126 |

ORIGINAL PAGE IS
OF POOR QUALITY

B-7

LMSC-HREC TM D306990

ORIGINAL PAGE IS
OF POOR QUALITY

ROCKETDYNE ROCKET NOZZLE TEST FACILITY BRISTOL RECORDED (DATEX) TEST DATA

12 SEP 1973

TEST PROGRAM NO. 7307...JET PLUME AND WALL PRESSURE CALIBRATION OF THE 0.019 SCALE S.S.V.NOZZLES

CONFIGURATION NO. 930 TEST MEDIUM = AIR

TEST NO. 84 CASE NO. 1 SINGLE COMPONENT FORCE BALANCE

AVERAGE VALUES FOR EACH TAP ARE DIVIDED INTO THE AVERAGE MODEL TOTAL PRESSURE (PT)

AVERAGE MODEL TOTAL PRESSURE (PT) = 515.474, AVERAGE TEST CELL AMBIENT PRESSURE (PA) = 0.290, PT/PA = 1777.923

| | | | | | | |
|---------|---------|---------|-----------|---------|--------|-------------------|
| 90.2403 | 91.0342 | 57.0540 | 59.7064 | 12.4846 | 5.1109 | TAP NO. 1 - 6 |
| 3.4247 | 0.0 | 0.0 | 0.0 | 0.0 | 0.0 | TAP NO. 7 - 12 |
| 1.0000 | 1.0014 | 1.0006 | 0.0 | 0.0 | 0.0 | TAP NO. 25 - 30 |
| 0.0 | 0.0 | 0.0 | 1777.9229 | 0.0 | 0.0 | TAP NO. 57 - 102 |
| 0.0 | 0.0 | 0.0 | 0.0 | 1.0148 | 0.0 | TAP NO. 121 - 126 |

ROCKETDYNE ROCKET NOZZLE TEST FACILITY BRISTOL RECORDED (DATEX) TEST DATA

12 SEP 1973

TEST PROGRAM NO. 7307...JET PLUME AND WALL PRESSURE CALIBRATION OF THE 0.019 SCALE S.S.V.NOZZLES

CONFIGURATION NO. 900 TEST MEDIUM = AIR

TEST NO. 90 CASE NO. 1 SINGLE COMPONENT FORCE BALANCE

AVERAGE VALUES FOR EACH TAP ARE DIVIDED INTO THE AVERAGE MODEL TOTAL PRESSURE (PT)

AVERAGE MODEL TOTAL PRESSURE (PT) = 598.204, AVERAGE TEST CELL AMBIENT PRESSURE (PA) = 0.825, PT/PA = 615.857

| | | | | | | |
|---------|---------|---------|----------|---------|--------|-------------------|
| 90.1460 | 90.7550 | 56.8156 | 58.5190 | 12.4910 | 5.0961 | TAP NO. 1 - 6 |
| 3.4080 | 0.0 | 0.0 | 0.0 | 0.0 | 0.0 | TAP NO. 7 - 12 |
| 1.0000 | 1.0005 | 1.0001 | 0.0 | 0.0 | 0.0 | TAP NO. 25 - 30 |
| 0.0 | 0.0 | 0.0 | 615.8574 | 0.0 | 0.0 | TAP NO. 57 - 102 |
| 0.0 | 0.0 | 0.0 | 0.0 | 1.0055 | 0.0 | TAP NO. 121 - 126 |

B-8

LMSC-HREC TM D306990